EAO SUBMILLIMETRE FUTURES PAPER SERIES, 2019

The East Asian Observatory*
James Clerk Maxwell Telescope
660 N. A'ohōkū Place, Hilo, Hawai'i, USA, 96720

1 About This Series

Submillimetre astronomy is an active and burgeoning field that is poised to answer some of the most pressing open questions about the universe. The James Clerk Maxwell Telescope, operated by the East Asian Observatory, is at the forefront of discovery as it is the largest single-dish submillimetre telescope in the world. Situated at an altitude of 4,092 metres on Maunakea, Hawai'i, USA, the facility capitalises on the 850 μm observing window that offers crucial insights into the cold dust that forms stars and galaxies. In 1997, the Submillimetre Common User Bolometer Array (SCUBA) was commissioned, allowing astronomers to detect the furthest galaxies ever recorded (so-called SCUBA galaxies) and develop our understanding of the earliest stages of star formation. Since 2011, its successor, SCUBA-2, has revolutionised submillimetre wavelength surveys by mapping the sky hundreds of times faster than SCUBA. The extensive data collected spans a wealth of astronomy sub-fields and has inspired world-wide collaborations and innovative analysis methods for nearly a decade. Building on the successes of these instruments, the East Asian Observatory is constructing a third generation 850 μm wide-field camera with intrinsic polarisation capabilities for deployment on the James Clerk Maxwell Telescope.

In May, 2019, the "EAO Submillimetre Futures" meeting was held in Nanjing, China to discuss the science drivers of future instrumentation and the needs of the submillimetre astronomy community. A central focus of the meeting was the new 850 μm camera. As a result of many fruitful discussions, a series of white papers was commissioned to outline prominent 850 μm science goals across a variety of related fields and to identify key properties of the instrument design. The five white papers included here focus on the following topics:

1. Continuum Surveys
2. Transient Science
3. Magnetic Fields
4. Evolved Stars
5. Submillimetre Galaxies

These topics are representative of some of the main research interests at the JCMT, though the list is by no means exhaustive.

Each paper presents context for the given scientific field, highlights key results, comments on the current status of the field, and discusses future endeavours assuming the proposed properties of the new instrument (see Section 2). In Section 3 we present an overview of each white paper, highlighting just a few of the next decade's 850 μm science cases. In Section 4, we discuss the synergy between future observing campaigns. Finally, in Section 5, we briefly summarise the JCMT and the new 850 μm camera in the context of global submillimetre astronomy.

2 The Proposed JCMT 850 micron Camera

The third generation dedicated 850 μm camera at the JCMT will boast a guaranteed increase of at least an order of magnitude in mapping speed for both compact and large continuum maps relative to SCUBA-2. In addition, it will have intrinsic polarisation capabilities, allowing for at least a factor of 20 increase in mapping speed for magnetic field studies. These improved speeds are achieved by means of a larger field of view, improved per-pixel sensitivity and improved stability and uniformity of the detector array. The instrument will be monochromatic, taking advantage of the 850 μm transmission window accessible to the JCMT. The main instrument properties are summarised in Table 1.

*Contact: Steve Mairs, JCMT Senior Scientist, s.mairs@eaobservatory.org

Table 1: Proposed Properties of the New 850 μm Camera

Property	Description
Wavelength	850 μm
FOV	12 arcmin
Detectors	7,272 Feedhorn Coupled MKIDs (TiN/Ti multilayers)
Dark NEP	$< 4 \times 10^{-17}$ W/Hz$^{1/2}$
Guaranteed Mapping Speed Increase	Compact Maps: 10x, Large Maps: 10x, Polarimetry Maps: 20x
Aspirational Mapping Speed Increase	Large Maps: 20x, Large Polarimetry Maps: 40x

The new detector array will be 3,636 1fλ spaced feedhorn coupled pixels each comprised of two detectors that measure orthogonal linear polarisation. By careful choice of the orientation of pixels across the focal plane, it will be possible to determine all Stokes parameters from a single scan observation, without the need for a rotating half wave plate. This allows polarisation mapping as a matter of course, with no overhead or penalties, while mapping continuum intensities.

While SCUBA-2's Transition Edge Sensor array remains the best large format submillimetre detector array in operational use, the expected per-pixel sensitivity on the sky of the new MKID array will be a factor of 3 more sensitive. In addition, the detector yield will be close to 100%, compared to SCUBA-2's typical on-sky yield of 60%. This will allow a field of view of 12', nearly double the size of its predecessor. Finally, the new array will be much less sensitive to the thermal stability of the focal plane and magnetic field pickup, both of which impact SCUBA-2 data reduction. The MKID detector response will be linear across the full range of sky power whereas SCUBA-2 detectors are prone to flux-jumps due to the limited dynamic range of available Superconducting Quantum Interference Device (SQUID) feedback.

The new 850 μm MKID instrument is scheduled to begin operations at JCMT by October 2022.

3 White Paper Overviews

3.1 Continuum Surveys

Knowledge of the physical factors that control the conversion of interstellar gas into molecular clouds, and then into stars, is of fundamental importance for understanding the star formation process and the evolution of galaxies. The fraction of dense gas observed may highly depend on cloud properties. This white paper addresses the need for a series of new surveys to sample different star-forming environments. Such studies are necessary in order to determine if, for example, there are universal thresholds for star-formation. The full details of the role of "ubiquitous" filamentary structures, including their formation and evolution are also still poorly understood. Perpendicular striations to main filaments, the overall kinematics of hub-filament systems, and alignment or misalignment with a surrounding magnetic field are all crucial metrics that require study and comparison with magnetized, self-gravitating simulations to construct a complete theory of star-formation.

This white paper summarises several galactic plane surveys performed by Herschel Space Observatory, the Caltech Submillimetre Observatory, The Atacama Pathfinder Experiment Telescope, and the Planck satellite, highlighting the synergy with the JCMT's Plane Survey, SCUBA-2 Ambitious Sky Survey (SASSY), Gould Belt Survey, and SCOPE Large Program. Despite these successful programs, there remains a variety of issues. Most of the submillimetre continuum surveys have been focused on Gould Belt clouds or the inner Galactic Plane with limited coverage of other areas. These well-studied molecular clouds do not broadly represent the star formation activity seen in regions like metal poor high-latitude clouds, the central molecular zone (CMZ) of the Milky Way, or starburst galaxies where densities, temperatures, and star formation efficiencies can be vastly different. Several open questions remain, such as: how and where do protostellar cores form? What is the relative importance of turbulence, B-field, gravity, and external pressure in core formation and evolution? Is there a universal density threshold for star formation? How do filaments form? How do filaments fragment and what is their role in producing cores? Do filaments have a universal width? How does the formation and evolution of molecular clouds inform these questions? Are there different star-formation processes for different galactic environments (galactic arms, high latitude, supernova remnants, etc)? What dominant factors regulate star formation efficiency?

The increased mapping speed of the new camera will allow for a census of molecular cloud structures over a very broad representation of galactic environments to unprecedented depths that require prohibitive exposure times with SCUBA-2. The authors outline several potential surveys with the new camera, including:

1. A 320 hour program to observe 9,677 Planck-identified objects with a background noise level of 5 mJy/beam.

2. A 130-200 hour program to perform observations of 1000 Planck Galactic Cold Cores (PGCCs). The sensitivity will be high enough to detect dust emission where HI is converted to H_2
3. A 250-400 hour program to observe 160 square degrees covered by the Herschel Space Observatory to probe the link between large-scale diffuse structures and dense structures.
4. A 600-900 hour program to perform an extensive galactic plane survey to unprecedented sensitivities.

3.2 Transient Science

The Transient Science white paper is mainly focused on protostellar variability and extensions to the JCMT Transient Survey Large Program. This survey, the first of its kind, began in 2015 and has shown that luminosity variations of deeply embedded protostars are efficiently reprocessed by their surrounding, dusty envelopes, creating brightness changes that can be detected at submillimetre wavelengths. This pioneering work performed using SCUBA-2 has opened a new field in time domain science, allowing astronomers to probe the characteristics of solar systems during their earliest stages of formation while constraining the frequency and amplitude of protostellar variability without the use of far-infrared space telescopes. These observational metrics are directly related to the physical properties of the disk-star system and help answer questions such as: How is infalling material transferred to the protostar through the circumstellar disk? Do protostars continually accrete mass or do they exhibit punctuated bursts of accretion? Can the amplitude and frequency of these events provide evidence to solve the "Luminosity Problem" or confirm protostellar lifetimes? Do high-mass stars and low-mass stars behave differently in their earliest stages of formation? What fraction of protostars undergo significant burst/dimming phases?

The new 850 μm camera would significantly improve the statistical sample of young protostars and allow for the detailed study of more distant, higher-mass regions than are studied in the SCUBA-2 era. From December 2015 to January 2020, 8 low-mass star-forming regions ($0^\circ.5$ diameter circular maps) have been observed to a depth of $\sim 15\,\mathrm{mJy/beam}$ at an approximately monthly cadence. Once the third generation continuum imager is deployed, the factor of 10 increase in mapping speed will allow at least 25% more protostellar sources than are currently being robustly tracked to be uncovered in these 8 fields for the same time investment. The increased sensitivities may also allow for the first detections of First Hydrostatic Cores. Conversely, the survey area could widen significantly with 80 fields observed in the same amount of time spent on 8 during the SCUBA-2 era. Full repeats of extensive SCUBA-2 surveys could be performed in a fraction of the time, allowing for multiple epochs of all nearby star-forming regions with high concentrations of known young stellar objects. For example, all 103 Gould Belt star-forming fields covered by SCUBA-2 could be observed to a depth of $5\,\mathrm{mJy/beam}$ (comparable to the original JCMT Gould Belt Survey sensitivity) in only 60 hours of moderate weather (PWV$\sim$2 mm, observatory weather grade 3). The increased detector sensitivity will also allow for survey expansions to more distant intermediate- and high-mass star forming regions with a robust relative flux calibration scheme. This will allow for the characterisation of the frequency and amplitude of submillimetre variability events through a range of masses and galactic environments. Combining this data with archival SCUBA and SCUBA-2 data will lead to $> 20\,\mathrm{yr}$ submillimetre light curves for bright sources.

The white paper also briefly summarises the following other science cases for submillimetre time-domain monitoring:

1. Investigating supernovae in starburst galaxies to provide a more accurate measurement of star formation and supernova rates.
2. Tracking the submillimetre brightness changes of active galactic nuclei to probe the innermost components of relativistic jets and determine the properties of their turbulent nature.
3. Studying the evolution of X-ray binary systems to track accreting matter from inflow to outflow over human timescales.
4. Monitoring the pulsations of asymptotic giant branch and other evolved stars in order to provide insight into the properties of their dust shells outflow variations.
5. Expanding studies of non-thermal radio flares from stellar reconnection, with feasibility demonstrated by the detection of a flare from the binary system JW 566.
6. Broadening transient-style observations over the next decade to allow for the discovery of new phenomena from nearby galaxies or the distant universe.

3.3 Magnetic Fields

In this white paper, the authors introduce the importance of studying magnetic fields on a variety of physical scales and note the need for wider and deeper polarimetric surveys. The JCMT is highlighted as the ideal telescope for imaging polarised emission, citing the BISTRO Large Program as a successful campaign focused on measuring the magnetic field orientation and strength in cloud cores, clumps, and filaments across the Gould Belt. In the current era, SCUBA-2 relies on the use of the POL-2 instrument to collect polarisation data. While these data have driven unprecedented

results in submillimetre observations of magnetic fields, they are insufficient to robustly answer many open questions about the role of magnetic fields on scales of individual stars through the dynamics of the intergalactic medium. The proposed 850 μm camera, however, does not require additional equipment such as POL-2's spinning half wave plate due to the nature of the orthogonal MKID detectors. This simplified optical path mitigates the effect of light loss and greatly improves the image fidelity and overall detector sensitivity, increasing the ability to probe magnetic fields to extraordinary depths.

The white paper is organised into four main scientific areas:

1. *Star Formation and the Galactic ISM:* Measuring magnetic field angles with respect to star-forming filamentary structure is not only important for better understanding molecular clouds themselves, but it is also critical in formulating a complete theory of star-formation. The improved mapping speed of the new camera will allow for observations of entire molecular clouds for the same time investment as one POL-2 field. The study of low density/non-self-gravitating filaments will be expanded to better understand the role of magnetic fields during the earliest stages of star formation over a variety of mass ranges and galactic environments. The new camera will revolutionise the statistics of the initial conditions of star formation by increasing the sample of magnetised dense core observations by an order of magnitude. Additionally, the improved instrumentation will bring forth systematic investigations of cloud cores hosting potential progenitors of proto-brown dwarfs or very low-mass YSOs and allow for followup target-of-opportunity polarimetric observations of protostellar flares to note any significant changes in magnetic field properties in the time domain.
2. *Late-stage Stellar Evolution:* Evolved stars have significant magnetic fields at their surfaces and in their envelopes. Current surveys have only sampled a small fraction of this emission with the Zeeman splitting technique. The field of view and sensitivity of the new camera will drastically aid in the understanding of the typical behaviour of magnetic fields in AGB stars and planetary nebulae by allowing for investigations of the dependence on angular momentum transfer from companions and of how mass-loss histories shape the outflow. Estimates indicate that the new instrument will be capable of observing tens to hundreds of evolved stars. Additionally, the proposed camera would open a new avenue to investigate the compression and seeding of magnetic fields in the vicinity of supernova remnants in both the Milky Way and nearby galaxies.
3. *Galactic-Scale Magnetic Fields:* 850 μm polarisation observations of a sample of spiral galaxies will provide a unique dataset to assess the magnetic field properties of high-density gas in a galactic context. The new camera will also allow for a survey of starburst galaxies and the affect of intense stellar feedback on magnetic fields. Aditionally, 850 μm observations of the Milky Way's galactic centre will allow the region around Sgr A* to be mapped in unprecedented detail, informing models of galactic evolution and providing insight into AGN physics such as jet launching and radiative feedback.
4. *Dust Grain Physics and Alignment Mechanisms:* Dust polarisation is currently understood in the paradigm of radiative alignment torque theory, wherein non-spherical dust grains align with their long axes perpendicular to the magnetic field. Understanding the conditions under which grains gain and lose this alignment by probing a variety of galactic environments with high sensitivity observations is critical to understanding the polarisation spectrum and the grain properties of different molecular cloud scales.

The paper concludes by highlighting future JCMT data synergies with molecular line magnetic field observations (Zeeman Effect and Goldreich-Kylafis Effect) and summarising the advantages of obtaining data in the 850 μm transmission window in the global context of other polarimeters.

3.4 Evolved Stars

Evolved stars play key roles in the chemical enrichment of the interstellar medium (ISM) and, in general, the Universe. The amounts of metals that are processed can be understood by careful observations of the mass loss rate, primarily when stars are in the Asymptotic Giant Branch (AGB) phase. Additionally, mass-loss also dictates the end of life scenario, directly informing the production of iron-peak elements and the turbulence of the ISM. In this white paper, the authors note that despite the importance of these processes, the mass loss is still poorly understood. For example, it is unclear when winds become relevant as it depends on the dust properties, which are poorly constrained. The 850 μm submilllimetre continuum is sensitive to both the size and composition of dust grains and it is free from extinction effects, but homogeneous samples of evolved stars at submillimetre wavelengths are rare since the weak dust emission is difficult to observe. These data are necessary, however, to understand the relationships between pulsations, dust formation, and mass loss.

The next decade will be focused on answering questions about enrichment and mass return: How much enrichment does each class of star undergo? What fraction of mass return does each class contribute overall to the ISM? Molecular line observations combined with continuum surveys and radiative transfer models will be able to robustly address these

open questions. Tracing the extended continuum emission at high sensitivity and dynamic range will be fundamental as it informs the variable mass-loss history of a star on timescales of centuries. The current Nearby Evolved Stars Survey (NESS), a SCUBA-2 Large Program, sample is focused on 400 stars. Taking advantage of the increased mapping speed could double this sample, increasing the distance to targets by a factor of $\sqrt{2}$.

The authors highlight that the order of magnitude mapping speed increase will be "transformative" for understanding mass-loss histories since each observation will result in a sensitivity close to the confusion limit. Monitoring the submillimetre variability of these sources is also fundamental in investigating the shocks and changes in luminosity that drive dust formation and destruction while fuelling chemical pathways. Submillimetre wavelengths can directly probe how variability affects the outflow around evolved stars, rather than making indirect inferences using optical or near-infrared data. Additionally, observing the large-scale magnetic fields in the envelope using the built-in polarisation capabilities of the camera can answer questions such as: How many evolved stars have large-scale magnetic fields? What is the typical geometry? Is there a correlation with evolutionary stage? There is also some debate as to the origin of the fields, whether they are produced by angular-momentum transfer from a companion or if another mechanism is required to explain their existence.

An example of what could be seen with the future instrument was constructed by compiling 40 hours of observations of Omichron Cet (Mira). A detailed radial profile of the surface brightness was uncovered for this source. The same (or better) profile could be constructed in only 4 hours of observation time with the new camera. Only 200 hours of observing time would be required to provide mass-loss histories for all 400 NESS stars. The improved image fidelity produced by MKIDs when compared with TES will also improve the ability to recover lower surface brightnesses, extending the "look-back time" of the mass loss history. To probe shorter timescales, the authors discuss combining JCMT data with interferometric observations or looking ahead to a next generation 450 μm instrument.

The white paper also presents synergies with observations performed at multiple wavelengths and discusses in detail the importance of molecular line emission paired with the continuum data. CO line emission, for example, allows for a comparison of the cold gas and the cold dust in extended regions over multiple epochs of mass loss. The JCMT is currently the only facility in the Northern Hemisphere that could reasonably observe these relatively higher-frequency lines in conjunction with the continuum.

3.5 Submillimetre Galaxies

In this white paper, the authors note the unique opportunity the JCMT has to trace the gas and dust contents the early Universe. Since the late 1990's, when SCUBA was used to discover the first population of high-redshift, dusty starburst galaxies, there has been a rich history of studying these objects at 850 μm using the JCMT. In recent years, with SCUBA-2, tracking the numbers of these ULIRG and HyLIRG galaxies (dust-embedded star formation rates of $> 100 - 1000 M_{\odot}/yr$) at z>6 suggests that there is active star formation at even earlier epochs (z>10 and beyond). Large-scale surveys of distant galaxies provide essential information to probe the cosmic star formation history, the formation and evolution of galaxy clusters, and the heavy element production of the Universe. Improved mapping capability at the JCMT will also inform structure formation on the largest scales, since clusters of galaxies are the most massive, bound structures in the local Universe. The authors highlight that studying these associations may reveal with more certainty the progenitors of massive elliptical galaxies in the cores of clusters (as these are related to major starbursts occurring long ago).

At high-redshifts, there are some difficulties reconciling the observations with theoretical models of star-formation rates and the properties of protocluster galaxies. Several surveys/Large Programs have been undertaken using the JCMT. These observations are paired with data obtained at shorter wavelengths from the Spitzer Space Telescope and the Herschel Space Observatory to derive an accurate submillimetre source number density over a wide redshift range. In general, the poor resolution and confusion limits of space telescopes produce a significant underestimate of the star formation rate at high-redshifts. The ground-based JCMT provides better sensitivity and resolution, but the telescope has so far mapped only relatively small areas of the sky, introducing large statistical uncertainties. The confusion limited SCUBA-2 surveys cover <5 square degrees, compared to the optical/near-IR/radio observations of 300 square degrees. To improve the statistics of ground-based surveys, larger-area and deeper surveys are urgently required to match the existing data at other wavelengths.

The order of magnitude increase in mapping speed will make the JCMT's new camera the most powerful tool in the search for these objects at z>7 and beyond. Next generation surveys will better constrain the cosmic star formation history, address the evolutionary connection between star formation and SMBH accretion over a wide range of redshift, shed new light on galaxy cluster formation, and reduce the overall statistical uncertainties in the current literature. The JCMT data will be essential in identifying high-z candidates based on colour. Protocluster candidates have an expected area density of $\sim$1 per 40 square degrees, and the new camera at JCMT will make it possible to perform a survey of 300 square degrees to a depth of 2 mJy/beam in 2,500 hours assuming a PWV between 0.8mm and 2.6mm (observatory

weather grades 2/3). This dramatically expanded survey area would allow for the selection of $\sim 10,000$ very high redshift dusty starburst galaxy candidates and include $\sim 5,000$ quasars, creating an unprecedented and unique potential for studying rare submillimetre emitters. Large-scale surveys such as this will make available a homogeneous sample of high redshift sources for markedly better statistical assessments of galaxy luminosity functions and evolution than exist today. With the 10 times faster mapping speed, the new 850 μm camera is expected to enlarge the current sample of z>5 dusty starburst galaxies by nearly two orders of magnitude. This submillimetre continuum data will undoubtedly initiate spectroscopic followups using ALMA, NOEMA, KMOS, and MUSE.

4 Synergy in Future Campaigns

From an observational perspective, there is a significant amount of overlap between the science goals presented in Section 3. The future surveys outlined in Section 3.1 will not only provide urgently needed continuum information to study cores, filaments, and other ISM structures but it will also offer unprecedented polarisation data in each field that will contribute to many of the goals outlined in Section 3.3. The same is true for the evolved star work presented in Section 3.4. In the SCUBA-2 era, the observing time required for polarisation observations to achieve the same sensitivity as continuum observations is several times longer. The factor of 20 increase in mapping speed for polarisation data with the new camera compared to the factor of 10 increase in speed for continuum maps significantly mitigates this difference and allows for more efficient use of telescope time. The polarisation mapping capability will make JCMT data extremely competitive, since most polarisation measurements rely on Planck satellite data, which has very poor angular resolution in comparison.

With the new camera, the 850 μm confusion limit (0.7 $\mathrm{mJy/beam}$) for a $0^{\circ}.5$ diameter circular field would be achieved after only 27-50 hours in moderate weather conditions (PWV 2mm), depending on the declination. A future generation Transient Survey (see Section 3.2) alone would be able to provide confusion limited maps for ancillary ISM studies of 10 such fields at the small cost of only 10.5 nights[2] per year over the course of three years. Spending the equivalent of 32 nights per year (9% of the observing time) over a decade of use with the new instrument would provide the maximum available continuum sensitivity at 850 μm for 100 fields, each with deep polarisation maps for no additional overhead. This would allow for an unprecedented statistical dataset of ISM structures in a variety of galactic environments. This singular dataset would provide information on molecular cloud, filament, and core formation (see Section 3.1), offer insights into the dynamical importance of magnetic fields in star-forming regions (see Sections 3.3), allow for the detection of potential proto-brown dwarfs and very low luminosity objects (VeLLOs; see Sections 3.3 and 3.2), dramatically increase our understanding of submillimetre variability across thousands of young stellar objects (see Section 3.2), act as a precursor for ground-breaking studies of long-term changes in magnetic fields in the time domain, and seed many more ideas for years to come.

5 The New Camera in A Global Context

The next decade is rife with opportunity for collaborative studies involving the JCMT and other world-class facilities. The JCMT is situated at a latitude of $19^{\circ}.5$N, allowing sight lines to both northern and southern hemisphere fields and with the new 850 μm camera, it will provide the crucial high-sensitivity, wide-field maps needed for advancing our understanding of a wide spectrum of topics.

While interferometers such as the Atacama Large Millimetre/submillimetre Array (ALMA) provide high resolution observations, they lose large-scale structures due to the short spacing problem and provide a field of view significantly smaller than the JCMT. Space telescopes provide information over very large-scales, but at the cost of low angular resolution. The JCMT provides data on the critical intermediate scales between interferometric observations and, for example, Planck all-sky maps. The 850 μm transmission window is a unique opportunity for the JCMT as Maunakea is at a high enough altitude to capitalise on these observations year-round.

As discussed in the white papers, the wide-area surveys provided by the JCMT's new camera will undoubtedly inspire follow-up continuum and spectroscopic observations at other Maunakea facilities and around the world such as the Large Millimetre Telescope (LMT), the Institute for Radio Astronomy in the Millimeter Range (IRAM) telescope, ALMA, and the European Space Observatory (ESO). There will also be an opportunity to combine the maps obtained with data from new facilities and instruments such as the 6-meter CCAT-prime telescope, the new Toltec instrument at the LMT, made from the same MKID arrays as the proposed JCMT camera, tuned to 1.1mm, the James Webb Space Telescope, and space telescopes of the 2030s. The resolution, field of view and mapping speed of the JCMT's new instrument will also complement data taken by polarimeters such as HAWC+, BLAST-TNG, TolTEC, NIKA-2, and A-MKID, while boasting an intrinsic advantage over all these facilities in its ability to map magnetic fields without the use of a half-wave plate or a polarising grid.

[2]Assuming 12 hour nights.

GALACTIC CONTINUUM SURVEYS WITH THE NEW 850 μm MKID CAMERA AT THE EAO/JCMT 15-M TELESCOPE

EAO SUBMILLIMETRE FUTURES PAPER SERIES, 2019

Tie Liu[*1] • **Di Li**[†2] • **David Eden**[3] • **James Di Francesco**[4] • **Jinhua He**[5,6] • **Sarah Sadavoy**[7,8]
Ken Tatematsu[9] • **Kee-Tae Kim**[10] • **Naomi Hirano**[11] • **Gary Fuller**[12] • **Yuefang Wu**[13]
Sheng-Yuan Liu[11] • **Ke Wang**[13] • **Mark Thompson**[14] • **Mika Juvela**[15] • **Isabelle Ristorcelli**[16]
L. Viktor Toth[17] • **Archana Soam**[18] • **Patricio Sanhueza**[19] • **Woojin Kwon**[10] • **Sung-ju Kang**[10]
John Richer[20] • **Jinjin Xie**[2] • **Yapeng Zhang**[21] • **Bingru Wang**[2] • **Derek Ward-Thompson**[22]
Julien Montillaud[23]

[1]*East Asian Observatory (JCMT) 660 N. A'ohōkū Place, Hilo, Hawai'i, USA, 96720*
[2]*National Astronomical Observatories, Chinese Academy of Sciences, Beijing 100101, China*
[3]*Astrophysics Research Institute, Liverpool John Moores University, IC2, Liverpool Science Park, 146 Brownlow Hill, Liverpool, L3 5RF, UK*
[4]*NRC Herzberg Astronomy and Astrophysics, 5071 West Saanich Rd, Victoria, BC, V9E 2E7, Canada*
[5]*Yunnan Observatories, Chinese Academy of Sciences, 396 Yangfangwang, Guandu District, Kunming, 650216, P. R. China*
[6]*Chinese Academy of Sciences South America Center for Astronomy, China-Chile Joint Center for Astronomy, Camino El Observatorio #1515, Las Condes, Santiago, Chile*
[7]*Harvard-Smithsonian Center for Astrophysics, 60 Garden Street, Cambridge, MA, 02138, USA*
[8]*Department for Physics, Engineering Physics and Astrophysics, Queen's University, Kingston, ON, K7L 3N6, Canada*
[9]*Nobeyama Radio Observatory, National Astronomical Observatory of Japan, National Institutes of Natural Sciences, Nobeyama, Minamimaki, Minamisaku, Nagano 384-1305, Japan*
[10]*Korea Astronomy and Space Science Institute, 776, Daedeokdae-ro, Yuseong-gu, Daejeon, 34055, Korea*
[11]*Academia Sinica Institute of Astronomy and Astrophysics, AS/NTU Astronomy-Mathematics Building, No 1. Sec. 4 Roosevelt Rd, Taipei, Taiwan*
[12]*Jodrell Bank Centre for Astrophysics, School of Physics and Astronomy, The University of Manchester, Oxford Road, Manchester M13 9PL, UK*
[13]*Department of Astronomy, Peking University, 100871, Beijing China*
[14]*Centre for Astrophysics Research, Science & Technology Research Institute, University of Hertfordshire, Hatfield, AL10 9AB, UK*
[15]*Department of Physics, P.O.Box 64, FI-00014, University of Helsinki, Finland*
[16]*IRAP, Université de Toulouse, CNRS, UPS, CNES, F-31400 Toulouse, France*
[17]*Eötvös Loránd University, Department of Astronomy, Pázmány, Péter sétány 1/A, H-1117, Budapest, Hungary*
[18]*SOFIA Science Center, USRA, NASA Ames Research Center, Moffett Field, CA, USA, 94035*
[19]*National Astronomical Observatory of Japan, National Institutes of Natural Sciences, 2-21-1 Osawa, Mitaka, Tokyo 181-8588, Japan*
[20]*Kavli Institute for Cosmology, Institute of Astronomy, University of Cambridge, Madingley Road, Cambridge, CB3 0HA, UK*
[21]*Department of Physics, The Chinese University of Hong Kong, Shatin, Hong Kong*
[22]*Jeremiah Horrocks Institute, University of Central Lancashire, Preston PR1 2HE, UK*
[23]*Institut UTINAM - UMR 6213 - CNRS - Univ Bourgogne Franche Comté, France, OSU THETA, 41bis avenue de l'Observatoire, 25000 Besançon, France*

[*] liutiepku@gmail.com
[†] dili@nao.cas.cn

ABSTRACT

This white paper gives a brief summary of Galactic continuum surveys with the next generation 850 μm camera at the James Clerk Maxwell Telescope (JCMT) in the next decade. This new camera will have mapping speeds at least 10-20 times faster than the present SCUBA-2 camera, and will enable deep ($<$10 mJy beam^{-1}) and extensive continuum surveys such as a wider ($-5^\circ < l < 240^\circ$, $|b| < 2 - 5^\circ$) Galactic Plane survey, a larger Gould Belt survey, and a follow-up survey of all Planck compact objects visible from the northern hemisphere. These surveys will provide a complete census of molecular clouds, filaments, and dense cores across the Galaxy, vital for studying star formation in various environments.

Keywords surveys · radio continuum: ISM · ISM: clouds · stars: formation

1 Introduction

Stars form in molecular clouds when dense condensations of dust and gas gravitationally collapse to form a central protostar. This young stellar object (YSO) accretes material from the surrounding cloud until it reaches the temperature and density required for nuclear fusion. Knowledge of the physical factors that control the conversion of interstellar gas into molecular clouds, and then into stars, is of fundamental importance for understanding the star formation process and the evolution of galaxies. Nevertheless, our current theories of star formation are still very limited.

Molecular clouds form stars in their deepest, high-extinction interiors. Such regions only account for small percentages of the sizes and masses of molecular material in these clouds. The key to understanding the formation of clouds themselves may lie in sensitive observations of their diffuse outermost extents. The outermost extents of clouds, where HI is converted to H_2 (and vice-versa) are difficult to probe. Through a combined analysis of HI narrow self-absorption, CO emission, dust emission, and extinction, (1) identified a striking "ring" of enhanced HI abundance in a molecular cloud (see left panel in *Figure* 1), resembling the “onion” shell description of a forming molecular cloud with ongoing H_2 formation. Such observations, however, are very rare, preventing us from a thorough understanding of cloud formation and evolution.

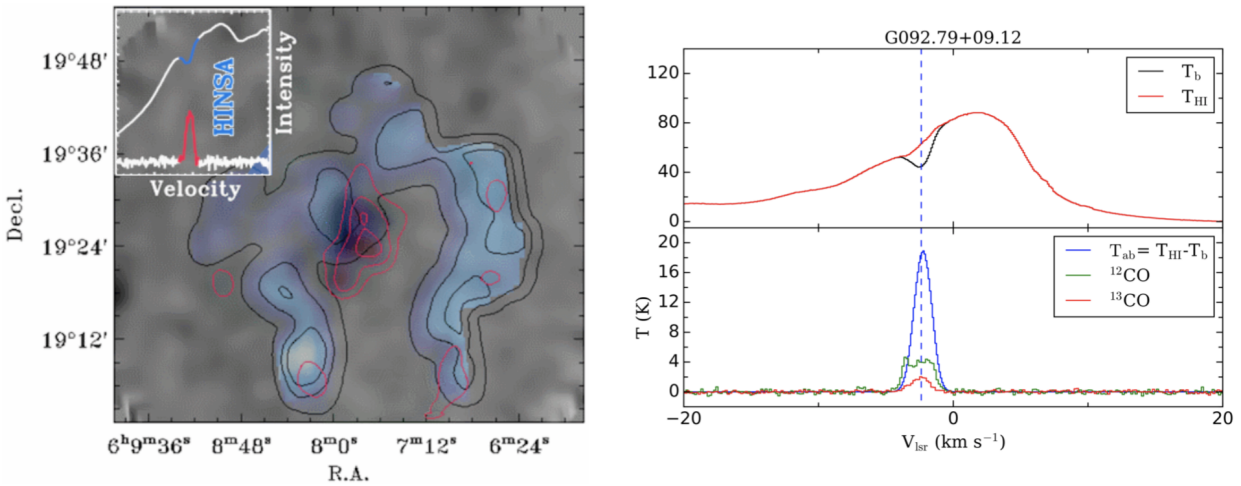

Figure 1: *Left:* The B227 molecular cloud (1). The gray scale image shows the 2MASS extinction; the black contours and blue shadow show the ratio of [HI]/[H_2]; and the red contours show the column density ratios of [^{13}CO]/[H_2].The upper left corner presents spectra of HI narrow self-absorption line and ^{13}CO J=1-0 emission line. *Right:* Spectra of PGCC G092.79+09.12 (Tang et al. 2019 submitted). Top panel: black and red solid lines are the observed HI and the recovered HI background spectrum $T_{\rm HI}$, respectively. Bottom panel: the profile of absorption temperature T_{ab} of HI (blue), ^{12}CO J=1-0 (green) and ^{13}CO J=1-0 spectrum (red).

Recent studies have defined a “threshold” surface density of about 120 $M_\odot$ pc^{-2} for star formation in nearby clouds (2; 3; 4), above which the vast majority of dense cores and YSOs are found. (5) compared various models of star formation to observations of nearby clouds and found that the mass of dense gas was the best predictor of the star formation rate (SFR). More recently, (6) found a similar threshold applied to more distant and massive clouds in the

Galactic Plane, using millimeter-continuum emission from the Bolocam Galactic Plane Survey (BGPS) (7) to measure the mass of dense gas. They further demonstrated that the average star formation rate per unit mass of dense gas (star formation efficiency; SFE) is remarkably constant over a large range of scales and conditions, ranging from Galactic molecular clouds to clouds in nearby galaxies to more distant galaxies (6).

However, the particular threshold or constant SFE may not apply in some extreme regions, especially those with lower metallicity or much stronger radiation fields (e.g. clouds in the central molecular zone,CMZ, (8)). In particular, the fraction of dense gas in various kinds of clouds may highly depend on cloud properties. Whether or not there is a single, universal density threshold for star formation can only be tested by investigating a complete and unbiased volume-limited sample of star-formation activity not only in the well-known dark clouds of the Galactic plane and Gould's Belt but also those currently unknown regions, potentially located in diffuse or small molecular clouds.

Whilst there is a broad-brush theory behind (low-mass) star formation, the initial conditions that lead a molecular cloud core to collapse and ultimately form a star is still far from fully understood. This limitation has a serious impact on our capability to extend the models of current star formation in our Galaxy to other environments such as low-metallicity galaxies or starburst galaxies. In the current paradigm, stars form within the compact (with sizes of 0.1 pc or less), cold ($T_{\rm k} \leq$10 K), and dense (n(H$_2$)$> 5 \times 10^4$ cm^{-3}) starless fragments in molecular clouds, usually dubbed "prestellar cores" (9). The prestellar core mass function in nearby clouds is very similar in shape to the stellar initial mass function (10; 11), hinting that there is a direct physical link between the initial conditions in prestellar cores and the star formation process (e.g. star formation mode (clustered or isolated), star formation efficiency and rate). However, it is unclear whether or not the core mass function is universal in clouds or if it changes across different environments.

Recent studies of nearby clouds by Herschel revealed a "universal" filamentary structure in the cold ISM (10). Filaments are commonly surrounded by a network of perpendicular striations. Filaments have been well predicted in simulations of supersonic turbulence with the absence of gravity, which can produce hierarchical structure with a lognormal density distribution seen in observations (12). Filaments in strongly magnetized turbulent clouds (e.g. B211/3, (13)) are formed preferentially perpendicular to the magnetic field lines, suggesting that magnetic fields have an important role in filament formation. Li et al. (2019; (14)) showed that a moderately strong magnetic field ($\mathcal{M}_{\mathcal{A}} \sim 1$) is crucial for maintaining a long and slender filamentary cloud for a long period of time $\sim$0.5 million years. Polarization observations of nearby filamentary clouds suggested a scenario in which local interstellar material has condensed into a gravitationally-unstable filament (with "supercritical" mass per unit length) that is accreting background material along field lines through the low-density striations (e.g., 15). The formation of filaments by self-gravitational fragmentation of sheet-like clouds was also seen in simulations of 1D compression (e.g. by an expanding HII region, an old supernova remnant, or collision of two clouds). For example, the asymmetric column density profiles of filaments in the Pipe Nebula have been attributed to the large-scale compressive flows generated by the winds of the nearby Sco OB2 association (16). Cloud-cloud collisions may also trigger the formation of these dense filaments (17). Although significant progress has been made in recent years, how filaments form in the cold ISM is still poorly understood.

The properties of filaments themselves are also far from well understood. One of the most striking results from Herschel observations in the Gould Belt clouds is the finding of an apparent characteristic width ($\sim$0.1 pc) of filamentary substructures (10). The origin of such a characteristic width is not well understood and this result is highly debated. Projection effects or artifacts in the data analysis may affect the inferred filament width (18). Some numerical simulations modeling the interplay between turbulence, strong magnetic field, and gravitationally driven ambipolar diffusion are indeed able to reproduce filamentary structures with widths peaked at 0.1 pc over several orders of magnitude in column density (e.g., 19; 20). Other simulations, however, find a wide range of filament widths (e.g. 21). It is unclear whether or not filaments have a universal width or under what conditions the width of a filament would deviate from 0.1 pc. Since we expect turbulence, magnetic fields, and external pressure to shape clouds and their filaments, we need a large census of filament properties and their host cloud properties to investigate how these filaments form and how they will in turn influence the types of cores and stars that will be produced.

2 Current Status

Prestellar cores are located in the coldest parts of molecular clouds. Early infrared surveys (e.g. IRAS, MSX, Spitzer, WISE) traced warm dust emission associated with protostellar objects or more evolved YSOs that are too old to assess the initial conditions of star formation. Extinction studies have assessed cloud structure and mass distributions, but these studies are mostly limited to low-latitude clouds where there are sufficient background stars to assess the dust content in the foreground clouds. Due to optical depth and depletion effects, molecular gas surveys (e.g., CO) are poor tracers of the densest parts of molecular clouds. Instead, the best probe of molecular cloud structures from the diffuse

cloud material to the small prestellar cores and the entire star formation process is from thermal dust emission of cold dust grains. We briefly summarize several representative (sub)mm continuum surveys in *Table 1*.

Table 1: **List of representative (sub)millimeter continuum surveys in the Galaxy**

Survey	Bands	Angular resolution	Survey region (°)	Sky Coverage	rms (mJy/beam)
BGPS/CSO	1.1 mm	33″	$-10.5 < l < 90.5, \lvert b\rvert < 0.5 - 1.5$	170 deg^2	11-53
ATLASGAL/APEX	870 μm	17″.5	$-80 < l < 60, \lvert b\rvert < 1 - 2$	∼400 deg^2	40-50
Hi-GAL/Herschel	70-500 μm	5″-35″	$-180 < l < 180, \lvert b\rvert < 1$	∼720 deg^2	
GBS/Herschel	70-500 μm	5″-35″	Gould Belt clouds	∼160 deg^2	
SASSy/JCMT	850 μm	14″.1	$60 < l < 240, \lvert b\rvert < 2$	∼720 deg^2	25-40
JPS/JCMT	850 μm	14″.4	$7 < l < 63, \lvert b\rvert < 1$	∼50 deg^2	8.4
GBS/JCMT	450-850 μm	7″.5-14″.5	Gould Belt clouds	∼24 deg^2	5
SCOPE	850 μm	14″.1	1235 Planck Galactic Cold Clumps	∼50 deg^2	6-10
Planck	0.35-10 mm	∼5′	All sky	∼41253 deg^2	

2.1 Galactic Plane surveys

The Herschel infrared Galactic Plane Survey (Hi-GAL, 22) observed the entire plane in five continuum bands between 70 μm and 500 μm. This survey provides the far-infrared and submillimeter continuum data to conduct self-consistent measurements of dust temperature and dust mass throughout the entire Galactic Plane, from the CMZ to the outer most regions of the Galaxy. Hi-GAL DR1 catalogues of the inner Milky Way contain 123210, 308509, 280685, 160972, and 85460 compact sources in the five bands (23). Elia et al. (2017; (24)) studied the physical parameters of those compact sources with respect to Galactic longitude and their association with spiral arms. They found only minor or no differences between the average evolutionary status of sources in the fourth and first Galactic quadrants, or between 'on-arm' and 'interarm' positions. They also found that the surface density of sources increases as they evolve from prestellar to protostellar, but decreases again in the majority of the most evolved clumps.

The Bolocam Galactic Plane Survey (BGPS) is a 1.1 mm continuum survey at 33" effective resolution of 170 deg^2 of the Galactic Plane visible from the northern hemisphere (25). It was conducted with the Bolocam instrument on the 10.4 m Caltech Submillimeter Observatory. The survey has detected approximately 8600 clumps over the entire area to a limiting non-uniform 1σ noise level in the range 11-53 mJy beam^{-1} in the inner Galaxy (26; 7). The majority of BGPS sources are molecular clumps. These clumps are large dense subregions in molecular clouds with supersonic turbulence (27) that are linked to cluster formation (26). (28) identified a subsample of 2223 (47.5%) starless clump candidates (SCCs) from BGPS objects and found that >75% of SCCs with known distances appear gravitationally bound.

The APEX Telescope Large Area Survey of the Galaxy (ATLASGAL) is one of the largest and most sensitive (rms∼40 to 50 mJy beam^{-1}) ground-based submillimetre (870 μm) surveys of the inner Galactic Plane (29). The ATLASGAL Compact Source Catalogue (CSC; 30; 31) includes ∼10,000 dense clumps. Urquhart et al. (2018; (32)) found that the vast majority of the detected clumps are capable of forming high-mass stars and 88 per cent are already associated with star formation at some level. They also found that all of the clumps are tightly correlated with the mid-plane of the Galaxy with a scale height of ∼26 pc. Li et al. (2016; (33)) found that almost 70% of the total 870 μm flux associated with the coherent structures in ATLASGAL survey resides in filaments. They also found that these filamentary structures are tightly correlated with the spiral arms in longitude and velocity, and that their semi-major axis is preferentially aligned parallel to the Galactic mid-plane, and therefore with the direction of large-scale Galactic magnetic field (33).

The James Clerk Maxwell Telescope (JCMT) Plane Survey (JPS; 34; 35) was originally planned to observe the entire Galactic Plane, but was scaled back to be a targeted, yet unbiased survey of the Inner Galactic Plane. The survey strategy consisted of observing six equally spaced fields of approximately 5° in longitude, 1°.7 in latitude centred at longitudes of l = 10°, 20°, 30°, 40°, 50°, and 60° and a latitude of b=0°. The rms obtained was at least 8.42 mJy beam^{-1}. A compact-source catalogue was produced for the JPS (34) resulting in 7813 sources, with 95 per cent completeness limits estimated to be 40 mJy beam^{-1} and 300 mJy for the peak and integrated flux densities, respectively. The increased resolution of the JPS survey breaks up sources in the ATLASGAL survey, allowing for a more accurate identification of cold, dense, star-forming clumps. Using the JPS 850 μm-continuum images in a larger-scale study, maps of the dense-gas mass fraction were produced, and a power-spectrum analysis found increases on the scales of individual molecular clouds (Eden et al., in preparation). Looking at individual regions, the JPS data finds that W43 appears to be a younger star-formation source than the rest of the Milky Way (35). The star-forming regions of W49 and W51 were

found to have consistent clump-mass functions but the luminosity function of W49 was found to be flatter, indicating it may be a candidate starburst region (36). Star-forming clumps were also found to be more centrally concentrated than those not housing a YSO, indicating that star formation is altering the morphology of a clump (34).

The SCUBA-2 Ambitious Sky Survey (SASSy;Thompson et al., in preparation; 37; 38) at the JCMT was originally designed as an all-sky survey with a goal of mapping the entire sky visible from the JCMT at a consistent rms. However, as with the JPS, this goal was scaled back and resulted in two surveys of the Outer Galaxy, SASSy-Perseus and SASSy-Outer-Galaxy with rms values of 25-40 mJy beam^{-1}. The combined surveys contain 3138 sources and provides a nice complement to the ATLASGAL survey that has similar sensitivity limits in the longitude range $300^\circ < l < 60^\circ$ (30; 31). A recent SASSy result extended the above results to greater Galactocentric radii, looking at the star-formation efficiency in the Outer Galaxy. They find that the star-formation efficiency decreases with distance from the CMZ (39), in contrast to previous studies looking at nearby clouds that found a constant star formation efficiency.

2.2 Gould Belt Clouds

Herschel/GBS is an extensive imaging survey of the densest portions of the Gould Belt with SPIRE at 250-500 μm and PACS at 110-170 μm. The main findings of Herschel/GBS are: (1) Herschel reveals a "universal" filamentary structure in the cold ISM (10, and references therein); (2) more than 70% of the prestellar cores and embedded protostars identified with Herschel are found within the densest filaments, i.e., those with column densities exceeding $\sim 7 \times 10^{21}$ cm^{-2} (10, and references therein); (3) the prestellar core mass function is very similar in shape to the stellar initial mass function (10; 11).

The JCMT Gould Belt Survey (GBS) was one of the first large legacy programs approved at the JCMT. With the aim of characterizing nearby star formation, the GBS utilized hundreds of hours to map thermal dust emission at 850 μm, as well as line emission over a more focused area, within nearby molecular clouds up to 500 pc in distance. Science topics addressed by the survey include the evolution of dust grains (e.g., 40), the virial properties of dense cores (e.g., 41), the influence of protostellar heating on dense cores (e.g., 42), the clustering properties of dense cores (e.g., 43), and the properties of filamentary structure (e.g., 44). Work on a final GBS catalogue of star-forming cores in Gould Belt clouds is ongoing and will be published in 2020. The GBS data are also providing an important dataset for a wide variety of other large surveys including the BISTRO polarization survey (45), the Green Bank Ammonia Survey (46), and the JCMT Transient Survey (47), as well as individual PI-led surveys such as an ALMA search for substructure within dense cores in the Ophiuchus molecular cloud (48).

2.3 The SCOPE survey of Planck Galactic Cold Clumps

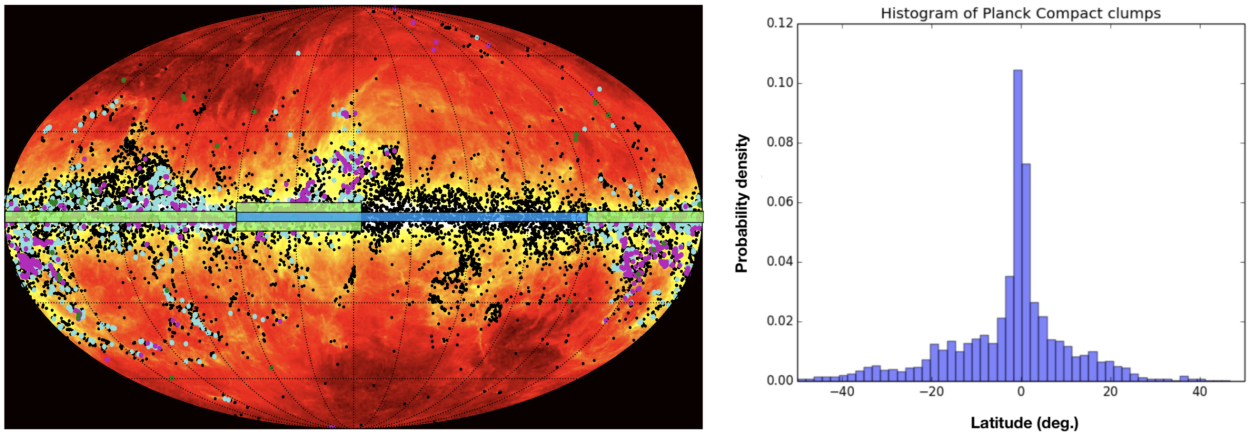

Figure 2: *Left:* All-sky distribution of the 13188 PGCC sources (black dots), the 2000 selected PGCC sources in the TOP survey (blue dots) and the 1200 PGCCs selected in the SCOPE survey overlaid on the 857 GHz Planck map. The green box outlines the sky coverage of the proposed JCMT Galactic Plane survey with the new 850 μm camera. The blue box outline the sky coverage of the ATLASGAL survey. *Right:* Distribution of Planck compact sources at 353 GHz as a function of Galactic latitude.

Planck is the third generation mission to measure the anisotropy of the cosmic microwave background (CMB), and it observed the sky in nine frequency bands (the 30, 44, 70, 100, 143, 217, 353, 545, and 857 GHz bands). The high frequency channels of Planck cover the peak thermal emission frequencies of dust colder than 14 K (49; 50),

indicating that Planck could probe the coldest parts of the ISM. There are 13188 cataloged Planck galactic cold clumps (PGCCs), which spread across the whole sky, i.e., from the Galactic plane to high latitudes, following the spatial distribution of the main molecular cloud complexes. The low dust temperature (<14 K) of PGCCs makes them likely to be pre-stellar objects or at the earliest stages of protostellar collapse (49; 50). The SCUBA-2 Continuum Observations of Pre-protostellar Evolution survey (SCOPE) is a legacy survey using SCUBA-2 at the JCMT to survey ∼1000 PGCCs at 850 μm at higher resolution than what can be obtained with Planck, aiming to conduct of census of cold dense cores in widely different environments (see left panel of Figure 2; 51; 52). SCOPE has resolved the PGCCs into more than 3000 dense cores, many of which are located in high-latitude ($|b| > 10^{\circ}$) or low density ($N < 5 \times 10^{21}$ cm^{-2}) clouds (52). Follow-up observations of the dense cores discovered in the SCOPE survey suggest that most of them are either starless cores or very young Class 0/I objects (53; 54; 55; 56), representing the earliest phases in pre-/proto-stellar evolution.

2.4 The need of new Galactic (sub)mm continuum surveys

The aforementioned previous surveys were limited by either low resolution (like Planck) or poor sensitivity (like BGPS, ATLASGAL, SASSy). Except for the all-sky Planck survey, all other previous continuum surveys have small sky coverage (<2% of the sky) and do not include high latitude or mid-latitude clouds. As shown in Table 1, most of the previous (sub)mm continuum surveys focused on Gould Belt clouds or the inner Galactic Plane with either limited coverage or limited resolution. A major portion of the Galaxy (e.g. intermediate-latitude or high-latitude clouds) has not been fully explored at (sub)millimeter bands with appropriate sensitivity and high angular resolution ($\times 10''$), which limits our knowledge of star formation and cloud evolution across the whole Galaxy.

These well studied Gould Belt clouds do not broadly represent the star formation activity seen in regions like metal poor high-latitude clouds, the CMZ of the Milky Way, or starburst galaxies, where densities, temperatures, and star formation efficiencies can be vastly different. There are still fundamental aspects of the initial conditions for star formation that remain unaddressed, which include but are not limited to:

• On small scales, how and where do prestellar cores (i.e. future star forming sites) form? Specifically, can prestellar cores form in less dense and metal poor high-latitude clouds, or short lived cloudlets? What is the interplay between turbulence, magnetic field, gravity, kinematics and external pressure in prestellar core formation and evolution? Is there really a "universal" density threshold or core mass function for core/star formation?

• On larger scales, how common are filaments in molecular clouds? How do they form? How do they fragment and what is their role in producing prestellar cores? Do filaments have a universal width?

• On cloud scales or galaxy scales, how do molecular clouds form from the diffuse atomic gas? Is there a universal dense-gas star formation law for clouds in various environments (e.g. spiral arms, interarm regions, high latitude, expanding HII regions, supernova remnants)? What factors determine and regulate star formation rates and efficiencies?

To address these questions, a census of a broader representation of star formation in the Galaxy is needed. That broader representation requires going beyond the dense gas in nearby clouds or toward the Galactic Plane to the entire spectrum of molecular clouds throughout the Galaxy. We want to compare and contrast star formation in clouds located in the CMZ, in spiral arms, in interarm regions, at high latitudes, and at high Galactocentric radii to span a range of Interstellar Radiation Fields (ISRFs), metallicities, pressures, and ionizations.

We have realized that the present SCUBA-2 instrument lacks the sensitivity and speed to conduct such large, unbiased surveys of all of these cloud regimes. Therefore, a new camera with much improved sensitivity and faster mapping speed is highly demanded.

3 The Next Decade

3.1 The new 850 μm MKID camera

The detector technology for the next generation 850 μm wide field camera is Microwave Kinetic Inductance Detectors (MKID), with intrinsic polarization mapping capability. These devices are much simpler to manufacture and operate than the TES detectors used in SCUBA-2 and are already being deployed on other large mm/submm telescopes such as the IRAM 30-m Telescope. The full field of view (FoV) of the new 7,272 MKID array will be 12 arcmin in diameter (almost twice as large as SCUBA-2). The focal plane will be filled with 3,636 1 fλ spaced feedhorn coupled pixels. More details of the new instrument can be found on the JCMT webpage.[3]

[3] https://www.eaobservatory.org/jcmt/instrumentation/continuum/

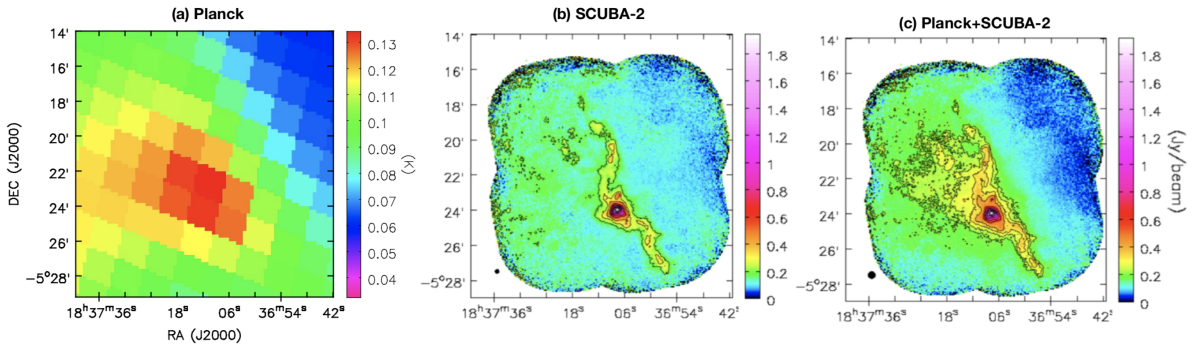

Figure 3: Images for PGCC G26.53+0.17 (51) (a) Planck 353 GHz data only (b) SCUBA-2 850 μm data only (c) Combined SCUBA-2 and Planck data

3.1.1 The capability of the new camera: Much faster scan speeds

The per-pixel sensitivity on the sky of the new camera will be a factor of 3 more sensitive than SCUBA-2. Between a larger FoV that almost doubles the exposure area in a larger Pong map and the more sensitive pixels, the new instrument will be 10$\times$ faster than SCUBA-2 to achieve a given sensitivity in a map. In the best case, the mapping speed can be increased by a factor of 20. The much improved mapping speeds of the new camera will enable deep and extensive continuum surveys (see section 3.2) within reasonable telescope time.

3.1.2 The capability of the new camera: Recovering more extended emission

The new camera will have the ability to recover more extended emission than the current camera SCUBA-2 benefiting from its improved pixel sensitivity, larger FOV and much faster scan speed. These data can be combined with Planck observations at 353 GHz in the Fourier domain to recover emission from all scales of molecular clouds (57). Panel (c) in Figure 3 presents one example of combining Planck data with SCUBA-2 data obtained from the SCOPE survey (51). The combined data resolves the Planck clump (panel a) and recovers more extended emission than the SCUBA-2 data alone (panel b). With the ability to recover more extended emission with the new camera, the process to recover the extended emission will be more accurate in the planned surveys mentioned in section 3.2.

3.1.3 The capability of the new camera: Intrinsic polarization mapping capability

Each pixel of the new camera is comprised of two detectors that measure orthogonal linear polarization. By careful choice of the orientation of pixels across the focal plane, it will be possible to determine all Stokes parameters from a single scan observation, without the need for a rotating half-wave plate. This would enable us to conduct dust polarization observations simultaneously in the proposed surveys. In contrast, the aforementioned previous surveys except the Planck survey did not have polarization information. Limited by its poor resolution, Planck did not provide resolved polarization information within clouds.

The proposed surveys in Section 3.2 have desired sensitivities of 2-10 mJy beam^{-1} in Stokes I to detect faint dust emission. This sensitivity will also capture dust polarization toward the bright filaments, clumps, and cores at the same time. Panels (a) and (b) of Figure 4 show the results of SCUBA-2/POL-2 observations of one bright filamentary cloud and one high-mass star-forming clump, respectively, whose mean surface brightness is $\sim$1 Jy beam^{-1}. The on-source time of those observations is $\sim$2 hrs with a sensitivity in Stokes I of $\sim$5-10 mJy beam^{-1}. The new camera will achieve comparable sensitivity and map coverage in about 10 minutes of on-source integration. As shown in Panel (c) of Figure 4, hundreds of clumps discovered in the previous JPS and ATLASGAL surveys show peak flux densities larger than 1 Jy beam^{-1}. Those clumps can be easily detected in polarization observations assuming polarization fractions of 1%. It is also possible to detect polarization in less bright sources by smoothing the Q and U maps.

3.2 New Galactic continuum surveys

Benefiting from its improved pixel sensitivity, larger FOV, much faster scan speed and intrinsic polarization mapping capability, extensive Galactic continuum surveys with the new camera will not only detect the entire spectrum of molecular clouds throughout the Galaxy but also provide their resolved polarization information. To this end, we propose the following Galactic continuum surveys with the new camera in next decade.

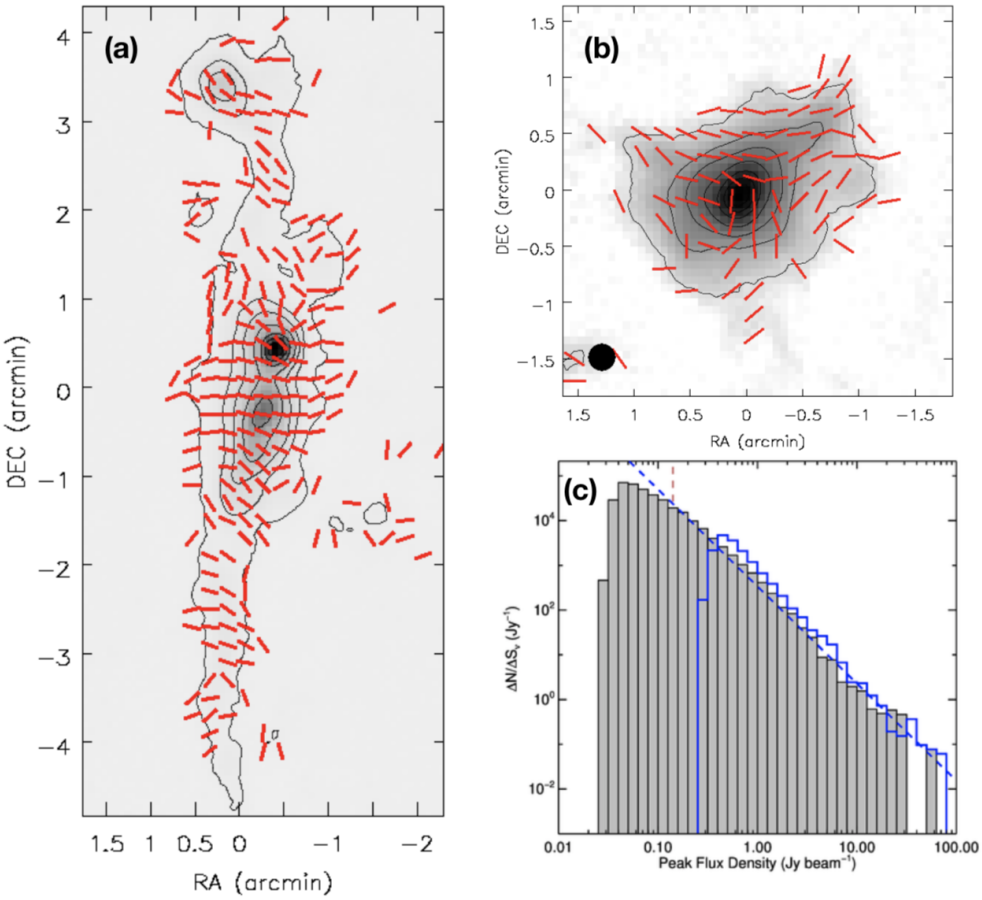

Figure 4: *(a):* JCMT POL-2 observations of a bright filamentary cloud (Soam, A. et al., 2019, submitted). The line segments show the inferred magnetic field morphology with a $S/N > 2$. The contours are [0.1, 0.5, 1, 2, 4, 8] Jy beam^{-1}. *(b):* JCMT POL-2 observations of a bright high-mass star-forming clump (58). The segments and contours are the same as in panel (a). *(c):* Peak flux density distributions for the JPS (grey-filled histogram) compared to the ATLASGAL distribution (blue histogram) (34). The dashed line indicates the least-squares fit to the JPS distribution.

3.2.1 An unbiased continuum survey of the local volume

The sky visible to the JCMT is a declination band in the range $-30^\circ \leq \delta \leq +70^\circ$, encompassing some 18,000 square degrees. A blind deep survey, however, is still impossible with the new camera.

Fortunately, the Planck satellite has done an all-sky multi-band continuum survey and discovered thousands of compact sources (59). There are 9677 Planck compact objects detected at 353 GHz that are visible to the JCMT. This sample contains both cold and warm/hot Galactic clumps. These objects are not included in the proposed Galactic Plane survey in Section 3.2.2 and represent an unbiased sample of (sub)mm continuum sources distributed in the local volume ($<$2 kpc) (50; 59). The Planck catalogue serves as a nice guide which makes the survey of dense cores in all the visible local volume ($<$1-2 kpc) possible.

The Planck observations of these objects, however, are at very low resolution ($\sim$5 arcmin) and do not resolve the structure of these sources. With the new camera, all 9677 of these objects can be followed up at 14-arcsec resolution (over a factor of 20 improvement) in CV Daisy mapping mode[4] with a total time of $\sim$320 hrs and a typical rms level of 5 mJy beam^{-1}. In addition, the larger FoV of the new camera will make the CV Daisy scan naturally larger on the sky and it will extend the central area from 3 arcmin (SCUBA-2) to at least 6 arcmin, where the map will have uniform coverage.

[4] https://www.eaobservatory.org/jcmt/instrumentation/continuum/scuba-2/observing-modes/#CV_Daisy

Pilot HI observations of PGCCs indicate that half of them show narrow self-absorption features in HI spectra (see the right panel of Figure 1; Tang et al. 2019, submitted). These objects are particularly interesting for studying the formation and evolution of molecular clouds (1). We plan to conduct a deep (2 mJy beam^{-1}) continuum survey of 1000 PGCCs that have been observed with ^{12}CO/^{13}CO J=1-0 lines in the TOP-SCOPE survey (51) and will be mapped in HI with the Five-hundred-meter Aperture Spherical radio Telescope (FAST). At this high sensitivity, we can detect dust emission in the warm ($\sim$40 K) and low density (A_V $\sim$1; or 850 μm flux of $\sim$10 mJy) cloud peripheries, where HI is converted to H_2. With the new camera, we need 0.2 hrs per source to achieve the desired sensitivity. The total time to complete this survey is about 200 hrs in Band 3 weather or 130 hrs in Band 2 weather.

Besides the surveys of Planck clumps, a re-visit to the Gould Belt cloud with the new camera is also very meaningful considering no polarization information provided by either Herschel GBS or JCMT GBS. Herschel GBS[5] has a much larger sky coverage (160 deg^2) than the previous JCMT GBS (50 deg^2). The clouds in Herschel GBS span a range of physical conditions, from active, cluster-forming complexes to quiescent regions with lower star formation activity. A future generation JCMT GBS could cover all clouds in the Herschel fields with a high and uniform sensitivity ($\sim$5 mJy beam^{-1}). With the new camera, it will take about 400 hrs in Band 3 weather or 250 hrs in Band 2 weather to complete a survey of the whole 160 deg^2 Herschel fields with the Pong 7200 mapping mode. The large spatial dynamic range of the proposed JCMT GBS in conjunction with Herschel GBS will probe the link between large-scale diffuse structures and dense structures (e.g., filaments or self-gravitating cores).

3.2.2 Galactic Plane survey

Observations of external galactic systems, especially grand-design structures, have shown that the majority of star formation is occurring within the spiral arms of galaxies, galaxies like the Milky Way (e.g., 31). The spiral arm structure within the Milky Way is confined to what is classically thought of as the Galactic Plane, although there is evidence of spiral arms leaving the mid-plane at extended Galactocentric radii (60). To understand star formation within the Milky Way and the extended Universe, we need to first understand how Galactic environments, ranging from large-scale features such as the spiral arms and the Galactic Bar to local triggering agents such as HII regions or star formation feedback, impact the star-formation process.

As shown in the right panel of Figure 2, a large number of Planck compact objects are distributed beyond the Galactic Plane. These sources indicate that star formation activities may occur in mid-latitude or high-latitude clouds. There are also many clumps at latitudes $1^\circ < |b| < 2^\circ$ that were not covered by previous Galactic Plane surveys. Filling in these gaps was the original intent of the "JPS" and "SASSy" surveys before being descoped. A new high resolution ($\sim$10 arcsec) and sensitivity ($<$10 mJy beam^{-1}) sub-millimeter Galactic Plane survey is needed to resolve the confusion in Hershel/Hi-GAL/Planck data and to detect objects in regions beyond the previous Galactic Plane surveys.

The new high-sensitivity MKID camera makes a "full" and wider Galactic Plane survey possible. One plausible Galactic Plane survey strategy is to observe the inner Plane ($-5^\circ < l < 60^\circ$) with a wide latitude range ($|b| < 5^\circ$; as wide as the Milky Way Imaging Scroll Painting (MWISP) project[6]) and to observe the remaining Plane ($60^\circ < l < 240^\circ$) visible to the JCMT with a narrower latitude range ($|b| < 2^\circ$). The sky coverage of this survey is outlined by the green box in the left panel of Figure 2. The desired rms level is $\sim$10 mJy beam^{-1} at 850 μm or a 3σ mass sensitivity of $\sim$0.1 $M_\odot$ for a point source out to a distance of 1 kpc assuming 20 K dust with a β of 2. With the new camera, it takes $\sim$900 hrs in Band 3 weather or $\sim$600 hrs in Band 2 weather to complete such a sensitive Galactic Plane survey with the Pong 7200 mapping mode[7].

3.2.3 Science goals of the new Galactic continuum surveys

The above surveys will provide a complete and unbiased census of molecular clouds, filaments, and dense clumps/cores in the local volume and in the Galactic Plane. JCMT has better resolution than the Herschel/SPIRE instrument and the new camera has ability to recover more extended emission than SCUBA-2. This will help resolve the widths of Herschel filaments in nearby ($<$1 kpc) clouds. Adding 850 μm data in SED fits will better constrain temperature and density profiles for dense filaments and also dense cores. From these surveys, we will thoroughly investigate star formation across the Galaxy, adressing the following goals:

* To build a complete database of molecular clouds in the Milky Way. To analyze molecular cloud distributions and properties across a range of Galactic environments (e.g. spiral arms, interarms, median/high latitude, expanding HII regions, supernova remnants). To compare Galactic molecular clouds with molecular clouds in

[5] http://www.herschel.fr/cea/gouldbelt/en/

[6] http://english.dlh.pmo.cas.cn/ic/in/

[7] https://www.eaobservatory.org/jcmt/instrumentation/continuum/scuba-2/observing-modes/#2-degree_Pong_map

nearby galaxies that are resolved in interferometric observations (e.g. ALMA). By combining JCMT data with Planck data, we will be able to detect faint and extended dust emission at the warm and low density cloud peripheries, where HI is converted to H_2. **Through a combined analysis of HI narrow self-absorption, CO emission, and dust emission, we will study the formation and evolution of molecular clouds.**

* The dense gas fraction in molecular clouds can be estimated from the 850 μm flux ratio between the JCMT data (that mainly traces dense gas) and the JCMT+Planck combined data (that recovers extended gas emission). Then we will evaluate whether extended or diffuse emission (non star forming gas) dominates the 850 μm flux in molecular clouds, and how does the dense gas fraction vary as a function of latitudes and longitudes. In particular, we will check whether or not there is a universal relation between star/core formation rate and surface mass density above a density threshold (or dense gas star formation law).
* In contrast to Herschel, JCMT observations have higher resolution and less confusion, and thus can more easily resolve filament widths and profile shapes. For example, assuming a typical filament width of 0.1 pc, the new camera will spatially resolve filaments beyond 1 kpc, whereas Herschel observations are generally restricted to 500 pc. In conjunction with molecular line Galactic Plane surveys (e.g., CHIMPS2[8], FUGIN[9], MWISP), we will conduct a complete census of velocity-coherent dense filaments in the Galactic Plane. We will detect filaments across the Galaxy and determine how universal they are in the ISM and how they are distributed relative to large-scale Galactic features (e.g., spiral arms and shells).
* For resolved filaments in nearby ($<$1 kpc) clouds, we will investigate the distributions of their masses, line masses, lengths and widths. We will study how these filament parameters change in different clouds. **Particularly, we will determine whether or not there is a characteristic width ($\sim$0.1 pc) of filamentary substructures in the ISM.**
* To investigate the role of magnetic fields in filament formation by studying the relative orientations between filaments and large-scale magnetic fields, and how the field structures change within filaments. To check whether magnetic fields are important in supporting filaments or clumps/cores against gravitational collapse. To study the fragmentation process of filaments and to determine which physical processes (magnetic fields, turbulence or gravity) dominate their fragmentation.
* To construct a complete sample of dense cores (with sizes of $\sim$0.1 pc) in clouds in the local volume ($<$2 kpc). We will then thoroughly study how core/clump mass functions and the core/clump formation efficiency change in different kinds of cloud. In particular, the new camera will be able to detect fainter cores with smoother structures in nearby clouds (e.g., Taurus) that were missed in previous SCUBA-2 surveys (e.g. SCOPE survey (51)). **The new surveys will provide a complete sample of dense cores for studying core evolution from very flattened starless phase to the centrally peaked protostellar phase.**
* To construct a complete catalogue of high-mass clumps ($M > 100\ M_\odot$, size$\sim$1 pc) throughout the whole Galactic Plane. To derive the clump mass function, clump formation efficiency and the fraction of clustered vs isolated high-mass core (or star) formation across the Galaxy. To evaluate the gravitational stability of a large ($\times$1000) sample of high-mass clumps through virial analysis by considering all supports from magnetic fields, turbulence and thermal pressure.
* To detect (sub)mm transient objects through multi-epoch observations (61).
* In particular, these surveys will provide a unique complete catalogue of dense cores/clumps for follow-up high-resolution molecular line/dust continuum studies with other mm/submm telescopes and interferometers (e.g., ALMA).

References

[1] Pei Zuo, Di Li, J. E. G. Peek, and others. Catching the Birth of a Dark Molecular Cloud for the First Time. *The Astrophysical Journal*, 867(1):13, Nov 2018.

[2] Amanda Heiderman, II Evans, Neal J., Lori E. Allen, Tracy Huard, and Mark Heyer. The Star Formation Rate and Gas Surface Density Relation in the Milky Way: Implications for Extragalactic Studies. *The Astrophysical Journal*, 723(2):1019–1037, Nov 2010.

[3] Charles J. Lada, Marco Lombardi, and João F. Alves. On the Star Formation Rates in Molecular Clouds. *The Astrophysical Journal*, 724(1):687–693, Nov 2010.

[4] Charles J. Lada, Jan Forbrich, Marco Lombardi, and João F. Alves. Star Formation Rates in Molecular Clouds and the Nature of the Extragalactic Scaling Relations. *The Astrophysical Journal*, 745(2):190, Feb 2012.

[8] https://www.eaobservatory.org/jcmt/science/large-programs/chimps2/

[9] https://nro-fugin.github.io

[5] II Evans, Neal J., Amanda Heiderman, and Nalin Vutisalchavakul. Star Formation Relations in Nearby Molecular Clouds. *The Astrophysical Journal*, 782(2):114, Feb 2014.

[6] Nalin Vutisalchavakul, II Evans, Neal J., and Mark Heyer. Star Formation Relations in the Milky Way. *The Astrophysical Journal*, 831(1):73, Nov 2016.

[7] Adam Ginsburg, Jason Glenn, Erik Rosolowsky, and others. The Bolocam Galactic Plane Survey. IX. Data Release 2 and Outer Galaxy Extension. *The Astrophysical Journal Supplement Series*, 208(2):14, Oct 2013.

[8] S. N. Longmore, J. Bally, L. Testi, and others. Variations in the Galactic star formation rate and density thresholds for star formation. *Monthly Notices of the Royal Astronomical Society*, 429(2):987–1000, Feb 2013.

[9] Paola Caselli. Observational Studies of Pre-Stellar Cores and Infrared Dark Clouds. In José Cernicharo and Rafael Bachiller, editors, *The Molecular Universe*, volume 280 of *IAU Symposium*, pages 19–32, Dec 2011.

[10] P. André, J. Di Francesco, D. Ward-Thompson, and others. From Filamentary Networks to Dense Cores in Molecular Clouds: Toward a New Paradigm for Star Formation. In Henrik Beuther, Ralf S. Klessen, Cornelis P. Dullemond, and Thomas Henning, editors, *Protostars and Planets VI*, page 27, Jan 2014.

[11] V. Könyves, Ph. André, A. Men'shchikov, and others. A census of dense cores in the Aquila cloud complex: SPIRE/PACS observations from the Herschel Gould Belt survey. *Astronomy & Astrophysics*, 584:A91, Dec 2015.

[12] Enrique Vazquez-Semadeni. Hierarchical Structure in Nearly Pressureless Flows as a Consequence of Self-similar Statistics. *The Astrophysical Journal*, 423:681, Mar 1994.

[13] P. Palmeirim, Ph. André, J. Kirk, and others. Herschel view of the Taurus B211/3 filament and striations: evidence of filamentary growth? *Astronomy & Astrophysics*, 550:A38, Feb 2013.

[14] Pak Shing Li and Richard I. Klein. Magnetized interstellar molecular clouds - II. The large-scale structure and dynamics of filamentary molecular clouds. *Monthly Notices of the Royal Astronomical Society*, 485(4):4509–4528, Jun 2019.

[15] N. L. J. Cox, D. Arzoumanian, Ph. André, and others. Filamentary structure and magnetic field orientation in Musca. *Astronomy & Astrophysics*, 590:A110, May 2016.

[16] N. Peretto, Ph. André, V. Könyves, and others. The Pipe Nebula as seen with Herschel: formation of filamentary structures by large-scale compression? *Astronomy & Astrophysics*, 541:A63, May 2012.

[17] Benjamin Wu, Jonathan C. Tan, Fumitaka Nakamura, and others. GMC Collisions as Triggers of Star Formation. II. 3D Turbulent, Magnetized Simulations. *The Astrophysical Journal*, 835(2):137, Feb 2017.

[18] G. V. Panopoulou, I. Psaradaki, R. Skalidis, K. Tassis, and J. J. Andrews. A closer look at the 'characteristic' width of molecular cloud filaments. *Monthly Notices of the Royal Astronomical Society*, 466(3):2529–2541, Apr 2017.

[19] Sayantan Auddy, Shantanu Basu, and Takahiro Kudoh. A Magnetic Ribbon Model for Star-forming Filaments. *The Astrophysical Journal*, 831(1):46, Nov 2016.

[20] Christoph Federrath. On the universality of interstellar filaments: theory meets simulations and observations. *Monthly Notices of the Royal Astronomical Society*, 457(1):375–388, Mar 2016.

[21] Rowan J. Smith, Simon C. O. Glover, and Ralf. S. Klessen. On the nature of star-forming filaments - I. Filament morphologies. *Monthly Notices of the Royal Astronomical Society*, 445(3):2900–2917, Dec 2014.

[22] S. Molinari, B. Swinyard, J. Bally, and others. Clouds, filaments, and protostars: The Herschel Hi-GAL Milky Way. *Astronomy & Astrophysics*, 518:L100, Jul 2010.

[23] S. Molinari, E. Schisano, D. Elia, and others. Hi-GAL, the Herschel infrared Galactic Plane Survey: photometric maps and compact source catalogues. First data release for the inner Milky Way: +68 $\geq$ l $\geq$ -70. *Astronomy & Astrophysics*, 591:A149, Jul 2016.

[24] Davide Elia, S. Molinari, E. Schisano, and others. The Hi-GAL compact source catalogue - I. The physical properties of the clumps in the inner Galaxy (-71.0 < ℓ < 67.0). *Monthly Notices of the Royal Astronomical Society*, 471(1):100–143, Oct 2017.

[25] James E. Aguirre, Adam G. Ginsburg, Miranda K. Dunham, and others. The Bolocam Galactic Plane Survey: Survey Description and Data Reduction. *The Astrophysical Journal Supplement Series*, 192(1):4, Jan 2011.

[26] Erik Rosolowsky, Miranda K. Dunham, Adam Ginsburg, and others. The Bolocam Galactic Plane Survey. II. Catalog of the Image Data. *The Astrophysical Journal Supplement Series*, 188(1):123–138, May 2010.

[27] Yancy L. Shirley, Timothy P. Ellsworth-Bowers, Brian Svoboda, and others. The Bolocam Galactic Plane Survey. X. A Complete Spectroscopic Catalog of Dense Molecular Gas Observed toward 1.1 mm Dust Continuum Sources with 7.5 <= l <= 194. *The Astrophysical Journal Supplement Series*, 209(1):2, Nov 2013.

[28] Brian E. Svoboda, Yancy L. Shirley, Cara Battersby, and others. The Bolocam Galactic Plane Survey. XIV. Physical Properties of Massive Starless and Star-forming Clumps. *The Astrophysical Journal*, 822(2):59, May 2016.

[29] F. Schuller, K. M. Menten, Y. Contreras, and others. ATLASGAL - The APEX telescope large area survey of the galaxy at 870 μm. *Astronomy & Astrophysics*, 504(2):415–427, Sep 2009.

[30] Y. Contreras, F. Schuller, J. S. Urquhart, and others. ATLASGAL - compact source catalogue: 330 < ℓ < 21. *Astronomy & Astrophysics*, 549:A45, Jan 2013.

[31] J. S. Urquhart, T. Csengeri, F. Wyrowski, and others. ATLASGAL - Complete compact source catalogue: 280<ℓ< 60. *Astronomy & Astrophysics*, 568:A41, Aug 2014.

[32] J. S. Urquhart, C. König, A. Giannetti, and others. ATLASGAL - properties of a complete sample of Galactic clumps. *Monthly Notices of the Royal Astronomical Society*, 473(1):1059–1102, Jan 2018.

[33] Guang-Xing Li, James S. Urquhart, Silvia Leurini, and others. ATLASGAL: A Galaxy-wide sample of dense filamentary structures. *Astronomy & Astrophysics*, 591:A5, Jun 2016.

[34] D. J. Eden, T. J. T. Moore, R. Plume, and others. The JCMT Plane Survey: first complete data release - emission maps and compact source catalogue. *Monthly Notices of the Royal Astronomical Society*, 469(2):2163–2183, Aug 2017.

[35] T. J. T. Moore, R. Plume, M. A. Thompson, and others. The JCMT Plane Survey: early results from the ℓ = 30 field. *Monthly Notices of the Royal Astronomical Society*, 453(4):4264–4277, Nov 2015.

[36] D. J. Eden, T. J. T. Moore, J. S. Urquhart, and others. Extreme star formation in the Milky Way: luminosity distributions of young stellar objects in W49A and W51. *Monthly Notices of the Royal Astronomical Society*, 477(3):3369–3382, Jul 2018.

[37] Todd MacKenzie, Filiberto G. Braglia, Andy G. Gibb, and others. A pilot study for the SCUBA-2 'All-Sky' Survey. *Monthly Notices of the Royal Astronomical Society*, 415(2):1950–1960, Aug 2011.

[38] Will Nettke, Douglas Scott, Andy G. Gibb, and others. The SCUBA-2 Ambitious Sky Survey: a catalogue of beam-sized sources in the Galactic longitude range 120-140. *Monthly Notices of the Royal Astronomical Society*, 468(1):250–260, Jun 2017.

[39] J. O. Djordjevic, M. A. Thompson, J. S. Urquhart, and J. Forbrich. Beyond the solar circle - trends in massive star formation between the inner and outer galaxy. *Monthly Notices of the Royal Astronomical Society*, 487(1):1057–1071, Jul 2019.

[40] S. I. Sadavoy, J. Di Francesco, D. Johnstone, and others. The Herschel and JCMT Gould Belt Surveys: Constraining Dust Properties in the Perseus B1 Clump with PACS, SPIRE, and SCUBA-2. *The Astrophysical Journal*, 767(2):126, Apr 2013.

[41] K. Pattle, D. Ward-Thompson, J. M. Kirk, and others. The JCMT Gould Belt Survey: first results from the SCUBA-2 observations of the Ophiuchus molecular cloud and a virial analysis of its prestellar core population. *Monthly Notices of the Royal Astronomical Society*, 450(1):1094–1122, Jun 2015.

[42] D. Rumble, J. Hatchell, R. A. Gutermuth, and others. The JCMT Gould Belt Survey: evidence for radiative heating in Serpens MWC 297 and its influence on local star formation. *Monthly Notices of the Royal Astronomical Society*, 448(2):1551–1573, Apr 2015.

[43] H. Kirk, D. Johnstone, J. Di Francesco, and others. The JCMT Gould Belt Survey: Dense Core Clusters in Orion B. *The Astrophysical Journal*, 821(2):98, Apr 2016.

[44] C. J. Salji, J. S. Richer, J. V. Buckle, and others. The JCMT Gould Belt Survey: properties of star-forming filaments in Orion A North. *Monthly Notices of the Royal Astronomical Society*, 449(2):1782–1796, May 2015.

[45] Derek Ward-Thompson, Kate Pattle, Pierre Bastien, and others. First Results from BISTRO: A SCUBA-2 Polarimeter Survey of the Gould Belt. *The Astrophysical Journal*, 842(1):66, Jun 2017.

[46] Rachel K. Friesen, Jaime E. Pineda, co-PIs, and others. The Green Bank Ammonia Survey: First Results of NH_3 Mapping of the Gould Belt. *The Astrophysical Journal*, 843(1):63, Jul 2017.

[47] Gregory J. Herczeg, Doug Johnstone, Steve Mairs, and others. How Do Stars Gain Their Mass? A JCMT/SCUBA-2 Transient Survey of Protostars in Nearby Star-forming Regions. *The Astrophysical Journal*, 849(1):43, Nov 2017.

[48] H. Kirk, M. M. Dunham, J. Di Francesco, and others. ALMA Observations of Starless Core Substructure in Ophiuchus. *The Astrophysical Journal*, 838(2):114, Apr 2017.

[49] Planck Collaboration, P. A. R. Ade, N. Aghanim, and others. Planck early results. XXIII. The first all-sky survey of Galactic cold clumps. *Astronomy & Astrophysics*, 536:A23, Dec 2011.

[50] Planck Collaboration, P. A. R. Ade, N. Aghanim, and others. Planck 2015 results. XXVIII. The Planck Catalogue of Galactic cold clumps. *Astronomy & Astrophysics*, 594:A28, Sep 2016.

[51] Tie Liu, Kee-Tae Kim, Mika Juvela, and others. The TOP-SCOPE Survey of Planck Galactic Cold Clumps: Survey Overview and Results of an Exemplar Source, PGCC G26.53+0.17. *The Astrophysical Journal Supplement Series*, 234(2):28, Feb 2018.

[52] D. J. Eden, Tie Liu, Kee-Tae Kim, and others. SCOPE: SCUBA-2 Continuum Observations of Pre-protostellar Evolution - survey description and compact source catalogue. *Monthly Notices of the Royal Astronomical Society*, 485(2):2895–2908, May 2019.

[53] Ken'ichi Tatematsu, Tie Liu, Satoshi Ohashi, and others. Astrochemical Properties of Planck Cold Clumps. *The Astrophysical Journal Supplement Series*, 228(2):12, Feb 2017.

[54] Tie Liu, Qizhou Zhang, Kee-Tae Kim, and others. Planck Cold Clumps in the λ Orionis Complex. I. Discovery of an Extremely Young Class 0 Protostellar Object and a Proto-brown Dwarf Candidate in the Bright-rimmed Clump PGCC G192.32-11.88. *The Astrophysical Journal Supplement Series*, 222(1):7, Jan 2016.

[55] Tie Liu, Pak Shing Li, Mika Juvela, and others. A Holistic Perspective on the Dynamics of G035.39-00.33: The Interplay between Gas and Magnetic Fields. *The Astrophysical Journal*, 859(2):151, Jun 2018.

[56] Hee-Weon Yi, Jeong-Eun Lee, Tie Liu, and others. Planck Cold Clumps in the λ Orionis Complex. II. Environmental Effects on Core Formation. *The Astrophysical Journal Supplement Series*, 236(2):51, Jun 2018.

[57] Yuxin Lin, Hauyu Baobab Liu, James E. Dale, and others. Cloud Structure of Three Galactic Infrared Dark Star-forming Regions from Combining Ground- and Space-based Bolometric Observations. *The Astrophysical Journal*, 840(1):22, May 2017.

[58] Tie Liu, Kee-Tae Kim, Sheng-Yuan Liu, and others. Compressed Magnetic Field in the Magnetically Regulated Global Collapsing Clump of G9.62+0.19. *The Astrophysical Journal Letters*, 869(1):L5, Dec 2018.

[59] Planck Collaboration, P. A. R. Ade, N. Aghanim, and others. Planck 2015 results. XXVI. The Second Planck Catalogue of Compact Sources. *Astronomy & Astrophysics*, 594:A26, Sep 2016.

[60] T. M. Dame and P. Thaddeus. A Molecular Spiral Arm in the Far Outer Galaxy. *The Astrophysical Journal Letters*, 734(1):L24, Jun 2011.

[61] Geumsook Park, Kee-Tae Kim, Doug Johnstone, and others. Submillimeter Continuum Variability in Planck Galactic Cold Clumps. *The Astrophysical Journal Supplement Series*, 242(2):27, Jun 2019.

SUBMILLIMETRE TRANSIENT SCIENCE IN THE NEXT DECADE

EAO SUBMILLIMETRE FUTURES PAPER SERIES, 2019

Steve Mairs[*1] • **Gregory Herczeg**[2] • **Doug Johnstone**[3] • **Jeong-Eun Lee**[4] • **Simon Coudé**[5]
Alexandra J. Tetarenko[1] • **Jenny Hatchell**[6] • **Aleks Scholz**[7] • **Bhavana Lalchand**[8] • **Wen-Ping Chen**[8]
Carlos Contreras Peña[6] • **Tim Naylor**[6] • **Kevin Lacaille**[9] • **Peter Scicluna**[10]

[1]*East Asian Observatory (JCMT) 660 N. A'ohōkū Place, Hilo, Hawai'i, USA, 96720*
[2]*Kavli Institute for Astronomy & Astrophysics, Peking University, Beijing, China*
[3]*NRC Herzberg Astronomy and Astrophysics, 5071 West Saanich Rd, Victoria, BC, V9E 2E7, Canada*
[4]*School of Space Research, Kyung Hee University, Giheung-gu Yongin-shi, Gyunggi-do, 17104, Korea*
[5]*SOFIA Science Center, USRA, NASA Ames Research Center, Moffett Field, CA, USA, 94035*
[6]*Physics and Astronomy, University of Exeter, Stocker Road, Exeter EX4 4QL, UK*
[7]*SUPA, School of Physics & Astronomy, North Haugh, St. Andrews, KY16 9SS, UK*
[8]*Graduate Institute of Astronomy, National Central University, 300 Zhongda Rd. Zhongli, Taoyuan 32001, Taiwan*
[9]*Department of Physics and Atmospheric Science, Dalhousie University, Halifax, NS, B3H 4R2, Canada*
[10]*Academia Sinica Institute of Astronomy and Astrophysics, AS/NTU Astronomy-Mathematics Building, No 1. Sec. 4 Roosevelt Rd, Taipei, Taiwan*

ABSTRACT

This white paper gives a brief summary of the time domain science that has been performed with the JCMT in recent years and highlights the opportunities for continuing work in this field over the next decade. The main focus of this document is the JCMT Transient Survey, a large program initiated in 2015 to measure the frequency and amplitude of variability events associated with protostars in nearby star-forming regions. After summarising the major accomplishments so far, an outline is given for extensions to the current survey, featuring a discussion on what will be possible with the new 850 μm camera that is expected to be installed in late 2022. We also discuss possible applications of submillimetre monitoring to active galactic nuclei, X-ray binaries, asymptotic giant branch stars, and flare stars.

1 Introduction

The initial phase of the growth of a protostar occurs steadily, driven by the gravitational infall of material in the surrounding, dusty envelope ($\sim 1000 - 10000$ AU). A protoplanetary disk ($\sim 0.1 - 100$ AU) forms early in this process [1]. Once formed, the disk channels most of the accreting material from the envelope to the protostar via a loss of angular momentum, likely due to viscous interactions and MHD instabilities. Finally, the mass is funnelled onto the protostar by the stellar magnetic field, which disrupts the disk at scales typically of order a few stellar radii [For a review on accretion processes, see 2]. Once a disk forms, the accretion rate is expected to be variable due to instabilities in both the inner and outer disk [see review by 3]. This variability in the rate of accretion has far-reaching implications for many of the most important aspects of star formation, including estimating protostellar lifetimes [4], reconciling a decades-old discrepancy between theoretical and observed brightnesses of young stars known as the "Luminosity Problem" [5, 6, 7], and describing the physical structure of the circumstellar disk that will go on to form planets [8, 9].

When a star accretes, most of the gravitational energy from the infall radius is converted into radiation [10]. Any change in the accretion rate is expected to lead to a similar change in the total luminosity of the protostar. The amplitudes and frequency of variability events associated with the changing accretion rate can inform us about the dominant physical drivers of unsteady mass accretion over time, but are virtually unconstrained in the literature. For example, bursts that last decades or even centuries suggest gravitational instabilities or processes in the outer disk, whereas short-term variability likely traces inner-disk/magnetic effects.

[*]s.mairs@eaobservatory.org

Many wide-field and all-sky monitoring optical and near-IR surveys, including VVV [11], ASAS-SN [12], Gaia alerts[2], Kepler K2 [13], WASP [14], and the Zwicky Transient Facility (ZTF, [15]; previously PTF) have made significant contributions to young star variability. Other monitoring campaigns, such as YSOVar [16], have been dedicated explicitly to monitoring star-forming regions to evaluate variability. These surveys have established the ubiquity of short-wavelength variability in optically-bright young stars, which are already nearly fully formed, but cannot probe the earliest, dominant stages of protostellar growth.

Accretion variability in the youngest sources has been challenging to study directly. While it has been inferred to be common based on population studies of bolometric temperatures and luminosities, such as the Spitzer cores-to-disks program and the Herschel HOPS survey [6, 17], at these stages the central protostar is heavily extincted by the nascent, dusty envelope. This dust, however, rapidly heats or cools in response to changes in the luminosity of the central source [18]. The envelope, which is well-traced by submillimetre observations, will brighten as the temperature increases (after, for example, a protostellar outburst associated with accretion) and it will dim with decreasing temperature. The typical timescale of these changes in submillimetre flux is expected to be weeks to months [18]. While the strongest signal from a protostellar outburst would be expected at mid to far-infrared wavelengths, there is a current lack of space telescopes available to carry out consistent, regular observations of star-forming regions. Therefore, in order to probe these critical stages of mass accretion in Young Stellar Objects (YSOs), we capitalise on longer wavelength data.

In an effort to investigate the changing mass accretion rate of stars during their earliest stages of formation, the James Clerk Maxwell Telescope (JCMT) Transient Survey Large Program was initiated [19]. This program was the first, dedicated survey to monitor deeply embedded YSOs at submillimetre wavelengths, opening a new field in time-domain astronomy. The Transient Survey employs the Submillimetre Common User Bolometer Array 2 (SCUBA-2) to observe 8 nearby (< 500 pc) star-forming regions (circular fields of 0.5° diameter) at an approximately monthly cadence. Due to the development of novel relative flux calibration techniques that have decreased the flux uncertainty by an unprecedented factor of $2-3$ [20], more than a half dozen protostellar variables have been confirmed, including the most luminous stellar flare ever recorded [21]. The early results from this survey have prompted both theoretical and observational follow-up studies by international teams within the JCMT partnership. In the following sections, we describe the current status and future prospects for the Transient Survey, and subsequently discuss other possible applications of time-monitoring in the submillimetre.

2 Current Status of Submillimetre Transient Science

The JCMT Transient Survey is the first dedicated program to monitor the light curves of compact, submillimetre sources. The survey began in December 2015 and will continue in its current form through at least January 2020. While submillimetre variability associated with young, deeply embedded YSOs has been found before for a few objects [e.g. 22], the construction and refining of a relative flux calibration pipeline that improves the flux uncertainty at the telescope by a factor of 2 to 3 [20] has made it possible to monitor 1643 sources, ~ 50 with an accuracy of $\sim 2\%$ and the remaining sample for any large changes. This JCMT large program has conclusively shown that $\sim 10-20\%$ of the 50 brightest sources vary in brightness over timescales of months to years. These long-term brightness changes are interpreted as the dusty envelopes' response to luminosity changes in embedded YSOs.

The first prominent detection of an obvious variable in the survey was associated with the source EC 53 [23], also known as V371 Ser [24]. The light curve shows a periodic trend of brightening and fading over a timescale of ~ 543 days (see left panel of Figure 1). The periodicity is interpreted as accretion variability in the inner disk surrounding EC 53, perhaps excited by binary interactions. This variation and continual rise in brightness is seen at both 450 and 850 μm and it is tightly correlated with near-infrared wavelengths [J, H, and K bands; Tim Naylor, Watson Varricatt; private communications, 23]. The periodic nature of both the near-infrared and submillimeter wavelengths make the system a unique laboratory to study protostellar outbursts and how they inform the physics of the accretion disk. The short period indicates a timescale similar to EXor outbursts, but the NIR spectral features obtained by IGRINS suggest FUor-like characteristics. This indicates that the cooling timescale at the disk midplane must be longer than the $\sim$1.5 year period, since the FUor-like NIR features can be explained by a hotter midplane than the surface of the disk. There are currently ongoing investigations into the scaling relationships and spectral index of the source across these wavelengths.

EC 53 is, so far, the only known periodic submillimetre variable identified in the eight Transient Survey fields. Additional examples of long-term variability, however, have been discovered by performing several statistical tests on the 1643 identified 850 μm sources across all observed regions [25]. These tests are part of an automated pipeline that is triggered each time new data is obtained. In total, ten submillimetre variables have been confirmed within the Transient survey (see Table 7 of [25]), while several additional candidates have been identified. HOPS 358 [26, 27], among the youngest and most deeply embedded YSOs in NGC 2068 (classified as a PACS Bright Red Source, [28]), has

[2] http://gsaweb.ast.cam.ac.uk/alerts/home

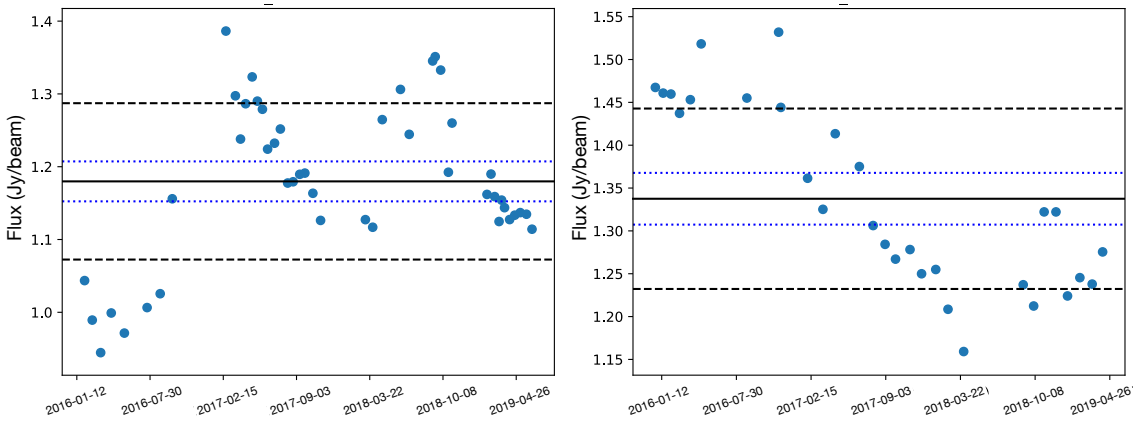

Figure 1: *Left:* The 850 μm light curve of EC 53. The variability period is $\sim$543 days. This variation is also seen at 450 microns, and at near-infrared wavelengths [23]. The blue (dotted) lines indicate the expected light curve standard deviation in the absence of variability, while the black (dashed) lines indicate the measured light curve standard deviation. *Right:* The 850 μm light curve of HOPS 358. After a stable period of over one year, the flux steadily declined, then began increasing again. Additional data is necessary to determine if this is a periodic trend.

a strong brightness variation seen in Figure 1. Further evidence of relatively long-term variability trends was found by identifying significant, robust changes in brightness (both brightening and fading) for 5 submillimetre sources observed 2-4 years apart by combining JCMT Transient Survey data with archival JCMT Gould Belt Survey [29], with further analysis of stochastic and secular variables in Lee et al. (in Prep).

In addition to this long-term variability associated with accretion rate changes, the Transient Survey has also uncovered a non-thermal, short-term variability event signalling what may have been the most luminous stellar radio flare on record [21]. On 2016 November 26, a bright point source was detected in the direction of the T Tauri Binary system known as JW 566 [30]. There has been no significant signal at this location during any of the other 26 Transient Survey observations, including data that was observed only 6 days previous to the flare. Upon further investigation, a light curve was constructed that showed the brightness of the source declining by 50% in less than 30 minutes. The resulting brightness temperature suggests a non-thermal origin. Short-timescale, non-thermal variability similar to this has been noted before at millimetre and radio wavelengths [31, 32, 33, 34] but this is the first detection in the submillimetre regime. The flare is interpreted as a magnetic reconnection event, releasing (gyro-)synchrotron radiation. Additional observations of short-term variability associated with T-Tauri stars or younger YSOs will help determine the amplitudes and frequencies of these events. This will be an important window into the dominant physics governing material in the scale of the inner accretion disk to the stellar surface. High resolution spectral follow-up studies are currently under preparation. New methods are also under development to search for additional faint, short-term variability events in each observed epoch. These results will be summarised in Lalchand et al. (In Prep).

In the case of the infrared wavelengths, if the emission can escape the envelope, the expected signal from an accretion burst should be much more significant as the YSO luminosity is being traced directly rather than tracing the temperature of the surrounding dust. However, near- and even mid-IR variability may also be caused by changes in extinction (for example, V1647 Ori), while far-IR and submillimetre variability may be caused only by changes in luminosity. This mid-infrared data (3.4 and 4.6 μm) is available toward the Transient Survey fields throughout much of the time the JCMT has been obtaining images with *WISE* and *NEOWISE* (Contreras, et al. in prep). In the left panel of Figure 2, we see a long-term brightening trend in both the MIR and Submillimetre data of an embedded YSO in the IC348 region. In the right panel of Figure 2, we see an example of a stochastic variable candidate in the Ophiuchus Core region with peaks and troughs in the mid-IR but not the submillimetre photometry. Using these observations as constraints, 3D and simplified 2D hydrodynamic modelling plus radiative transfer of protostellar variability has been developed to interpret the SED variability of generic variables [35, 36] and for EC 53 specifically (Baek et al. in prep). These models are needed to convert the submillimetre variability into a change in source luminosity while also allowing us to investigate the envelope structure, including outflow cavities and viewing inclination.

The JCMT Transient Survey has also motivated several ALMA programs to resolve the changes in flux at high spatial resolution. The calibration methods developed throughout this single-dish program are now being applied in pilot ALMA surveys to understand whether it is possible to apply the same techniques to interferometric data [e.g. 37].

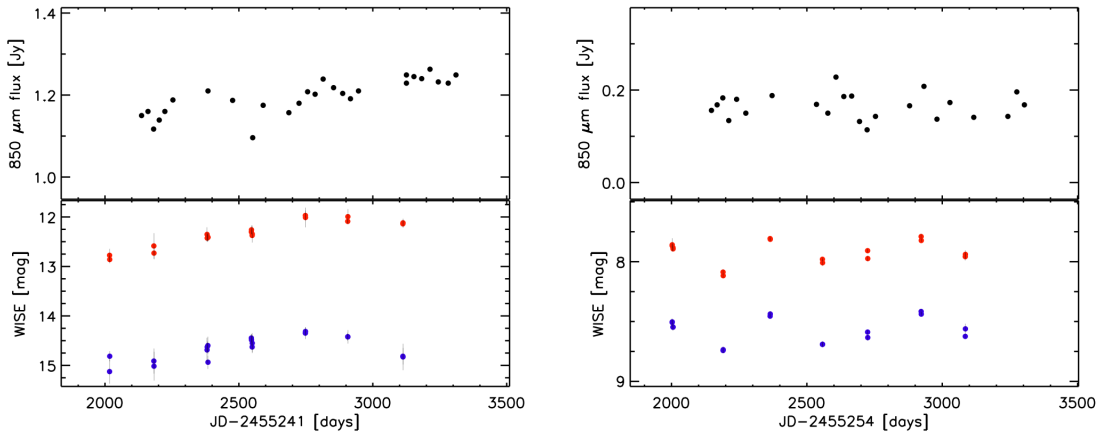

Figure 2: Preliminary figures from Contreras, et al. in prep. *Left:* A confirmed long-term variable in the IC348 field at 3.4 (blue), 4.6 (red), and 850 μm (black). *Right:* A stochastic variable candidate in the Ophiuchus Core field. The colour scheme is the same as the left panel.

3 The Next Decade

3.1 The Near Future: SCUBA-2

The JCMT Transient Survey has definitively shown that variability associated with young stellar objects can be identified and characterised at submillimetre wavelengths. The current observing strategy of a monthly cadence toward 8 nearby star-forming regions has proven to be successful. Therefore, similar observations will be continued in the next generation programs in order to extend the 4-year timeframe, to better quantify any underlying timescales through periodogram analyses, and to construct deeper maps of fields densely populated with YSOs. The benefit of longer timescales was shown by [29], where Transient Survey data was compared with Gould Belt Survey data taken 2-4 years previous. A slow, long-term change in brightness can only be detected and verified over many years. The longer the timescale, the more sensitive the analysis is to identifying these "secular" variables. Additionally, with 3-4 more years of data collected on these same regions, several epochs obtained close in time can be combined in chunks to reduce the RMS background noise. By sacrificing some time resolution in this manner, fainter sources with long-term trends would be tracked with more certainty.

While the baseline large program will remain the same in principle, there are several ways to improve the observations in the near future. In regions that have the highest density of YSOs, a higher cadence of 1-2 weeks can be adopted. This increase in cadence will double the observing time for these fields with the current technology, but allow for the detection of shorter-period variability modes for bright sources while providing a factor of $\sqrt{2}$ decrease in RMS noise relative to the current large program over monthly timescales. The increase in sensitivity over one month would allow for a significantly more robust calibration of $\sim$25% more protostellar sources than are currently being tracked (see Section 3.2 for more details).

While observing at a higher cadence can increase the monthly sensitivity of observed fields, targeting additional fields also bolsters the amount of sources observed and improves statistics. Further to the 8 fields that are currently being observed by the JCMT Transient Survey, there are 5-8 other regions that were observed by the Gould Belt Survey that have a high density of compact sources associated with known YSOs (this is necessary for relative flux calibration). These regions span Southern Orion A [38], The W40 complex [39], and IC 5146 [40]. The benefit of targeting these regions is that they can be compared to observations taken before 2016 in order to investigate long-term secular variability. An additional 8 regions would double the amount of observing time required for the survey.

There is also significant interest from the community to expand the scope of the survey to regular observations of intermediate and high-mass star forming regions such as NGC 2264 [e.g. 41], IC 3196 [e.g. 42], or the nearby Planck Galactic Cold Clumps already observed by the JCMT throughout the TOP-SCOPE large program [43]. The further distances of these regions ensure the observation of more protostars per unit area at the cost of source confusion within the field. High-mass protostars likely undergo more energetic events, and the presence of high-mass protostars means that the field will contain many more low-mass protostars to build the survey's statistics. An initial analysis of SCUBA-2 observations towards 12 TOP-SCOPE fields [44] identified one candidate variability event in a high-mass star-forming

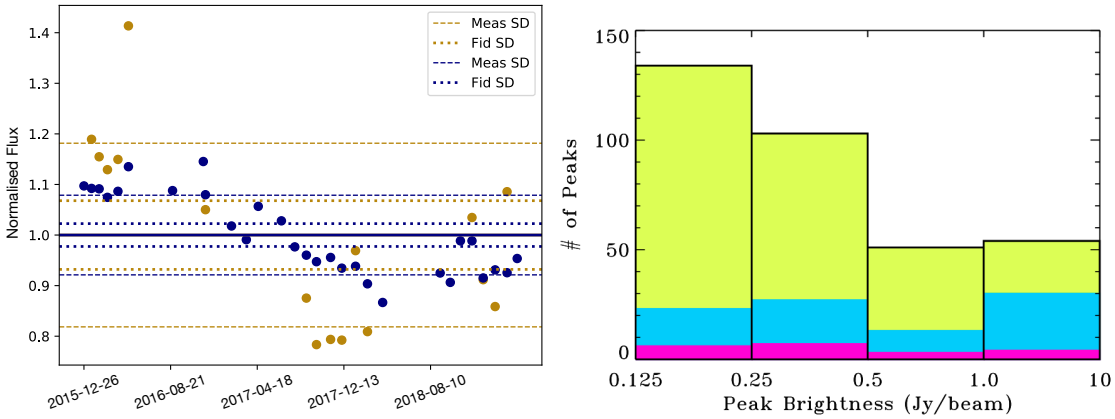

Figure 3: *Left:* HOPS 358 light curve shown at 450 (gold) and 850 μm (blue). Dashed lines show the measured standard deviation in each light curve while dotted lines show the expected standard deviation. *Right:* From [19]. Distribution of 342 sources that have compact 850 μm emission with peak brightness above 0.125 Jy/beam for all eight regions in our survey (yellow). The purple and blue histograms, respectively, show the number of sources associated with one or more disks and protostars. Based on the analysis of [20], with the current SCUBA-2 set-up, we can achieve 2–3% accuracy for the 105 peaks brighter than 0.5 Jy/beam and 10% for the 237 sources with brightness 0.125-0.5 Jy/beam.

region, but the analysis was limited because only the region was observed only three times. Improvements to the relative flux calibration pipeline would need to be made to ensure consistently measured light curves for these further regions.

Outside of the main large program that will continue to monitor variability over selected regions, there are several opportunities for complementary PI projects. For example, Target of Opportunity (ToO) time will be vital if another survey, (e.g. ZTF or Gaia Alerts) announces the detection of an event at a different wavelength (ToOs were triggered using ALMA and IGRINS as a result of the JCMT observations of EC 53), or, if simultaneous observations involving multiple facilities are to be coordinated. The relationship between the JCMT and The Submillimetre Array (SMA) will be invaluable during these times, observing the same event from the same physical location. Interferometers such as the SMA and the Atacama Large Millimetre/submillimetre Array (ALMA) offer resolution and sensitivity to observe small fluctuations in brightness at the scale of the disk where episodic accretion may be driven. Recently, [37] presented novel methods for comparing time-series interferometric observations using Combined Array for Research in Millimeter-wave Astronomy (CARMA) and ALMA 1.3mm observations of deeply embedded protostars in Serpens taken 9 years apart. High resolution spectroscopic follow-ups of variability events at facilities such as Gemini, Keck, and SOFIA are also being pursued to evaluate the physical cause of the instability by evaluating inner disk heating and binarity.

3.2 Beyond SCUBA-2

Despite the successes of the JCMT Transient Survey so far, the current program is limited by statistics due to the depth of each observation and the small number of observed fields. Figure 3 shows a histogram of more than 300 850 μm compact emission sources with peak brightnesses above 0.125 Jy/beam identified over all 8 survey regions [19]. The purple and blue histograms show the fraction of those sources associated with one or more known Class II (disk) object or Class 0/I/Flat spectrum protostar, respectively. The typical RMS noise in a given 850 μm Transient Survey image is approximately 0.015 Jy/beam. For sources that have a peak brightness greater than 0.5 Jy/beam, the relative calibration uncertainty is $\sim 2-3\%$. There are 105 emission sources detected in this brightness range, 42 of which are known to be protostellar. Expanding this high-accuracy bracket to include all sources brighter than 0.125 Jy/beam would allow for the robust tracking of an additional 237 emission sources, 51 of which are known to be protostellar. Achieving this accuracy with SCUBA-2 requires a background RMS noise of ~ 0.005 Jy/beam, 3 times fainter than the current value. This factor of ~ 10 increase in observing time required is prohibitive with SCUBA-2 but achievable with the proposed 850 μm MKID camera.

The new JCMT instrument is expected to increase the mapping speed by a factor of 10 from the combination of more sensitive detectors and a wider field of view. As shown in Figure 3, this would dramatically increase the number of monitored young stellar objects, bolstering the ability to observe robust variability events for the same amount of observing time ($\sim$50 hours per year). In the first 3 years of using the new 850 μm camera, we expect more than a factor of 3 increase in variability detections in the regions that are currently monitored by both increasing the number of sources we can analyse at $\sim 2\%$ precision and by uncovering smaller-scale variability on the bright objects in our current

survey. Fainter events are expected to occur more frequently than their brighter counterparts. More short-timescale flares such as JW 566 [21] will also be detected. In addition to tracking the flux variability of known YSOs, detecting significant variable flux associated with identified "starless cores" could lead to the discovery of first hydrostatic cores or deeply embedded protostars that were previously missed. Circular fields of 0°.5 diameter are ideal for monitoring YSO variability at a range of distances. Therefore, gaining an increased mapping speed with respect to SCUBA-2 solely by covering a larger field of view to the same depth will not be of benefit to the goals of YSO transient science, but may benefit other projects.

Future generation surveys with the new camera would uncover variability in more clouds spanning a variety of galactic environments. Wider area coverage is essential in order to dramatically increase the sample size of observed YSOs while allowing for cross-comparisons of light curves for stars forming in different physical conditions. With SCUBA-2 technology, the projects and survey expansions previously discussed in Section 3 require significant increases in observing time to achieve a fraction of what would be possible with the new camera assuming time investments comparable to what is currently spent on variability studies. As an example, the entire JCMT Gould Belt Survey area (103 0°.5 diameter circular fields) could be monitored monthly to a depth of 0.015 Jy/beam for an investment of only 10 hours per year more than the current survey (a total of 60 hours per year, or 5 observing nights, in Band 3 weather), which only covers 8 such fields. Alternatively, a full repeat of these fields to a depth of 0.005 Jy/beam (similar to the original survey and three times deeper than a single scan obtained by the current JCMT transient survey) could be performed in the same amount of time. This single epoch of all survey fields at such a deep sensitivity would provide critical flux information on thousands of compact sources when compared to the data obtained in $\sim$2015.

The MKID detectors in the new camera will be much more stable than the current TES detectors in SCUBA-2, based on tests performed for similar arrays [45, 46]. This stability is expected to translate into a lower uncertainty in the relative flux calibration, improving the confidence with which more distant and higher mass star-forming regions can be measured. In 30 hours of Band 3/4 observing time with the MKID detectors, all the fields in the SCOPE survey [43] could be revisited. Additionally, there is a wealth of star-forming regions previously observed by the JCMT such as M17, DR 21, and S255[3] that have great potential in showcasing variability associated with intermediate and high-mass forming stars.

Characterising the frequency and amplitude of submillimetre variability events through a range of masses and galactic environments over several year timescales will be essential in determining a complete theory of star formation. The constant monitoring of regions over a several year timescale would also result in the deepest submillimetre maps ever obtained of these regions, creating many opportunities for ancillary science. Expanding the scope of this new field of time domain science with a factor of 10 increase in observing efficiency will ensure new discoveries and the initiation of related studies for many years. These unique insights into the nature and evolution of the youngest stars will only be possible with the new 850 μm camera at the JCMT.

3.3 A Note Concerning 450 μm Data

Throughout all of these future prospects, JCMT Transient science will benefit greatly from the 450 μm data that is collected simultaneously with the 850 μm data. While the main focus of the Transient monitoring has been based on the 850 μm data, there is ongoing work to make full use of the simultaneous 450 μm data and to compare light curves of more evolved, less embedded YSOs across several mid to near-infrared filters. The relative flux calibration at 450 μm is more challenging due to the higher impact of atmospheric water vapour on the quality of the data. Despite this, preliminary studies have shown that >60% of the data can be recovered and flux calibrated to an uncertainty of 4-6% (Mairs et al. In Prep). The simultaneity of this data is paramount in studying variability events at these wavelengths, especially when considering short-term, non-thermal events such as JW 566's stellar flare [21]. While the 850 μm data can detect and reliably trace variability over time, additional wavelengths are necessary to constrain the physical conditions that are responsible for the event. So far, very good agreement is observed when comparing the 450 and 850 μm light curves of known variable sources (see Figure 3 for an example). Studies on the scaling relations, spectral indices, and phase shifts of these sources are ongoing, though preliminary efforts show stronger variations at 450 μm than at 850 μm, consistent with theoretical expectations.

3.4 Other science cases for submillimetre monitoring

Our focus in this white paper and in our initial application for submillimetre monitoring has been variable protostars. In contrast, optical monitoring surveys are designed to find supernovae, with applications for novae as well as more exotic phenomenon, like tidal disruption events and mergers of neutron stars [e.g. 47, 48]. Since dust obscures some transient events at optical wavelengths, ground- and space-based monitoring surveys are starting to monitor smaller regions on

[3] See the JCMT Archive: https://www.cadc-ccda.hia-iha.nrc-cnrc.gc.ca/en/jcmt/

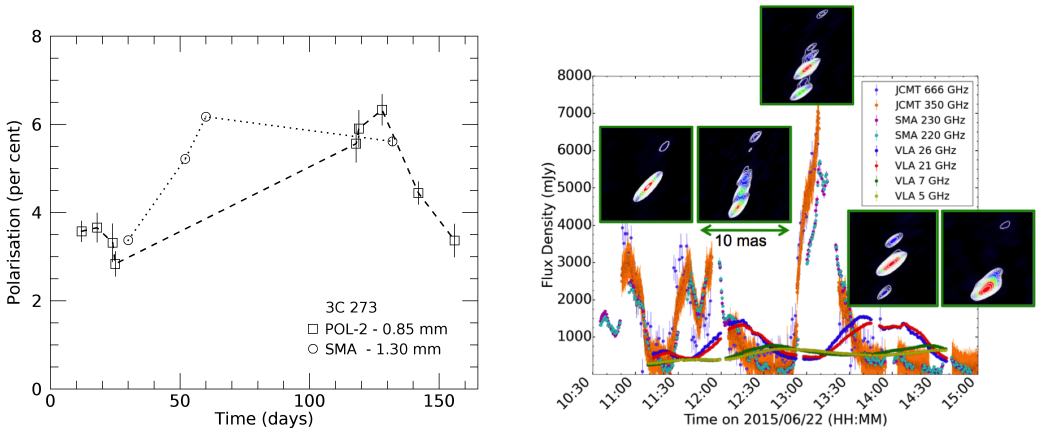

Figure 4: *Left:* Temporal variability (in days) of the polarization towards 3C 273 as a percentage of the continuum intensity at 850 μm (POL-2, shown as squares) and 1.3 mm (SMA, shown as circles). These data were obtained in 2016 by the POL-2 commissioning team as part of a polarimetric monitoring campaign of radio-loud active galactic nuclei. *Right:* Time resolved light curves of the jet launched from the stellar mass black hole V404 Cygni, taken simultaneously in an unprecedented 8 different bands [52]. We detect rapid flux variability, in the form of multiple, large scale flaring events, which coincide with the launching of discrete jet ejecta (shown in inset panels of high angular resolution images taken with the Very Long Baseline Array; [53]). This work represents the first time-resolved submillimetre study of XRB jets, and demonstrates the paramount importance of the submillimetre bands in understanding the rapidly evolving jets in XRB systems.

the sky in the near and mid-IR [49, 50]. The detection of distant variable phenomenon will always be challenging for the JCMT because of the beam size and the sparse density of galaxies on the sky. However, a new and more sensitive detector would open unique and powerful capabilities for monitoring eruptive phenomenon beyond nearby star-forming regions, including the distant universe and nearby galaxies, such as M31 and M33. Several specific science cases are described below.

Supernovae: Some core-collapse supernovae in starburst galaxies may be hidden from the view of optical observers but would be detected in the mid-IR and submillimetre, thereby providing a more accurate measurement of the star formation and supernova rates in the most active star-forming galaxies [51]. Submillimetre monitoring of supernovae would also provide direct measurements of the feedback of supernovae by dust heating, and non-thermal emission as the supernova shock wave interacts with the surrounding interstellar medium.

Active Galactic Nuclei: Synchrotron radiation from radio-loud active galactic nuclei (AGN) produces variable non-thermal emission [e.g. 54] that probes the innermost components of relativistic jets, which are launched by accretion events onto supermassive black holes [e.g. 55]. The highly turbulent nature of the magnetized medium found within shocks along these relativistic jets may be responsible for their observed temporal variability in both continuum and polarised intensity [e.g. 56, 57]. Such a variability in polarisation has successfully been observed at 850 μm on a timescale of days for the blazar 3C 273 using the POL-2 polarimeter at the JCMT (see Figure 4). However, there is also evidence for intraday variability in the polarization of blazars at millimetre wavelengths [58]. Similar flaring has been detected from Sgr A* at our galactic center [59]. Even larger variability attributed to tidal disruption events may be deeply obscured by dusty torus. A submillimetre camera capable of sensitive, high-cadence polarimetric measurements would therefore be an invaluable asset to probe the shortest coherence timescales of magnetized turbulence in AGN jets and other related variability of supermassive black holes.

X-ray binaries: Stellar mass black holes existing in X-ray binary (XRB) systems in our own Galaxy (i.e., binary systems containing a black hole accreting matter from a companion star) also launch highly variable relativistic synchrotron jets [60]. When compared to AGN, the rapid evolutionary timescales of XRBs (days to months, rather than 10^6 yrs), offers a distinct observational advantage, allowing us to watch the jet and accretion flow change on real human timescales. While XRB jets emit across a wide range of frequencies, the submillimetre bands uniquely probe the jet base region, where the jets are first launched and accelerated. Detecting and characterizing rapid flux variability in jet emission from multiple XRBs can allow us to track accreting matter from inflow to outflow, and probe detailed jet properties that are difficult, if not impossible, to measure by traditional spectral and imaging methods (e.g., size scales, speed, the sequence of events leading to jet launching; [e.g. 61, 62, 63, 64]). While XRB jet variability studies have been mainly confined to the higher frequency bands (optical, infrared), recently Tetarenko et al. [52, 65] have extended these time

domain studies into the radio and submillimetre bands, utilizing sophisticated Bayesian modelling and time domain techniques (e.g., cross correlation analyses, Fourier analyses) to directly connect jet variability properties to internal jet physics (see Figure 4). However, with current instrumentation (e.g., SCUBA-2 of JCMT), these studies could only probe jet variability in the brightest XRB systems, showing hundreds of mJy to Jy flux density levels. A more sensitive submillimetre camera would allow us to sample fainter, more common XRB jets, and significantly probe variability over much shorter timescales.

Evolved Stars: The pulsations of AGB and other evolved stars may affect their dust shells, leading to variable continuum emission [66]. submillimetre monitoring of evolved stars presents a number of advantages over the traditional optical/NIR observations. Not only is the submillimetre free from extinction, and avoids confusion caused by changes in spectral type by primarily detecting the circumstellar emission, but it has the potential to directly probe the influence of the variations on the outflow, rather than having to infer them indirectly: radio photospheres, dust and molecules all contribute to the submillimetre emission. By studying variability in the submillimetre and relating that to the behaviour of the stars themselves (as probed in the optical and NIR) we can unravel the influence of the pulsations on the inner envelope, where the outflow is launched. This is particularly interesting for the most optically-thick (i.e. highest mass-loss rate) sources, where even the mid-infrared is obscured, and for supernova progenitors, where it may shed light on the mechanisms driving pre-supernova mass loss, the most important unknown in the ultimate evolution of massive stars. Typically, one hour of integration spread over several epochs should be sufficient to smoothly sample the light curve for most nearby sources.

Flare stars: Non-thermal radio flares from stellar reconnection may also be a potential area of expansion for JCMT, with feasibility demonstrated by the detection of a flare from JW 566 [21]. Most observations of radio flares have focused on longer wavelengths, however coordinated observations that include the submillimetre and radio wavelengths would lead to a spectral index that would correspond to the electron opacity, while monitoring simultaneous to X-ray emission reveals connections between electron acceleration in magnetic fields and the production of high-energy photons [67].

3.5 JCMT in a Global Context

A new 850 μm camera at the JCMT would be uniquely capable of carrying out effective, consistent submillimetre Transient science observations due to its fast mapping speed in combination with a relatively wide field of view. The physical location of the JCMT in Hawai'i provides the capability of covering both northern and some southern fields. All this leads to plentiful synergies with other facilities in the coming decade. For example, pairing JCMT data with future monitoring campaigns undertaken by the Large Millimetre Telescope (LMT), the Institute for Radio Astronomy in the Millimeter Range (IRAM) 30-m dish, and near-future facilities such as the James Webb Space Telescope (JWST) and the Cornell Caltech Atacama Telescope Prime (CCAT-p). Follow-up studies on JCMT-discovered variable sources with the Atacama Large Millimetre/Submillimetre array (ALMA) will also be highly beneficial for probing the characteristics of the youngest stars. Since the JCMT will remain the most stable and reliable facility for 850 μm monitoring, the potential for new and continuing collaborations is strong world-wide. JCMT Transient science will drive the development of innovative programmatic infrastructure to combine data at multiple wavelengths over rapid timescales, ushering in next-generation instrumentation and ambitious science goals with the space telescopes of the 2030s.

References

[1] Jes K. Jørgensen, Doug Johnstone, Helen Kirk, and others. Current Star Formation in the Ophiuchus and Perseus Molecular Clouds: Constraints and Comparisons from Unbiased Submillimeter and Mid-Infrared Surveys. II. *The Astrophysical Journal*, 683(2):822–843, Aug 2008.

[2] Lee Hartmann, Gregory Herczeg, and Nuria Calvet. Accretion onto Pre-Main-Sequence Stars. *Annual Review of Astronomy and Astrophysics*, 54:135–180, Sep 2016.

[3] Philip J. Armitage. Physical processes in protoplanetary disks. *arXiv e-prints*, page arXiv:1509.06382, Sep 2015.

[4] Stella S. R. Offner and Christopher F. McKee. The Protostellar Luminosity Function. *The Astrophysical Journal*, 736(1):53, Jul 2011.

[5] Scott J. Kenyon, Lee W. Hartmann, Karen M. Strom, and Stephen E. Strom. An IRAS Survey of the Taurus-Auriga Molecular Cloud. *The Astronomical Journal*, 99:869, Mar 1990.

[6] II Evans, Neal J., Michael M. Dunham, Jes K. Jørgensen, and others. The Spitzer c2d Legacy Results: Star-Formation Rates and Efficiencies; Evolution and Lifetimes. *The Astrophysical Journal Supplement Series*, 181(2):321–350, Apr 2009.

[7] Michael M. Dunham, Lori E. Allen, II Evans, Neal J., and others. Young Stellar Objects in the Gould Belt. *The Astrophysical Journal Supplement Series*, 220(1):11, Sep 2015.

[8] Jaehan Bae, Lee Hartmann, Zhaohuan Zhu, and Richard P. Nelson. Accretion Outbursts in Self-gravitating Protoplanetary Disks. *The Astrophysical Journal*, 795(1):61, Nov 2014.

[9] Eduard I. Vorobyov and Shantanu Basu. Variable Protostellar Accretion with Episodic Bursts. *The Astrophysical Journal*, 805(2):115, Jun 2015.

[10] Steven W. Stahler. Deuterium and the Stellar Birthline. *The Astrophysical Journal*, 332:804, Sep 1988.

[11] D. Minniti, P. W. Lucas, J. P. Emerson, and others. VISTA Variables in the Via Lactea (VVV): The public ESO near-IR variability survey of the Milky Way. *New Astronomy*, 15(5):433–443, Jul 2010.

[12] B. J. Shappee, J. L. Prieto, D. Grupe, and others. The Man behind the Curtain: X-Rays Drive the UV through NIR Variability in the 2013 Active Galactic Nucleus Outburst in NGC 2617. *The Astrophysical Journal*, 788(1):48, Jun 2014.

[13] S. B. Howell, C. Sobeck, M. Haas, and others. The K2 Mission: Characterization and Early Results. *The Publications of the Astronomical Society of the Pacific*, 126:398, April 2014.

[14] D. L. Pollacco, I. Skillen, A. Collier Cameron, and others. The WASP Project and the SuperWASP Cameras. *The Publications of the Astronomical Society of the Pacific*, 118(848):1407–1418, Oct 2006.

[15] Roger M. Smith, Richard G. Dekany, Christopher Bebek, and others. The Zwicky transient facility observing system. In *Proceedings of the SPIE*, volume 9147 of *Society of Photo-Optical Instrumentation Engineers (SPIE) Conference Series*, page 914779, Jul 2014.

[16] M. Morales-Calderón, J. R. Stauffer, L. A. Hillenbrand, and others. Ysovar: The First Sensitive, Wide-area, Mid-infrared Photometric Monitoring of the Orion Nebula Cluster. *The Astrophysical Journal*, 733:50, May 2011.

[17] William J. Fischer, S. Thomas Megeath, Elise Furlan, and others. The Herschel Orion Protostar Survey: Luminosity and Envelope Evolution. *The Astrophysical Journal*, 840(2):69, May 2017.

[18] Doug Johnstone, Benjamin Hendricks, Gregory J. Herczeg, and Simon Bruderer. Continuum Variability of Deeply Embedded Protostars as a Probe of Envelope Structure. *The Astrophysical Journal*, 765(2):133, Mar 2013.

[19] Gregory J. Herczeg, Doug Johnstone, Steve Mairs, and others. How Do Stars Gain Their Mass? A JCMT/SCUBA-2 Transient Survey of Protostars in Nearby Star-forming Regions. *The Astrophysical Journal*, 849(1):43, Nov 2017.

[20] Steve Mairs, James Lane, Doug Johnstone, and others. The JCMT Transient Survey: Data Reduction and Calibration Methods. *The Astrophysical Journal*, 843(1):55, Jul 2017.

[21] Steve Mairs, Bhavana Lalchand, Geoffrey C. Bower, and others. The JCMT Transient Survey: An Extraordinary Submillimeter Flare in the T Tauri Binary System JW 566. *The Astrophysical Journal*, 871(1):72, Jan 2019.

[22] Emily J. Safron, William J. Fischer, S. Thomas Megeath, and others. Hops 383: an Outbursting Class 0 Protostar in Orion. *The Astrophysical Journal*, 800(1):L5, Feb 2015.

[23] Hyunju Yoo, Jeong-Eun Lee, Steve Mairs, and others. The JCMT Transient Survey: Detection of Submillimeter Variability in a Class I Protostar EC 53 in Serpens Main. *The Astrophysical Journal*, 849(1):69, Nov 2017.

[24] Klaus W. Hodapp, Rolf Chini, Ramon Watermann, and Roland Lemke. Eruptive Variable Stars and Outflows in Serpens NW. *The Astrophysical Journal*, 744(1):56, Jan 2012.

[25] Doug Johnstone, Gregory J. Herczeg, Steve Mairs, and others. The JCMT Transient Survey: Stochastic and Secular Variability of Protostars and Disks In the Submillimeter Region Observed over 18 Months. *The Astrophysical Journal*, 854(1):31, Feb 2018.

[26] E. Furlan, W. J. Fischer, B. Ali, and others. The Herschel Orion Protostar Survey: Spectral Energy Distributions and Fits Using a Grid of Protostellar Models. *The Astrophysical Journal Supplement Series*, 224(1):5, May 2016.

[27] Steve Mairs, Graham S. Bell, Doug Johnstone, and others. Sixteen month decline in the 850 micron continuum brightness of the young stellar object HOPS 358 in NGC 2068. *The Astronomer's Telegram*, 11583:1, Apr 2018.

[28] Amelia M. Stutz, John J. Tobin, Thomas Stanke, and others. A Herschel and APEX Census of the Reddest Sources in Orion: Searching for the Youngest Protostars. *The Astrophysical Journal*, 767(1):36, Apr 2013.

[29] Steve Mairs, Doug Johnstone, Helen Kirk, and others. The JCMT Transient Survey: Identifying Submillimeter Continuum Variability over Several Year Timescales Using Archival JCMT Gould Belt Survey Observations. *The Astrophysical Journal*, 849(2):107, Nov 2017.

[30] B. F. Jones and Merle F. Walker. Proper Motions and Variabilities of Stars Near the Orion Nebula. *The Astronomical Journal*, 95:1755, Jun 1988.

[31] Geoffrey C. Bower, Richard L. Plambeck, Alberto Bolatto, and others. A Giant Outburst at Millimeter Wavelengths in the Orion Nebula. *The Astrophysical Journal*, 598(2):1140–1150, Dec 2003.

[32] M. Massi, J. Forbrich, K. M. Menten, and others. Synchrotron emission from the T Tauri binary system V773 Tauri A. *Astronomy & Astrophysics*, 453(3):959–964, Jul 2006.

[33] D. M. Salter, M. R. Hogerheijde, and G. A. Blake. Captured at millimeter wavelengths: a flare from the classical T Tauri star DQ Tauri. *Astronomy & Astrophysics*, 492(1):L21–L24, Dec 2008.

[34] J. Forbrich, K. M. Menten, and M. J. Reid. A 1.3 cm wavelength radio flare from a deeply embedded source in the Orion BN/KL region. *Astronomy & Astrophysics*, 477(1):267–272, Jan 2008.

[35] Benjamin MacFarlane, Dimitris Stamatellos, Doug Johnstone, and others. Observational signatures of outbursting protostars - I: From hydrodynamic simulations to observations. *arXiv e-prints*, page arXiv:1906.01960, Jun 2019.

[36] Benjamin MacFarlane, Dimitris Stamatellos, Doug Johnstone, and others. Observational signatures of outbursting protostars – II: Exploring a wide range of eruptive protostars. *arXiv e-prints*, page arXiv:1906.01966, Jun 2019.

[37] Logan Francis, Doug Johnstone, Michael M. Dunham, Todd R. Hunter, and Steve Mairs. Identifying Variability in Deeply Embedded Protostars with ALMA and CARMA. *The Astrophysical Journal*, 871(2):149, Feb 2019.

[38] S. Mairs, D. Johnstone, H. Kirk, and others. The JCMT Gould Belt Survey: a first look at Southern Orion A with SCUBA-2. *Monthly Notices of the Royal Astronomical Society*, 461(4):4022–4048, Oct 2016.

[39] D. Rumble, J. Hatchell, K. Pattle, and others. The JCMT Gould Belt Survey: evidence for radiative heating and contamination in the W40 complex. *Monthly Notices of the Royal Astronomical Society*, 460(4):4150–4175, Aug 2016.

[40] D. Johnstone, S. Ciccone, H. Kirk, and others. The JCMT Gould Belt Survey: A First Look at IC 5146. *The Astrophysical Journal*, 836(1):132, Feb 2017.

[41] N. Peretto, Ph. André, and A. Belloche. Probing the formation of intermediate- to high-mass stars in protoclusters. A detailed millimeter study of the NGC 2264 clumps. *Astronomy & Astrophysics*, 445(3):979–998, Jan 2006.

[42] Aurora Sicilia-Aguilar, Veronica Roccatagliata, Konstantin Getman, and others. A Herschel view of IC 1396 A: Unveiling the different sequences of star formation. *Astronomy & Astrophysics*, 562:A131, Feb 2014.

[43] Tie Liu, Kee-Tae Kim, Mika Juvela, and others. The TOP-SCOPE Survey of Planck Galactic Cold Clumps: Survey Overview and Results of an Exemplar Source, PGCC G26.53+0.17. *The Astrophysical Journal Supplement Series*, 234(2):28, Feb 2018.

[44] Geumsook Park, Kee-Tae Kim, Doug Johnstone, and others. Submillimeter continuum variability in Planck Galactic cold clumps. *arXiv e-prints*, page arXiv:1905.12147, May 2019.

[45] Nathan P. Lourie, Peter A. R. Ade, Francisco E. Angile, and others. Preflight characterization of the BLAST-TNG receiver and detector arrays. In *Millimeter, Submillimeter, and Far-Infrared Detectors and Instrumentation for Astronomy IX*, volume 10708 of *Society of Photo-Optical Instrumentation Engineers (SPIE) Conference Series*, page 107080L, Jul 2018.

[46] Sean Bryan. The TolTEC Camera for the LMT Telescope. In *Atacama Large-Aperture Submm/mm Telescope (AtLAST)*, page 36, Jan 2018.

[47] T. W. S. Holoien, J. S. Brown, K. Z. Stanek, and others. The ASAS-SN bright supernova catalogue - III. 2016. *Monthly Notices of the Royal Astronomical Society*, 471(4):4966–4981, Nov 2017.

[48] Matthew J. Graham, S. R. Kulkarni, Eric C. Bellm, and others. The Zwicky Transient Facility: Science Objectives. *Publications of the Astronomical Society of the Pacific*, 131(1001):078001, Jul 2019.

[49] C. Contreras Peña, P. W. Lucas, R. Kurtev, and others. Infrared spectroscopy of eruptive variable protostars from VVV. *Monthly Notices of the Royal Astronomical Society*, 465(3):3039–3100, Mar 2017.

[50] Mansi M. Kasliwal, John Bally, Frank Masci, and others. SPIRITS: Uncovering Unusual Infrared Transients with Spitzer. *The Astrophysical Journal*, 839(2):88, Apr 2017.

[51] Haojing Yan, Zhiyuan Ma, John F. Beacom, and James Runge. Revealing Dusty Supernovae in High-redshift (Ultra)Luminous Infrared Galaxies through Near-infrared Integrated Light Variability. *The Astrophysical Journal*, 867(1):21, Nov 2018.

[52] A. J. Tetarenko, G. R. Sivakoff, J. C. A. Miller-Jones, and others. Extreme jet ejections from the black hole X-ray binary V404 Cygni. *Monthly Notices of the Royal Astronomical Society*, 469(3):3141–3162, Aug 2017.

[53] James C. A. Miller-Jones, Alexandra J. Tetarenko, Gregory R. Sivakoff, and others. A rapidly changing jet orientation in the stellar-mass black-hole system V404 Cygni. *Nature*, 569(7756):374–377, Apr 2019.

[54] E. I. Robson, J. A. Stevens, and T. Jenness. Observations of flat-spectrum radio sources at $\lambda 850$ μm from the James Clerk Maxwell Telescope - I. 1997 April to 2000 April. *Monthly Notices of the Royal Astronomical Society*, 327:751–770, November 2001.

[55] A. P. Marscher. Relativistic Jets in Active Galactic Nuclei. In P. A. Hughes and J. N. Bregman, editors, *Relativistic Jets: The Common Physics of AGN, Microquasars, and Gamma-Ray Bursts*, volume 856 of *American Institute of Physics Conference Series*, pages 1–22, September 2006.

[56] S. G. Jorstad, A. P. Marscher, J. A. Stevens, and others. Multiwaveband Polarimetric Observations of 15 Active Galactic Nuclei at High Frequencies: Correlated Polarization Behavior. *The Astronomical Journal*, 134:799–824, August 2007.

[57] A. P. Marscher. Turbulent, Extreme Multi-zone Model for Simulating Flux and Polarization Variability in Blazars. *The Astrophysical Journal*, 780:87, January 2014.

[58] J. W. Lee, S.-S. Lee, S. Kang, D.-Y. Byun, and S. S. Kim. Detection of millimeter-wavelength intraday variability in polarized emission from S5 0716+714. *Astronomy & Astrophysics*, 592:L10, August 2016.

[59] F. Yusef-Zadeh, H. Bushouse, M. Wardle, and others. Simultaneous Multi-Wavelength Observations of Sgr A* During 2007 April 1-11. *The Astrophysical Journal*, 706(1):348–375, Nov 2009.

[60] R. Fender. *Compact Stellar X-Ray Sources*. Cambridge University Press, 2006.

[61] P. Casella, T. J. Maccarone, K. O'Brien, and others. Fast infrared variability from a relativistic jet in GX 339-4. *Monthly Notices of the Royal Astronomical Society*, 404(1):L21–L25, May 2010.

[62] P. Uttley and P. Casella. Multi-Wavelength Variability. Accretion and Ejection at the Fastest Timescales. *Space Science Reviews*, 183:453–476, 2014.

[63] F. M. Vincentelli, P. Casella, T. J. Maccarone, and others. Characterization of the infrared/X-ray subsecond variability for the black hole transient GX 339-4. *Monthly Notices of the Royal Astronomical Society*, 477:4524–4533, July 2018.

[64] J. Malzac, M. Kalamkar, F. Vincentelli, and others. A jet model for the fast IR variability of the black hole X-ray binary GX 339-4. *Monthly Notices of the Royal Astronomical Society*, 480:2054–2071, 2018.

[65] A. J. Tetarenko, P. Casella, J. C. A. Miller-Jones, and others. Radio frequency timing analysis of the compact jet in the black hole X-ray binary Cygnus X-1. *Monthly Notices of the Royal Astronomical Society*, 484(3):2987–3003, Apr 2019.

[66] Planck Collaboration, M. Arnaud, F. Atrio-Barandela, and others. Planck intermediate results. XVIII. The millimetre and sub-millimetre emission from planetary nebulae. *Astronomy & Astrophysics*, 573:A6, Jan 2015.

[67] Jan Forbrich, Mark J. Reid, Karl M. Menten, and others. Extreme Radio Flares and Associated X-Ray Variability from Young Stellar Objects in the Orion Nebula Cluster. *The Astrophysical Journal*, 844(2):109, Aug 2017.

MAGNETIC FIELDS STUDIES IN THE NEXT DECADE

EAO SUBMILLIMETRE FUTURES PAPER SERIES, 2019

Ray S. Furuya[*1] • **Kate Pattle**[2] • **Simon Coudé**[3] • **Tao-Chung Ching**[4] • **Steve Mairs**[5]
Sarah Sadavoy[6,7] • **Peter Scicluna**[8] • **Archana Soam**[3] • **Chakali Eswaraiah**[4] • **Samar Safi-Harb**[9]

[1]*Institute of Liberal Arts and Sciences, Tokushima University, Minami Jousanajima-machi 1-1, Tokushima 770-8502, Japan*
[2]*Institute of Astronomy and Department of Physics, National Tsing Hua University, Hsinchu 30013, Taiwan, R.O.C.*
[3]*SOFIA Science Center, USRA NASA Ames Research Center Moffett Field, CA 94035, U.S.A.*
[4]*CAS Key Laboratory of FAST, National Astronomical Observatories, Chinese Academy of Sciences, Datun Road, Chaoyang District, Beijing 100101, People's Republic of China*
[5]*East Asian Observatory (JCMT) 660 N. A'ohōkū Place, Hilo, HI, 96720, U.S.A.*
[6]*Harvard-Smithsonian Center for Astrophysics, 60 Garden Street, Cambridge, MA, 02138, USA*
[7]*Department for Physics, Engineering Physics and Astrophysics, Queen's University, Kingston, ON, K7L 3N6, Canada*
[8]*Academia Sinica Institute of Astronomy and Astrophysics, AS/NTU Astronomy-Mathematics Building, No 1. Sec. 4 Roosevelt Rd, Taipei, Taiwan*
[9]*Dept of Physics and Astronomy, Faculty of Science, University of Manitoba, Winnipeg, MR R3T 2N2 Canada*

ABSTRACT

Magnetic fields are ubiquitous in our Universe, but remain poorly understood in many branches of astrophysics. A key tool for inferring astrophysical magnetic field properties is dust emission polarimetry. The James Clerk Maxwell Telescope (JCMT) is planning a new 850 μm camera consisting of an array of 7272 paired Microwave Kinetic Inductance Detectors (MKIDs), which will inherently acquire linear polarization information. The camera will allow wide-area polarization mapping of dust emission at $14''$-resolution, allowing magnetic field properties to be studied in a wide range of environments, including all stages of the star formation process, Asymptotic Giant Branch stellar envelopes and planetary nebula, external galaxies including starburst galaxies and analogues for the Milky Way, and the environments of active galactic nuclei (AGN). Time domain studies of AGN and protostellar polarization variability will also become practicable. Studies of the polarization properties of the interstellar medium will also allow detailed investigation of dust grain properties and physics. These investigations would benefit from a potential future upgrade adding 450 μm capability to the camera, which would allow inference of spectral indices for polarized dust emission in a range of environments. The enhanced mapping speed and polarization capabilities of the new camera will transform the JCMT into a true submillimetre polarization survey instrument, offering the potential to revolutionize our understanding of magnetic fields in the cold Universe.

1 Introduction

Our Universe is threaded by magnetic fields (also known as B-fields), whose presence is deduced from their effects on the astrophysical generation of electromagnetic radiation, or on the propagation of that radiation through the interstellar or intergalactic media (ISM and IGM respectively) [e.g. 1], and so through observation of polarized astrophysical signal. Magnetic fields can significantly affect the dynamics of all phases of the ISM, being coupled to the neutral material by Alfvénic flux freezing ("frozen in") [2].These magnetic fields may be primordial [3] or generated or amplified by dynamo effects [1], and can be dissipated by magnetic reconnection [4]. In order to address some of the most pressing questions in modern astrophysics and cosmology we require knowledge of the structure and strength of magnetic fields in the ISM and IGM, the physical roles that they play, and the conditions under which they affect gas dynamics.

[*]rsf@tokushima-u.ac.jp

Submillimetre emission polarimetry is a key tool for deducing magnetic field properties in cold ($\lesssim 100$ K) gas. Polarized continuum emission arises from non-spherical dust grains aligned with their major axes perpendicular to their local magnetic field [5]: a powerful tracer of plane-of-sky ISM magnetic field direction, as dust makes up 1% of the ISM by mass [6], and is widely used as a proxy for molecular hydrogen [7]. Emission polarimetry is unique in its dynamic range and wide mapping area. Polarized signal is down to column densities $\sim 10^{20}$ cm^{-2} in space-based observations [8], while submillimetre dust emission remains optically thin at even the highest ISM gas densities [7]. Dust polarization fraction ranges from a maximum of $\sim 20\%$ in the diffuse ISM [8] to $\lesssim 1\%$ in the densest parts of molecular clouds [e.g. 9], and so polarization observations require a sensitivity $\gtrsim 10^2$ times better than is needed in unpolarized light.

Methods for quantifying the dynamic importance of magnetic fields inferred from emission polarimetry are well-established. Plane-of-sky magnetic field strength is inferred using the Davis-Chandrasekhar-Fermi (DCF) method [10, 11], which takes deviations in magnetic field angle to result from Alfvénic distortion by non-thermal motions. The dynamic importance of the magnetic field relative to gravity is assessed using the mass-to-flux ratio, the critical value of which indicates a structure too massive to be supported by its internal magnetic field, while importance relative to non-thermal ISM motions is assessed using the Alfvén Mach number, the ratio of gas velocity dispersion to Alfvén velocity [2]. The dynamic importance of magnetic fields can also be characterised through their morphology [e.g 12].

The James Clerk Maxwell Telescope (JCMT) is a 15 m telescope operating in the wavelength range $450 - 1100\,\mu$m, with a resolution of $14''$ at 850 μm, near the summit of Maunakea in Hawaii. The JCMT has for decades been a world leader in submillimetre emission polarimetry, hosting the UKT Polarimeter [13], the SCUPOL polarimeter [14, 15] on the SCUBA camera [16], and now the POL-2 polarimeter [17, 18] on the SCUBA-2 camera [19]. Each of these has measured polarization by inserting a half-wave plate into a camera's light path, progressing from a sensitivity of ~ 200 mJy beam^{-1} in a single pixel [UKT Polarimeter, 13], to ~ 1 mJy beam^{-1} over > 5000 pixels [POL-2, 18, 20]. The JCMT has made the first detections of magnetic fields in protostellar envelopes with the UKT Polarimeter [21, 22]; in the centre of a starburst galaxy [23] and in a starless core [24] with SCUPOL; and in a photoionized column with POL-2 [25]. The JCMT has made most DCF measurements of magnetic field strength in the ISM to date [26].

Other recent advances have been the *Planck* Space Observatory [8] all-sky polarization maps, and the polarimetric capabilities of the Atacama Large Millimeter/submillimeter Array (ALMA) [e.g. 27]. The $5'$-resolution *Planck* all-sky maps reveal the large-scale polarization structure of the Milky Way, but at best coarsely resolve molecular clouds. Conversely, ALMA can map detailed magnetic fields around individual compact objects but, with a maximum observable size scale $\sim 1''$, cannot provide larger-scale context. With a resolution $\sim 10''$, the JCMT bridges this gap (see Figure 1), flexibly providing information on how Galactic-scale magnetic fields couple to fields on the smallest scales in the ISM, through both wide-area surveys [20] and high-sensitivity mapping of individual sources [e.g. 28].

The JCMT is planning a major instrumentation upgrade. First light for a new 850μm camera is planned for October 2022, with 450μm capability added in 2024. A new large heterodyne array is planned for 2026. The new camera will have a $12'$ field of view, twice that of SCUBA-2, with a focal plane filled with 3636 pixels, each comprising two Microwave Kinetic Induction Detectors (MKIDs), measuring orthogonal linear polarizations from a single scan observation without a half-wave plate. Native observation of polarized signal, and the improved capabilities of MKIDs over the SCUBA-2 bolometers, will result in a guaranteed $20\times$ increase in polarization mapping speed over POL-2, and an aspirational $40\times$ increase. As shown in Figure 2, this will allow entire molecular clouds to be mapped in the time currently required to map a single POL-2 field. This will transform the JCMT into a true polarimetric survey instrument, while retaining its ability to map sources of particular scientific interest to unprecedented depth in polarized light.

In this white paper we present potential science goals for the new JCMT camera. While we primarily focus on the 850 μm polarimetric capabilities of the camera, we also discuss how the proposed studies could be enhanced by 450 μm polarimetric data. Where relevant we discuss time-domain magnetic field studies. Section 2 considers star formation and the Galactic ISM; Section 3, evolved stars and stellar remnants; Section 4, magnetic fields in external galaxies, our own Galactic centre, and active galactic nuclei; Section 5, dust grain physics; Section 6, potential synergies with heterodyne instruments; and Section 7, synergies with other polarimeters. Section 8 summarizes the white paper.

2 Magnetic fields in star formation

Molecular clouds: Stars form in molecular clouds, the gas dynamics of which are regulated by an interplay between turbulent pressure, magnetic fields and self-gravity [e.g. 33]. These cold molecular clouds form out of the warm ISM, which is heated both by supernova shocks and by cosmic rays trapped by the galactic magnetic field [34]. Proposed formation mechanisms include multiple-shock compression of atomic clouds embedded in a weak galactic-scale magnetic field [35], or colliding flows in a magnetized warm ISM [36], among other models. Thus, galactic-scale magnetic fields may be integral to setting the initial conditions for the formation of stars within molecular clouds.

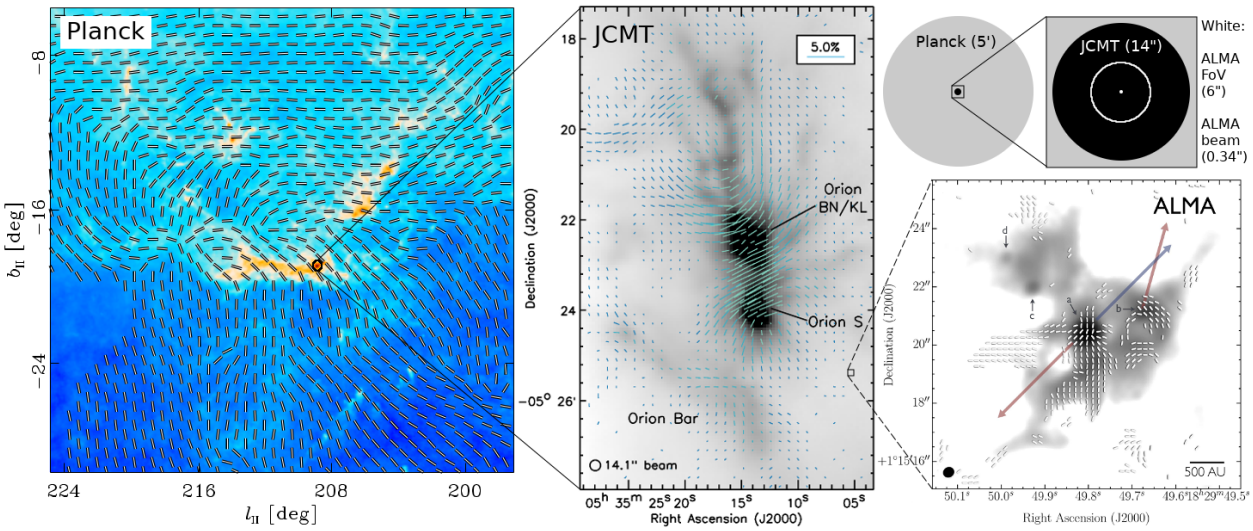

Figure 1: A comparison of JCMT, *Planck* and ALMA polarization observations. All vectors are rotated by 90° to trace magnetic field direction. *Left: Planck* observations of the Orion Molecular Cloud [8]. *Centre:* JCMT observations of the OMC-1 region in the centre of Orion [29]. Note the significant deviations from the large-scale field morphology. The total area observed with the JCMT is shown as a black circle on the left-hand panel. *Lower right:* ALMA observations of the Serpens SMM 1 protostar [30],located at comparable distance to Orion [31, 32]. The extent of the ALMA observations is shown as a black square on the central panel (Serpens MM1 is not located in the marked region). *Upper right:* The resolutions of *Planck* (grey), the JCMT (black) and ALMA (filled white circle), and the field of view of ALMA Cycle 7 polarization observations (open white circle; $1/3$ of the $18''$ ALMA primary beam). ALMA beam size depends on array configuration; the beam shown is representative of the data in the lower right-hand panel.

Both *Planck* [8, 37] and extinction polarimetric observations [38] suggest that large-scale magnetic fields in molecular clouds are bi-modal, being preferentially aligned either parallel or perpendicular to the major axis of the cloud. The relationship between magnetic fields and filamentary structure within clouds remains uncertain. Recent observations of the Vela C complex by BLAST-Pol [39] and of IRDCs by POL-2 [40], along with optical and NIR extinction polarimetric results [e.g. 41, 42], show that magnetic fields on the peripheries of self-gravitating filaments are generally perpendicular to the filaments' major axes (see Figure 3). However, these magnetic fields may be aligned with low-density substructures (sometimes called 'striations') which are themselves perpendicular to the filaments' major axes [42]. These striations may comprise material being accreted onto filaments along magnetic field lines [43]. These observations tell us about overall field-filament alignment within molecular clouds, but do not provide sufficient resolution to determine the the behaviour of magnetic field inside filaments. Conservation of magnetic flux requires that magnetic fields either pass through filaments [e.g. 44] or wrap around them [e.g. 45]. Sensitive high-resolution polarization observations would distinguish between these cases, informing the role of magnetic fields in filamentary accretion and fragmentation.

POL-2 observations of nearby molecular clouds suggest that within dense filaments, relationships between field and filament direction can become more complex. For example, the centre of the OMC-1 molecular cloud – the nearest region of high-mass star formation – shows a field geometry that may have been significantly distorted by large-scale motion of material under gravity [29, see Figure 1]. However, the surface-brightness limitation and relatively small extent of a POL-2 observation [18] and the insensitivity of SCUBA-2 to large-scale structure [47] limits our current ability to deduce the properties of magnetic fields within filamentary structure, particularly in low-density non-self-gravitating filaments. To determine the existence or otherwise of magnetically-supported filaments, higher-sensitivity polarization observations with < 0.1 pc linear resolution are needed [48]. The new 850-μm camera will allow entire molecular clouds to be mapped in polarized light at $14''$ resolution, equivalent to ~ 0.01 pc in nearby molecular clouds.

Feedback from massive stars drives the dynamics and regulates the evolution of the molecular clouds in which they form [49]. Intense UV radiation and/or winds from OB stars as well as supernova feedback drive the expansion of HII regions, creating structures such as photoionized columns (also known as pillars or elephant trunks) in the photodissociation regions (PDRs) at the interface between molecular and ionized material. The role of magnetic fields in PDR evolution remains poorly constrained [e.g. 50, 51]. POL-2 has recently made the first map of magnetic fields within the famous 'Pillars of Creation' in M16 [25, see Figure 4], finding that the magnetic field is dynamically important, but unable to

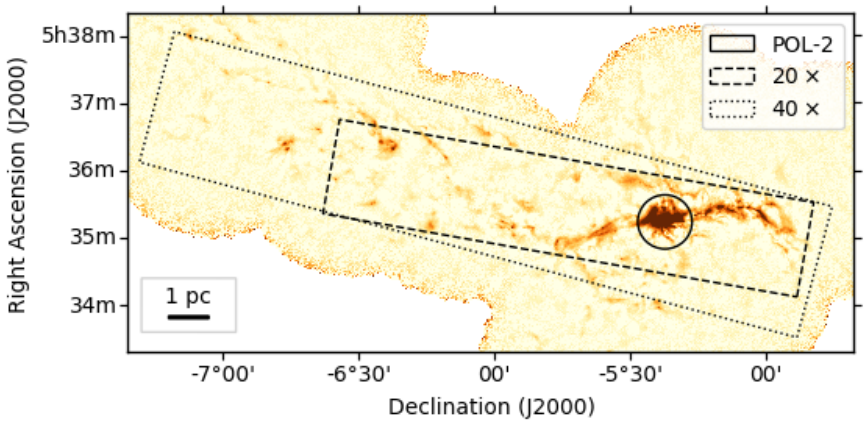

Figure 2: A comparison of polarization mapping speed between POL-2 and the proposed new camera. Image shows a SCUBA-2 850 μm map of the Orion A molecular cloud [46]. The 'integral filament' is on the right of the image (North is located to image right). Solid circle shows the full extent of a current POL-2 field, centred on the OMC-1 region. Rectangles mark the area observable in the same time with $20\times$ (dashed) and $40\times$ (dotted) mapping speed.

prevent the columns' destruction by the oncoming ionization front. However, the improved mapping speed of the new camera will allow the entire PDR associated with an open HII region to be mapped in the time currently required to map individual columns, allowing investigation of the role of magnetic fields in the large-scale evolution of HII regions.

Time estimate: Given a $20\times$ increase in mapping speed, with 14 hours of observing time in Band 2 weather, 0.6 square degrees of the sky could be observed to a depth of 1.5 mJy/beam, as shown in Figure 2. This would allow mapping of full molecular clouds to the depth currently achieved in single pointing observations by the BISTRO (B-Fields in Star-forming Region Observations) Survey [20], fulfilling the science goals described above.

Starless and prestellar cores: A key indicator of the relative importance of magnetic fields in the gravitational collapse of cores to form YSOs, and of the magnetic fields in YSOs themselves, is the strength and morphology of magnetic fields in starless cores. Starless cores are overdensities in star-forming regions which, if gravitationally bound (a 'prestellar core' [52]), will go on to form an individual star or system of stars [53]. A detailed understanding of how starless cores form and evolve is necessary in order to understand the functional form of the Initial Mass Function [54].

Being extended, low-surface-brightness objects, starless cores remain particularly challenging to observe. The JCMT has been responsible for nearly all polarimetric observations of starless cores to date, both with SCUPOL [55] and more recently with POL-2 [e.g. 56]. Isolated starless cores generally appear to have a smooth and well-ordered magnetic field, with detectable polarization across the cores [e.g. 57]. An example of a starless core observed with POL-2 is shown in Figure 4. Despite being gravitationally unstable [e.g. 58], none of the prestellar cores so far observed unambiguously show the 'hourglass' magnetic field which would indicate ambipolar-diffusion-driven collapse [59]. The role of magnetic fields in the physics of prestellar core formation and collapse thus remains unclear. However, very few starless cores have been observed in polarized light, due to the prohibitive amount of time required for a detection, and observations are strongly biased towards the very highest-surface-brightness cores. With $20\times$ increased mapping speed, the new JCMT camera would allow at least an order of magnitude increase in the number of starless cores detectable, and would allow investigation of whether the uniform fields seen in bright cores are the norm, and to systematically search for cores showing signs of magnetically regulated collapse.

Debate continues over whether high-mass stars form from the monolithic collapse of prestellar cores, analogously to low-mass stars, or through competitive accretion or other dynamic processes [49]. If high-mass prestellar cores exist, they are likely to require significant magnetic support [e.g. 62]. Archival data from the SCUPOL Legacy Catalogue toward a set of bright massive cores in the G 11.11-0.12 region has been used to propose that one of these sources is a magnetically supported high-mass starless core [62]. Most detections of high-mass star-forming cores to date have been made using interferometric observations [e.g. 63, 64] in which any extended lower-density periphery will be resolved out. The new JCMT camera will allow entire IRDCs to be surveyed in polarized light, searching for polarization geometries consistent with magnetic support, and for existing high-mass core candidates to be surveyed systematically, allowing the debate over magnetically-supported high-mass starless cores to be put onto a statistical footing.

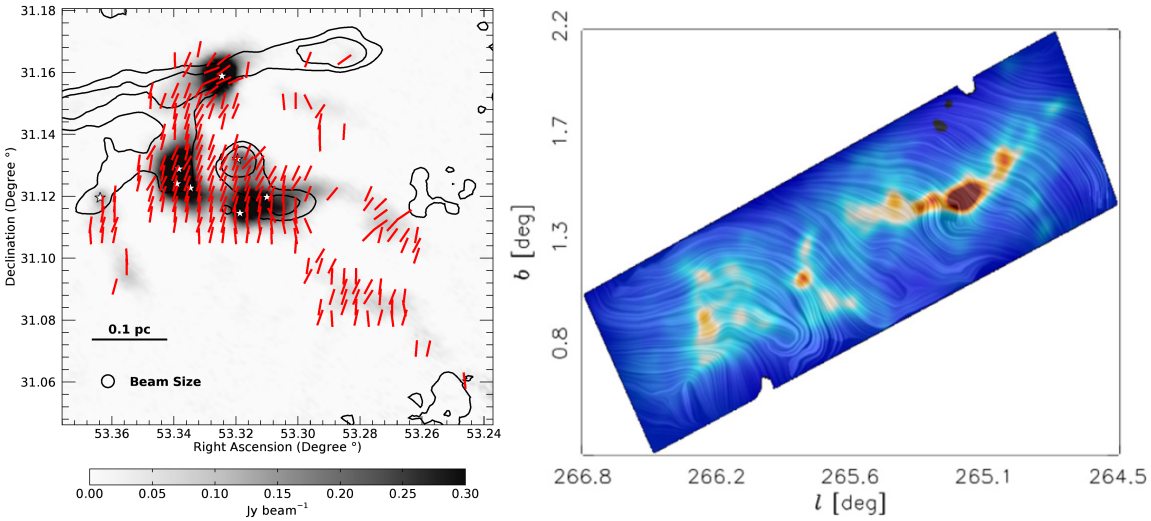

Figure 3: Examples of magnetic fields in molecular clouds. *Left:* Plane-of-sky magnetic field structure observed with POL-2 in the nearby ($\sim$ 300 pc) Perseus B1 low-mass star-forming region [60]. Image shows 850 μm intensity; contours show ^{12}CO J=3-2 integrated intensity (10 and 20 K km s^{-1}) measured with HARP [47]. Embedded YSOs are marked with star symbols. *Right:* Plane-of-sky magnetic field morphology observed with BLAST-Pol in the early-stage molecular cloud Vela C ($\sim$ 700 pc) [61].

Time estimate: Given a 20$\times$ increase in mapping speed, the well-studied prestellar core L1544 (peak 850μm brightness $\sim$ 300 mJy/beam) could be observed to a sensitivity of 0.5 mJy/beam with 5 hours of Band 1 observations, allowing 3-σ detection of 0.5% polarization on-peak. A survey of 20 such cores would thus require only 100 hours of observing time.

Protostellar systems: Protostellar cores, dense cores with a size $\sim$ 0.1 pc containing embedded hydrostatic objects, either young stellar objects (YSOs) or their precursors, are generally warmer, brighter and more centrally condensed than their starless counterparts, and so are less challenging to observe. Protostellar cores, containing complex internal structures (discs, accretion flows, etc.), are good interferometric targets [65]. However, single-dish observations provide information on the environments of these cores unobtainable with interferometers. The new JCMT camera offers the opportunity to perform unbiased surveys of the magnetic environments of protostellar cores in nearby molecular clouds.

Recent interferometric observations suggest that the dynamic importance of magnetic fields in protostellar cores may vary widely: the majority have outflows randomly oriented with respect to the magnetic field direction (on scales $\sim 10^2$ – 10^3 AU), suggesting a weak magnetic field, while a minority show parallel outflow and field directions, suggesting a dynamically important field [65]. A large dust polarization survey could investigate whether this behaviour persists on core-to-filament scales ($\gtrsim$0.1 pc), and whether there is a difference in large-scale magnetic environment between the two populations of protostellar cores. Such a survey would offer a strong legacy set of data, and would identify targets for interferometric follow-up. Studying magnetic fields from core scales down to the scales of disks ($\lesssim 10^2$ AU) is vital to understand the origin of those disks and the formation of jets and outflows, in order to determine whether field misalignment, turbulence, or non-ideal magnetohydrodynamic (MHD) processes are at play [e.g., 66, 67, 68].

A further unanswered question is of the role played by magnetic fields in the formation of brown dwarfs [69]. The improved sensitivity and mapping speed of the new JCMT camera will allow for systematic investigation of cloud cores hosting very low luminosity objects (VeLLOs; integrated luminosity $\lesssim 0.1\,L_\odot$), potential progenitors of either proto-brown dwarfs or very low-mass YSOs [e.g. 70]. A large sample of VeLLOs could include first hydrostatic cores (FHSCs) – the much-searched-for adiabatic first kernel of mass which precedes a core's collapse to make a YSO. Regardless of whether VeLLOs are FHSCs or very young YSOs, their outflows are too weak to affect the magnetic fields in their host cores, and so they offer the possibility of mapping the initial field structure in protostellar cores [71].

Time-domain science: A long-standing question in star formation is of the rate at which a YSO gains mass from its surroundings [73], and of the role of magnetic fields in regulating this process. While YSOs are inherently variable objects [e.g., 74, 75], sporadic episodes of elevated mass accretion can be observed at the earliest stages of a YSO's life at far-infrared (FIR) and submillimetre wavelengths [76]. The frequency and amplitude of this variability give insight into the physical drivers of unsteady accretion. The JCMT Transient Survey first showed that submillimetre protostellar variability is robustly observable [77, 78, 79]. When a YSO enters a burst phase, the surrounding material

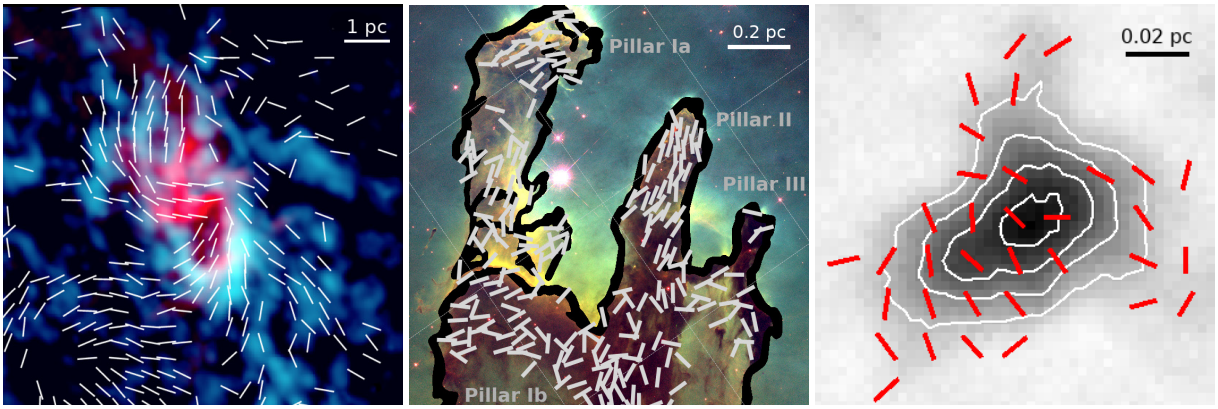

Figure 4: JCMT POL-2 observations of magnetic fields in the Milky Way Galaxy, on a range of scales. In all panels, POL-2 850μm polarization vectors have uniform length and are rotated to trace magnetic field direction. *Left*: The centre of the Milky Way, Sagittarius A*, and its circumnuclear disk (SMA imaging; blue) and mini-spiral (6 cm continuum Jansky Very Large Array imaging; red) [72]. *Middle*: The 'Pillars of Creation' photoionized columns in M16 (Hubble Space Telescope image) [25]. *Right*: The Ophiuchus C starless core (SCUBA-2 850μm image) [c.f. 56].

reprocesses the excess energy and the submillimetre flux increases with dust temperature [76, 79]. Monitoring potential changes in the magnetic field in the accreting material over timescales of weeks to years will give insight into the physical conditions of these systems. Radio observations have also shown short-timescale (hours) synchrotron flares associated with T Tauri stars [e.g. 80, 81]. The JCMT recently made the first submillimetre observation of a similar event in the JW 566 T Tauri Binary System [82], thought to be the most powerful of its kind recorded. Fast-followup target-of-opportunity polarimetric observations of the dusty regions associated with such flares will be compared with archival data to note any significant changes in magnetic field properties, even over short timescales.

Time estimate: For a YSO with peak 850μm brightness $\sim$ 1000 mJy/beam (such as the variable source EC53 [83]), a sensitivity $\sim$ 3.3 mJy/beam would be required in order to make a 3-σ detection of 1% changes in polarization. Given a 20$\times$ increase in mapping speed, this could be achieved in approximately 10 minutes of Band 2 observing time. This would make both wide-area YSO polarization surveys covering entire molecular clouds and long-term and target-of-opportunity monitoring of protostellar variability feasible.

450 μm science: Comparison of 450 μm and 850 μm measurements of polarization in molecular clouds and cores will allow study of differing polarization structures in warm and cold dust populations along the line of sight, thereby producing quasi-three-dimensional magnetic field models [e.g 67]. The potential of such studies is demonstrated by recent FIR polarimetric observations of Orion A, showing that the magnetic field structure observed at 850 μm (Figure 1) gives way in the FIR to a polarization structure that traces the bipolar structure produced by the BN/KL explosion [84]. The 450μm capabilities of the new camera will allow such comparisons to be made as a matter of course.

3 Late-stage Stellar Evolution

AGB stars and planetary nebulae: The new JCMT camera will significantly improve our knowledge of magnetic fields in asymptotic giant branch (AGB) stars and planetary nebulae by allowing the study of magnetic fields in circumstellar material, and so of the typical magnetic field geometry within a circumstellar envelope, how magnetic fields regulate mass-loss phenomena in AGB stars (or vice versa), and of the relationship between stellar and circumstellar magnetic fields. Cool evolved stars have significant magnetic fields both at their surfaces [85] and in their envelopes [e.g. 86, 87], measurements of which currently use Zeeman splitting either of atomic lines from the stellar photosphere or of maser transitions of molecules in the circumstellar material. However, these measurements sample only a small fraction of the gas associated with the stars, while photospheric lines may be affected by starspots, and masers inherently sample only high-density, population-inverted, molecular gas in the inner outflow. An overall view of magnetism in evolved stars requires observations of the overall magnetic field structure of the circumstellar envelope.

Debate continues as to whether magnetic fields in AGB stars are produced by angular-momentum transfer from a companion. Statistics of the presence and morphology of the large-scale field will allow comparison to models of the expected population of companions, and with known binary stars. Comparison between field morphology and mass-loss history will reveal whether magnetic fields play any role in shaping the outflow. Correlating magnetic field properties with evolutionary stage will explore how fields evolve with the stars, and if they play a role in the changes that occur as

stars evolve off the AGB. Moreover, along with supernovae, AGB stars have been considered as major sites of dust grain production. Data provided by the new camera would thus provide new observational constraints on dust grain physics.

Time estimate: ALMA observations of IRC+10216, the brightest AGB star in the submillimetre [88], suggest that POL-2 might need $\sim$ 30 hours of Band 1 weather to detect 5%-polarized emission in the outer envelope. A 20$\times$ increase in speed would make the brightest sources observable in 1–2 hours each. A large program could thus observe tens or hundreds of evolved stars and map the polarization in their envelopes, particularly if informed by the results of the ongoing Nearby Evolved Stars Survey (NESS) Large Program, or by future continuum mapping with the new camera.

Supernova remnants: ISM properties control galactic evolution by regulating star formation rate, while stars return much of their material to the ISM through dense winds or supernova explosions at the end of their lives. These supernovae send shock waves into the ISM, producing supernova remnants (SNRs) which disperse heavy elements, while also compressing and seeding magnetic field lines [e.g., 89, 90]. The origin of magnetic fields in SNRs and their link to the magnetic field of their host galaxy is an important open question, with few objects studied in detail [e.g., 91, 92]. While submillimetre observations offer a new, independent way of probing magnetic fields, only a few SNRs have been mapped in submillimetre polarization to date.With the 20$\times$ increase in mapping speed of the new JCMT camera, 850 μm polarization observations of SNRs will be achievable for large numbers of objects, opening a new field of study for the JCMT. A polarization survey of the nearby galaxies M31 and M33 will help link our understanding of the global view of their star formation with their magnetic field morphology: while most extragalactic SNRs will be very compact, their high polarization fractions mean they should be detectable with the new JCMT camera.

The new camera will also enable novel studies in the field of pulsar wind nebulae (PWNe), a subclass of core-collapse supernovae. These are non-thermal, polarized synchrotron bubbles inflated by the loss of rotational energy from fast-spinning neutron stars. It is believed that dust grains are able to penetrate into the nebula given the low pulsar velocity, thus making circum-pulsar disks [93]. Future observations of a large sample of PWNe (in their different stages of evolution) will open a new window into the discovery of circum-pulsar disks in which planets may form.

SNR magnetic field studies are important not only to understand the particle acceleration mechanism operating in SNR shocks, but also to address the larger questions of cosmic magnetism and the origin of cosmic rays driving future large radio telescopes such as the Square Kilometer Array and the next generation VLA (ngVLA), and the γ-ray Cherenkov Telescope Array. Observations made with the new JCMT camera will serve as pathfinder science for these instruments.

Time estimate: 850μm polarization is detected in 9 hours of mixed Band 1/2 POL-2 commissioning observations of the Crab Nebula SNR. A similar detection would thus be achievable in approximately 30 minutes with a 20$\times$ increase in mapping speed. Fainter SNRs would thus be detectable with a few hours of observing time.

4 Galactic-Scale Magnetic Fields

Spiral Galaxies: The disk of our galaxy is threaded by a large-scale magnetic field, mostly parallel to its spiral arms [e.g., 8, 94]. Similar fields have also been observed in nearby galaxies [95, 96], indicating that these fields are closely tied to the dynamics of spiral galaxies [97], and are likely sustained by a dynamo effect created by differential rotation and star formation occurring within them [e.g., 98]. However, Faraday rotation measures have shown the existence of a field reversal in the inner region of our galaxy [e.g., 99], which has not yet been observed elsewhere, and which could indicate anisotropic turbulence in galactic magnetic fields, or perturbation by satellite galaxies [97].

Submillimetre dust polarization observations in nearby spiral galaxies will allow insight into the magnetic properties of the high-density gas, which will serve as templates to better understand our own galaxy's magnetic field [8]. Several of these nearby galaxies were successfully detected at 450 μm and 850 μm by the JINGLE survey using the SCUBA-2 camera on the JCMT [100], and so the new camera will have the required sensitivity to detect polarization in these objects. The new camera's larger field of view will allow the first 850 μm polarization surveys of the M31 and M33 galaxies, as discussed above. These extragalactic polarization data sets can be analyzed similarly to those of molecular clouds, providing information about the magnetic and turbulent properties of galactic-scale magnetic fields [101].

Time estimate: M31 occupies approximately 3 square degrees on the sky. To map this area to 1.5 mJy/beam sensitivity in 850μm polarized light with the new camera would require approximately 70 hours of Band 2 time, making polarization surveys of nearby spiral galaxies eminently feasible.

Starburst Galaxies: Galactic magnetic field strengths $\sim$100 μG are observed in starburst (intensely star-forming) galaxies [e.g., 102]. In comparison, the Milky Way's large-scale field strength is $\sim$ 5 μG, similar to M31 and M33 [97]. While the origin of starburst galaxies' strong magnetic fields is not well-understood, their interaction with galactic outflows may have magnetized the IGM in the early universe [e.g., 103]. The new JCMT camera will significantly

expand our knowledge of the magnetic field structure in the densest regions of starburst galaxies, helping to explain the nature of these fields and how they are maintained in environments of intense stellar feedback [e.g., 23, 97, 104].

Time estimate: The starburst galaxy M82 has a peak 850μm brightness of 1400 mJy/beam and a median polarization fraction of 2.8% [23]. A 5-σ detection of this polarization fraction could be achieved in less than 3 minutes in Band 2 weather with the new camera, and fainter starbursts could be observed in minutes or hours.

Super-Massive Black Holes and Active Galactic Nuclei: The role of magnetic fields in galactic evolution can be investigated through observations of Sagittarius A*, the super-massive black hole (SMBH) at the centre of our galaxy. While Sgr A* is currently quiescent, its accretion behaviour provides information on AGN physics, such as jet launching mechanisms and galactic-scale feedback, unobtainable in more distant sources. Similarly to AGN such as Cygnus A [105], Sgr A* hosts a circumnuclear disc (CND) with a rotating molecular torus housing ionized streamers [106, 107]. POL-2 observations of the CND (Figure 4) show that the magnetic field and the CND align on larger scales, while the innermost field lines align with the streamers [72, 108], suggesting that the CND and the streamers are an inflow system. Observations with the new JCMT camera will allow the large-scale magnetic environment of the Galactic centre and Sgr A* to be mapped in unprecedented detail. These combined with observations of Sgr A* itself from the Event Horizon Telescope [109, 110], of which the JCMT is a part, will revolutionize our understanding of how SMBHs acquire mass, and so how magnetic fields influence the galactic-scale feedback effects that regulate galactic evolution.

Time estimate: The POL-2 polarization vectors of the Galactic Centre shown in Figure 1 were achieved in ~ 14.5 hours of mixed Band 1/2 time, with a sensitivity ~ 1.6 mJy/beam [72]. With the new camera, such an observation could be made in ~ 45 minutes, making a deep, wide-area survey of the Galactic Centre quickly practicable.

Time-domain science: Among the most extreme environments in which magnetic fields have been detected are jets launched from accretion events onto SMBHs in radio-loud AGN [e.g. 111]. The 850 μm emission of these objects is dominated by highly-polarized synchrotron radiation from relativistic electrons accelerated along magnetic field lines [e.g. 112], and the turbulent nature of the magnetized medium found within shocks along these relativistic jets may cause their observed temporal variability in polarized intensity [e.g. 113, 114].

Time estimate: Variable AGN polarization is detected between 40-minute Band 2 850 μm POL-2 observations (sensitivity ~ 7 mJy/beam) [18]. The new camera would decrease the observing time per measurement to 2 minutes, making a daily observing campaign possible. Such high-cadence measurements would provide a statistically-significant AGN variability data set on timescales of days, and would allow precise measurements of intra-day variability [e.g. 115].

450 μm science: The smaller beam size of the JCMT at 450 μm may help to detect polarized emission from radio-loud AGN by reducing the effect of beam dilution on the measured signal. More importantly, while synchrotron emission is typically the main source of emission in these AGN, their 850 μm polarization can be contaminated by dust emission, [116]. This dust component would typically be an order of magnitude brighter than the synchrotron emission at 450 μm, thus lifting the degeneracy between the thermal and non-thermal components at 850 μm. Combined 450 μm and 850 μm polarimetric data of flat-spectrum radio-loud AGN such as blazars can also be used to probe the electron density and magnetic field properties in the inner components of relativistic jets launched by SMBHs [e.g. 113, 115, 117].

5 Dust grain physics and alignment mechanisms

For polarization observations to trace magnetic fields, a fraction of the ISM dust population must consist of non-spherical grains with major axes preferentially aligned perpendicular to the local magnetic field direction [5]. The most promising theory for how this occurs is the Radiative Alignment Torques (RATs) paradigm [119], in which irregular grains are spun up by anisotropic radiation. [120]. If grain alignment is driven by an incident radiation field, its effectiveness should decrease with increasing extinction [119, 120]. A systematic decrease in polarization fraction towards high-extinction lines of sight (often called a 'polarization hole') is indeed commonly observed [e.g. 9, 60, 121], implying loss of grain alignment, an effect most pronounced in starless cores which have no internal source of photons [122, 123]. However, non-Gaussian noise properties of polarization measurements can lead to a predisposition for a lack of grain alignment to be inferred at low-to-intermediate signal-to-noise [124]. Higher-sensitivity observations will allow observation of starless and protostellar cores in a wider range of environments, elucidating the conditions under which grains lose alignment with the magnetic field, and so constraining the size distribution of grains in high-density regions.

Simple models predict an approximately flat submillimetre polarization spectrum (the variation of polarization fraction with wavelength) in molecular clouds [125]. However, polarization spectra have been found to have a minimum at 350 μm [e.g. 125, 126]. While this is possible in the RAT paradigm [127], the predicted variation in polarization fraction with wavelength is too small to explain the apparent 350 μm minimum. However, recent work combining BLAST-Pol 250–500 μm and Planck 850 μm observations have shown a polarization spectrum which is flat to within 10–20% across the submillimetre in nearby molecular clouds [128, 129]. Comparing polarization spectra observed on

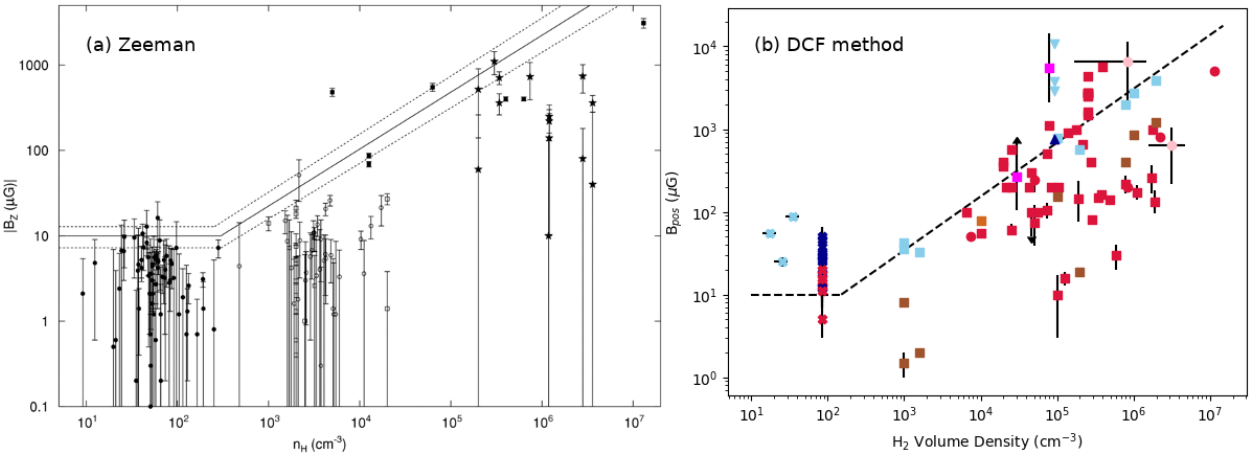

Figure 5: A comparison between magnetic field strengths determined (a) directly from Zeeman splitting measurements [118] and (b) indirectly using the DCF method [26]. The left-hand plot compares H volume density to line-of-sight field strength. The right-hand plot compares H_2 volume density to plane-of-sky field strength. The dashed line shown in both panels is the upper-limit field strength inferred from the Zeeman measurements in panel (a).

$\sim 5'$ scales with those observed on $\sim 10''$ scales will allow investigation of how grain properties vary from molecular cloud scales to filament/core scales, and of the dependence of grain growth on temperature, density and radiation field.

450μm science: Replacing Planck's $5'$ beam with the JCMT's $12''$ resolution will produce detailed submillimetre polarization spectra through synthesis with BLAST-TNG [130] and SOFIA [131], with $36''$-resolution (BLAST 500 μm). The upgrade to include 450 μm imaging could replace BLAST-TNG's 500 μm band, further improving the resolution.

6 Synergy with molecular line magnetic field observations

Zeeman Effect: The most direct measurement of astrophysical magnetic field strength is through Zeeman splitting of paramagnetic spectral lines. Such line-of-sight field strength measurements, using either thermal lines (e.g., HI, OH and CN) or maser lines (e.g., H_2O), have only been achieved toward a limited number of sources [e.g. 132]. Although magnetic field strengths inferred from dust emission using DCF analysis are comparatively indirect, they can, through wide-area mapping, simultaneously provide both the field structure and its strength in the plane of the sky [e.g. 26]. While Zeeman and DCF measurements probe different magnetic field components, the two are broadly consistent with and complement each other (Figure 5) [26], and can be combined to estimate total magnetic field strength [58]. A more complex approach is to combine polarization, Zeeman and ion-to-neutral molecular line width ratios in order to determine the angle of the magnetic field with respect to the line of sight [133, 134].

With its enhanced sensitivity, the new JCMT camera will allow estimates of magnetic field strengths to be obtained even in the lower-density periphery of molecular clouds. We will therefore have a more complete knowledge of magnetic field strengths over a larger range of gas densities, as shown in Figure 5. Polarization maps made using the new camera will thus provide a valuable reference for the planning of future measurements of the Zeeman effect as well as providing opportunities to infer three-dimensional magnetic field properties, and driving associated theoretical studies.

Goldreich-Kylafis effect: Molecular line polarization can arise from the Goldreich-Kylafis (GK) effect [135], in which molecular line emission may in certain circumstances be linearly polarized either parallel or perpendicular to the plane-of-sky magnetic field. The GK effect can complement emission polarimetry, occurring in regions where polarized dust emission is to faint to detect: for example, dust polarization can be used to probe magnetic fields in the high-column-density circumstellar material around YSOs, while fields in the low-column-density lobes of molecular outflows can be probed using the GK effect. Spectropolarimetric observations can also be used to probe the structure of magnetic fields in position-position-velocity space in order to, for example, disentangle the magnetic field of the galactic spiral arms. Wide-field Galactic plane observations made using the new JCMT camera, complemented with targeted observations of the GK effect with the forthcoming heterodyne array, might for the first time reveal the magnetic field structures of individual spiral arms, and the connection between galactic-scale and cloud-scale magnetic fields.

7 Synergies with other polarimeters

As discussed in Section 1, and elsewhere above, the resolution, field of view and mapping speed of the JCMT makes it an excellent bridge between *Planck* all-sky polarization maps and interferometric polarization imaging with ALMA and other similar instruments such as the Submillimeter Array (SMA). The new JCMT camera will both perform targeted high-resolution follow-up of *Planck* observations and undertake wide-area surveys from which targets for interferometric follow-up can be selected. The new JCMT camera will also perform pathfinder science for forthcoming large radio telescopes such as the Square Kilometer Array (SKA) and the next generation VLA (ngVLA).

The new JCMT camera will also synergize with other current and forthcoming single-dish polarization instruments [26]. HAWC+ [131], currently operating on the airborne SOFIA observatory, is an FIR polarimeter operating in the wavelength range 53–214μm with resolution 4.8–18.2$''$. HAWC+ is optimized to observe a warmer dust population than the JCMT; as discussed in Section 5, synthesis of polarization observations across the FIR/submillimetre regime is essential to understanding how dust properties and magnetic fields vary with gas temperature and density. BLAST-TNG [136], a balloon-borne polarimeter planned to fly from Antarctica in December 2019, operates at 250–500μm with resolutions 30–60$''$. Flight in Antarctica mean that BLAST-TNG can observe a limited number of Southern-sky targets, with declinations largely not observable by the JCMT, making the two instruments complementary.

TolTEC [137], the camera currently being commissioned at the LMT, will operate at wavelengths 1.1–2.1mm, with resolution 5.0–9.8$''$. NIKA-2 [138], a camera currently being commissioned at the IRAM 30m telescope, will operate at 1.2 and 2.0mm with resolutions of 11 and 18$''$. Both cameras will offer a polarization mode. Synthesis of JCMT 850μm and 450μm observations with these data will further add to polarization spectra across the wavelength range of dust continuum emission, while the higher surface brightness of cold dust at 450μm and 850μm will enhance the JCMT's ability to detect cold and dense sources over that of millimetre cameras. Moreover, comparison of millimetre and submillimetre observations of sources with significant non-thermal emission will allow the effects of synchrotron radiation to be disentangled from continuum emission (c.f. Section 4). The A-MKID camera [139], currently being commissioned at APEX, will operate at 350μm and 850μm with resolutions of 8 and 19$''$, and will offer a polarization mode. Observing declinations $< +50^{\circ}$, A-MKID may prove to be an effective Southern-sky counterpart to the JCMT.

All of these single-dish polarimeters modulate signal using a half-wave plate or polarizing grid [26]. The new JCMT camera will therefore have an intrinsic advantage in its ability to measure polarization natively, making it unique in its ability to provide polarization information as a standard component of an astrophysical observation.

8 Executive Summary

The James Clerk Maxwell Telescope (JCMT), which has long been at the forefront of submillimetre polarization instrumentation, is proposing a next-generation 850 μm camera. In this white paper we have presented the science case for the polarimetric capabilities of this camera. The JCMT's current POL-2/SCUBA-2 system has provided its user community with an outstanding and unique imaging polarimeter, and has resulted in numerous international collaborations and the global exchange of knowledge and ideas. The science goals and instrumentation requirements described in this work are based on wide-ranging discussions both across and beyond the JCMT community.

The new JCMT camera will be a vital tool with which to address fundamental questions of the role of magnetic fields in galactic astronomy and star formation, and also to pursue such studies beyond the Milky Way by analysing the magnetic field properties of galaxies as a whole. Key questions in such galactic and extra-galactic studies would include that of the role of magnetic fields in determining star formation efficiency and the origin of the Initial Mass Function, and in determining a galaxy's structure, ISM thermal balance, and global star formation rate. The JCMT is vital to such studies as, with a mapping size of tens of arcminutes and an angular resolution of 14$''$at 850μm, and operating in the optimal wavelength regime for detection of cold and dense material. The new JCMT camera's enhanced sensitivity and wide field of view will make it unique in its ability to serve as a wide-area survey instrument with which to study the interplay between self-gravity, turbulence and magnetism which drives the evolution of the cold ISM, and so to resolve questions crucial to our understanding of cosmic star-formation history.

References

[1] J. L. Han. Observing Interstellar and Intergalactic Magnetic Fields. *Annual Review of Astronomy and Astrophysics*, 55(1):111–157, Aug 2017.

[2] H. Alfvén. Existence of Electromagnetic-Hydrodynamic Waves. *Nature*, 150(3805):405–406, Oct 1942.

[3] D. Grasso and H. R. Rubinstein. Magnetic fields in the early Universe. *Phys. Rep.*, 348(3):163–266, Jul 2001.

[4] Ethan T. Vishniac and A. Lazarian. Reconnection in the Interstellar Medium. *The Astrophysical Journal*, 511(1):193–203, Jan 1999.

[5] L. Davis, Jr. and J. L. Greenstein. The Polarization of Starlight by Aligned Dust Grains. *The Astrophysical Journal*, 114:206, September 1951.

[6] R. C. Bohlin, B. D. Savage, and J. F. Drake. A survey of interstellar H I from Lalpha absorption measurements. II. *The Astrophysical Journal*, 224:132–142, Aug 1978.

[7] R. H. Hildebrand. The determination of cloud masses and dust characteristics from submillimetre thermal emission. *QJRAS*, 24:267–282, Sep 1983.

[8] Planck Collaboration, P. A. R. Ade, N. Aghanim, and others. Planck intermediate results. XIX. An overview of the polarized thermal emission from Galactic dust. *Astronomy & Astrophysics*, 576:A104, Apr 2015.

[9] Jungmi Kwon, Yasuo Doi, Motohide Tamura, and others. A First Look at BISTRO Observations of the ρ Oph-A core. *The Astrophysical Journal*, 859(1):4, May 2018.

[10] Leverett Davis. The Strength of Interstellar Magnetic Fields. *Physical Review*, 81(5):890–891, Mar 1951.

[11] S. Chandrasekhar and E. Fermi. Magnetic Fields in Spiral Arms. *The Astrophysical Journal*, 118:113, Jul 1953.

[12] J. D. Soler, P. Hennebelle, P. G. Martin, and others. An Imprint of Molecular Cloud Magnetization in the Morphology of the Dust Polarized Emission. *The Astrophysical Journal*, 774(2):128, Sep 2013.

[13] Alistair M. Flett and Alexander G. Murray. First results from a submillimetre polarimeter on the James Clerk Maxwell Telescope. *Monthly Notices of the Royal Astronomical Society*, 249:4P, Mar 1991.

[14] A. G. Murray, R. Nartallo, C. V. Haynes, F. Gannaway, and P. A. R. Ade. An Imaging Polarimeter for SCUBA. In A. Wilson, editor, *The Far Infrared and Submillimetre Universe.*, volume 401 of *ESA Special Publication*, page 405, Aug 1997.

[15] J. S. Greaves, W. S. Holland, T. Jenness, and others. A submillimetre imaging polarimeter at the James Clerk Maxwell Telescope. *Monthly Notices of the Royal Astronomical Society*, 340(2):353–361, Apr 2003.

[16] W. S. Holland, E. I. Robson, W. K. Gear, and others. SCUBA: a common-user submillimetre camera operating on the James Clerk Maxwell Telescope. *Monthly Notices of the Royal Astronomical Society*, 303(4):659–672, Mar 1999.

[17] P. Bastien, E. Bissonnette, A. Simon, and others. POL-2: The SCUBA-2 Polarimeter. In Pierre Bastien, Nadine Manset, Dan P. Clemens, and Nicole St-Louis, editors, *Astronomical Polarimetry 2008: Science from Small to Large Telescopes*, volume 449 of *Astronomical Society of the Pacific Conference Series*, page 68, Nov 2011.

[18] Per Friberg, Pierre Bastien, David Berry, and others. POL-2: a polarimeter for the James-Clerk-Maxwell telescope. In *Proceedings of the SPIE*, volume 9914 of *Society of Photo-Optical Instrumentation Engineers (SPIE) Conference Series*, page 991403, Jul 2016.

[19] W. S. Holland, D. Bintley, E. L. Chapin, and others. SCUBA-2: the 10 000 pixel bolometer camera on the James Clerk Maxwell Telescope. *Monthly Notices of the Royal Astronomical Society*, 430(4):2513–2533, Apr 2013.

[20] Derek Ward-Thompson, Kate Pattle, Pierre Bastien, and others. First Results from BISTRO: A SCUBA-2 Polarimeter Survey of the Gould Belt. *The Astrophysical Journal*, 842(1):66, Jun 2017.

[21] N. R. Minchin, D. Ward-Thompson, and G. J. White. A submillimetre continuum study of S 140/L 1204: the detection of three new submillimetre sources and a self-consistent model for the region. *Astronomy & Astrophysics*, 298:894, Jun 1995.

[22] Motohide Tamura, J. H. Hough, and Saeko S. Hayashi. 1 Millimeter Polarimetry of Young Stellar Objects: Low-Mass Protostars and T Tauri Stars. *The Astrophysical Journal*, 448:346, Jul 1995.

[23] J. S. Greaves, W. S. Holland, T. Jenness, and T. G. Hawarden. Magnetic field surrounding the starburst nucleus of the galaxy M82 from polarized dust emission. *Nature*, 404:732–733, April 2000.

[24] D. Ward-Thompson, J. M. Kirk, R. M. Crutcher, and others. First Observations of the Magnetic Field Geometry in Prestellar Cores. *The Astrophysical Journal Letters*, 537(2):L135–L138, Jul 2000.

[25] Kate Pattle, Derek Ward-Thompson, Tetsuo Hasegawa, and others. First Observations of the Magnetic Field inside the Pillars of Creation: Results from the BISTRO Survey. *The Astrophysical Journal Letters*, 860(1):L6, Jun 2018.

[26] Kate Pattle and Laura Fissel. Submillimeter and far-infrared polarimetric observations of magnetic fields in star-forming regions. *Frontiers in Astronomy and Space Sciences*, 6:15, 2019.

[27] C. L. H. Hull, P. Mocz, B. Burkhart, and others. Unveiling the Role of the Magnetic Field at the Smallest Scales of Star Formation. *The Astrophysical Journal Letters*, 842:L9, June 2017.

[28] Hsi-Wei Yen, Bo Zhao, I. Ta Hsieh, and others. JCMT POL-2 and ALMA Polarimetric Observations of 6000-100 au Scales in the Protostar B335: Linking Magnetic Field and Gas Kinematics in Observations and MHD Simulations. *The Astrophysical Journal*, 871(2):243, Feb 2019.

[29] Kate Pattle, Derek Ward-Thompson, David Berry, and others. The JCMT BISTRO Survey: The Magnetic Field Strength in the Orion A Filament. *The Astrophysical Journal*, 846(2):122, Sep 2017.

[30] Charles L. H. Hull, Josep M. Girart, Łukasz Tychoniec, and others. ALMA Observations of Dust Polarization and Molecular Line Emission from the Class 0 Protostellar Source Serpens SMM1. *The Astrophysical Journal*, 847(2):92, Oct 2017.

[31] Marina Kounkel, Lee Hartmann, Laurent Loinard, and others. The Gould's Belt Distances Survey (GOBELINS) II. Distances and Structure toward the Orion Molecular Clouds. *The Astrophysical Journal*, 834(2):142, Jan 2017.

[32] Gisela N. Ortiz-León, Sergio A. Dzib, Marina A. Kounkel, and others. The Gould's Belt Distances Survey (GOBELINS). III. The Distance to the Serpens/Aquila Molecular Complex. *The Astrophysical Journal*, 834(2):143, Jan 2017.

[33] Mordecai-Mark Mac Low and Ralf S. Klessen. Control of star formation by supersonic turbulence. *Reviews of Modern Physics*, 76(1):125–194, Jan 2004.

[34] M. G. Wolfire, D. Hollenbach, C. F. McKee, A. G. G. M. Tielens, and E. L. O. Bakes. The Neutral Atomic Phases of the Interstellar Medium. *The Astrophysical Journal*, 443:152, Apr 1995.

[35] Shu-ichiro Inutsuka, Tsuyoshi Inoue, Kazunari Iwasaki, and Takashi Hosokawa. The formation and destruction of molecular clouds and galactic star formation. An origin for the cloud mass function and star formation efficiency. *Astronomy & Astrophysics*, 580:A49, Aug 2015.

[36] Fabian Heitsch, James M. Stone, and Lee W. Hartmann. Effects of Magnetic Field Strength and Orientation on Molecular Cloud Formation. *The Astrophysical Journal*, 695(1):248–258, Apr 2009.

[37] Planck Collaboration, P. A. R. Ade, N. Aghanim, and others. Planck intermediate results. XXXV. Probing the role of the magnetic field in the formation of structure in molecular clouds. *Astronomy & Astrophysics*, 586:A138, Feb 2016.

[38] Hua-bai Li, Min Fang, Thomas Henning, and Jouni Kainulainen. The link between magnetic fields and filamentary clouds: bimodal cloud orientations in the Gould Belt. *Monthly Notices of the Royal Astronomical Society*, 436(4):3707–3719, Dec 2013.

[39] Dylan L. Jow, Ryley Hill, Douglas Scott, and others. An application of an optimal statistic for characterizing relative orientations. *Monthly Notices of the Royal Astronomical Society*, 474(1):1018–1027, Feb 2018.

[40] Tie Liu, Pak Shing Li, Mika Juvela, and others. A Holistic Perspective on the Dynamics of G035.39-00.33: The Interplay between Gas and Magnetic Fields. *The Astrophysical Journal*, 859(2):151, Jun 2018.

[41] Jia-Wei Wang, Shih-Ping Lai, Chakali Eswaraiah, and others. Multiwavelength Stellar Polarimetry of the Filamentary Cloud IC5146. I. Dust Properties. *The Astrophysical Journal*, 849(2):157, Nov 2017.

[42] P. Palmeirim, Ph. André, J. Kirk, and others. Herschel view of the Taurus B211/3 filament and striations: evidence of filamentary growth? *Astronomy & Astrophysics*, 550:A38, Feb 2013.

[43] P. André, J. Di Francesco, D. Ward-Thompson, and others. From Filamentary Networks to Dense Cores in Molecular Clouds: Toward a New Paradigm for Star Formation. In Henrik Beuther, Ralf S. Klessen, Cornelis P. Dullemond, and Thomas Henning, editors, *Protostars and Planets VI*, page 27, Jan 2014.

[44] Kohji Tomisaka. Magnetohydrostatic Equilibrium Structure and Mass of Filamentary Isothermal Cloud Threaded by Lateral Magnetic Field. *The Astrophysical Journal*, 785(1):24, Apr 2014.

[45] Jason D. Fiege and Ralph E. Pudritz. Helical fields and filamentary molecular clouds - I. *Monthly Notices of the Royal Astronomical Society*, 311(1):85–104, Jan 2000.

[46] C. J. Salji, J. S. Richer, J. V. Buckle, and others. The JCMT Gould Belt Survey: constraints on prestellar core properties in Orion A North. *Monthly Notices of the Royal Astronomical Society*, 449(2):1769–1781, May 2015.

[47] S. I. Sadavoy, J. Di Francesco, D. Johnstone, and others. The Herschel and JCMT Gould Belt Surveys: Constraining Dust Properties in the Perseus B1 Clump with PACS, SPIRE, and SCUBA-2. *The Astrophysical Journal*, 767:126, April 2013.

[48] D. Arzoumanian, Ph. André, P. Didelon, and others. Characterizing interstellar filaments with Herschel in IC 5146. *Astronomy & Astrophysics*, 529:L6, May 2011.

[49] J. C. Tan, M. T. Beltrán, P. Caselli, and others. Massive Star Formation. In Henrik Beuther, Ralf S. Klessen, Cornelis P. Dullemond, and Thomas Henning, editors, *Protostars and Planets VI*, page 149, Jan 2014.

[50] William J. Henney, S. Jane Arthur, Fabio de Colle, and Garrelt Mellema. Radiation-magnetohydrodynamic simulations of the photoionization of magnetized globules. *Monthly Notices of the Royal Astronomical Society*, 398(1):157–175, Sep 2009.

[51] Jonathan Mackey and Andrew J. Lim. Effects of magnetic fields on photoionized pillars and globules. *Monthly Notices of the Royal Astronomical Society*, 412(3):2079–2094, Apr 2011.

[52] D. Ward-Thompson, P. F. Scott, R. E. Hills, and P. Andre. A Submillimetre Continuum Survey of Pre Protostellar Cores. *Monthly Notices of the Royal Astronomical Society*, 268:276, May 1994.

[53] P. J. Benson and P. C. Myers. A Survey for Dense Cores in Dark Clouds. *The Astrophysical Journal Supplement*, 71:89, Sep 1989.

[54] F. Motte, P. Andre, and R. Neri. The initial conditions of star formation in the rho Ophiuchi main cloud: wide-field millimeter continuum mapping. *Astronomy & Astrophysics*, 336:150–172, Aug 1998.

[55] Brenda C. Matthews, Christie A. McPhee, Laura M. Fissel, and Rachel L. Curran. The Legacy of SCUPOL: 850 μm Imaging Polarimetry from 1997 to 2005. *The Astrophysical Journal Supplement*, 182(1):143–204, May 2009.

[56] Junhao Liu, Keping Qiu, David Berry, and others. The JCMT BISTRO Survey: The Magnetic Field in the Starless Core ρ Ophiuchus C. *The Astrophysical Journal*, 877(1):43, May 2019.

[57] Richard M. Crutcher, D. J. Nutter, D. Ward-Thompson, and J. M. Kirk. SCUBA Polarization Measurements of the Magnetic Field Strengths in the L183, L1544, and L43 Prestellar Cores. *The Astrophysical Journal*, 600(1):279–285, Jan 2004.

[58] J. M. Kirk, D. Ward-Thompson, and R. M. Crutcher. SCUBA polarization observations of the magnetic fields in the pre-stellar cores L1498 and L1517B. *Monthly Notices of the Royal Astronomical Society*, 369(3):1445–1450, Jul 2006.

[59] T. C. Mouschovias. Nonhomologous contraction and equilibria of self-gravitating, magnetic interstellar clouds embedded in an intercloud medium: star formation. II. Results. *The Astrophysical Journal*, 207:141–158, Jul 1976.

[60] Simon Coudé, Pierre Bastien, Martin Houde, and others. The JCMT BISTRO Survey: The Magnetic Field of the Barnard 1 Star-forming Region. *The Astrophysical Journal*, 877(2):88, Jun 2019.

[61] L. M. Fissel, P. A. R. Ade, F. E. Angilè, and others. Balloon-Borne Submillimeter Polarimetry of the Vela C Molecular Cloud: Systematic Dependence of Polarization Fraction on Column Density and Local Polarization-Angle Dispersion. *The Astrophysical Journal*, 824:134, June 2016.

[62] T. Pillai, J. Kauffmann, J. C. Tan, and others. Magnetic Fields in High-mass Infrared Dark Clouds. *The Astrophysical Journal*, 799(1):74, Jan 2015.

[63] Ya-Wen Tang, Paul T. P. Ho, Patrick M. Koch, Stephane Guilloteau, and Anne Dutrey. Dust Continuum and Polarization from Envelope to Cores in Star Formation: A Case Study in the W51 North Region. *The Astrophysical Journal*, 763(2):135, Feb 2013.

[64] Tao-Chung Ching, Shih-Ping Lai, Qizhou Zhang, and others. Magnetic Fields in the Massive Dense Cores of the DR21 Filament: Weakly Magnetized Cores in a Strongly Magnetized Filament. *The Astrophysical Journal*, 838(2):121, Apr 2017.

[65] Charles L. H. Hull and Qizhou Zhang. Interferometric observations of magnetic fields in forming stars. *Frontiers in Astronomy and Space Sciences*, 6:3, Mar 2019.

[66] P. Hennebelle and S. Fromang. Magnetic processes in a collapsing dense core. I. Accretion and ejection. *Astronomy & Astrophysics*, 477:9–24, January 2008.

[67] D. Seifried, R. Banerjee, R. E. Pudritz, and R. S. Klessen. Turbulence-induced disc formation in strongly magnetized cloud cores. *Monthly Notices of the Royal Astronomical Society*, 432:3320–3331, July 2013.

[68] J. Masson, G. Chabrier, P. Hennebelle, N. Vaytet, and B. Commercon. Ambipolar diffusion in low-mass star formation. I. General comparison with the ideal magnetohydrodynamic case. *Astronomy & Astrophysics*, 587:A32, March 2016.

[69] G. Chabrier, A. Johansen, M. Janson, and R. Rafikov. Giant Planet and Brown Dwarf Formation. In Henrik Beuther, Ralf S. Klessen, Cornelis P. Dullemond, and Thomas Henning, editors, *Protostars and Planets VI*, page 619, Jan 2014.

[70] T. Liu, Q. Zhang, K.-T. Kim, and others. Planck Cold Clumps in the λ Orionis Complex. I. Discovery of an Extremely Young Class 0 Protostellar Object and a Proto-brown Dwarf Candidate in the Bright-rimmed Clump PGCC G192.32-11.88. *The Astrophysical Journal Supplement*, 222:7, January 2016.

[71] A. Soam, Jugmi Kwon, G. Maheswar, Motohide Tamura, and Chang Won Lee. First Optical and Near-infrared Polarimetry of a Molecular Cloud Forming a Proto-brown Dwarf Candidate. *The Astrophysical Journal Letters*, 803(2):L20, Apr 2015.

[72] P. Y. Hsieh, P. M. Koch, W. T. Kim, and others. Magnetized Inflow Accretion. In C. Matulonis and H. Parsons, editors, *East Asian Observatory News*, volume 4, pages 12–14, Sep 2018.

[73] Lee Hartmann, Gregory Herczeg, and Nuria Calvet. Accretion onto Pre-Main-Sequence Stars. *Annual Review of Astronomy and Astrophysics*, 54:135–180, Sep 2016.

[74] II Evans, Neal J., Michael M. Dunham, Jes K. Jørgensen, and others. The Spitzer c2d Legacy Results: Star-Formation Rates and Efficiencies; Evolution and Lifetimes. *The Astrophysical Journal Supplement Series*, 181(2):321–350, Apr 2009.

[75] Jan Forbrich, Mark J. Reid, Karl M. Menten, and others. Extreme Radio Flares and Associated X-Ray Variability from Young Stellar Objects in the Orion Nebula Cluster. *The Astrophysical Journal*, 844(2):109, Aug 2017.

[76] Doug Johnstone, Benjamin Hendricks, Gregory J. Herczeg, and Simon Bruderer. Continuum Variability of Deeply Embedded Protostars as a Probe of Envelope Structure. *The Astrophysical Journal*, 765(2):133, Mar 2013.

[77] Gregory J. Herczeg, Doug Johnstone, Steve Mairs, and others. How Do Stars Gain Their Mass? A JCMT/SCUBA-2 Transient Survey of Protostars in Nearby Star-forming Regions. *The Astrophysical Journal*, 849(1):43, Nov 2017.

[78] Steve Mairs, Doug Johnstone, Helen Kirk, and others. The JCMT Transient Survey: Identifying Submillimeter Continuum Variability over Several Year Timescales Using Archival JCMT Gould Belt Survey Observations. *The Astrophysical Journal*, 849(2):107, Nov 2017.

[79] Doug Johnstone, Gregory J. Herczeg, Steve Mairs, and others. The JCMT Transient Survey: Stochastic and Secular Variability of Protostars and Disks In the Submillimeter Region Observed over 18 Months. *The Astrophysical Journal*, 854(1):31, Feb 2018.

[80] Ray S. Furuya, Hiroko Shinnaga, Kouichiro Nakanishi, Munetake Momose, and Masao Saito. A Giant Flare on a T Tauri Star Observed at Millimeter Wavelengths. *Publications of the Astronomical Society of Japan*, 55:L83–L87, Dec 2003.

[81] J. Forbrich, K. M. Menten, and M. J. Reid. A 1.3 cm wavelength radio flare from a deeply embedded source in the Orion BN/KL region. *Astronomy & Astrophysics*, 477(1):267–272, Jan 2008.

[82] Steve Mairs, Bhavana Lalchand, Geoffrey C. Bower, and others. The JCMT Transient Survey: An Extraordinary Submillimeter Flare in the T Tauri Binary System JW 566. *The Astrophysical Journal*, 871(1):72, Jan 2019.

[83] Hyunju Yoo, Jeong-Eun Lee, Steve Mairs, and others. The JCMT Transient Survey: Detection of Submillimeter Variability in a Class I Protostar EC 53 in Serpens Main. *The Astrophysical Journal*, 849(1):69, Nov 2017.

[84] D. T. Chuss, B.-G. Andersson, J. Bally, and others. HAWC+/SOFIA Multiwavelength Polarimetric Observations of OMC-1. *The Astrophysical Journal*, 872:187, February 2019.

[85] A. Lèbre, M. Aurière, N. Fabas, and others. Search for surface magnetic fields in Mira stars. First detection in χ Cygni. *Astronomy & Astrophysics*, 561:A85, Jan 2014.

[86] F. Herpin, A. Baudry, C. Thum, D. Morris, and H. Wiesemeyer. Full polarization study of SiO masers at 86 GHz. *Astronomy & Astrophysics*, 450(2):667–680, May 2006.

[87] W. H. T. Vlemmings, E. M. L. Humphreys, and R. Franco-Hernández. Magnetic Fields in Evolved Stars: Imaging the Polarized Emission of High-frequency SiO Masers. *The Astrophysical Journal*, 728(2):149, Feb 2011.

[88] Thavisha E. Dharmawardena, Francisca Kemper, Peter Scicluna, and others. Extended Dust Emission from Nearby Evolved Stars. *Monthly Notices of the Royal Astronomical Society*, 479(1):536–552, Sep 2018.

[89] M. R. M. Leão, E. M. de Gouveia Dal Pino, D. Falceta-Goncalves, C. Melioli, and F. G. Geraissate. Local star formation triggered by supernova shocks in magnetized diffuse neutral clouds. *Monthly Notices of the Royal Astronomical Society*, 394(1):157–173, Mar 2009.

[90] J. L. West, S. Safi-Harb, T. Jaffe, and others. The connection between supernova remnants and the Galactic magnetic field: A global radio study of the axisymmetric sample. *Astronomy & Astrophysics*, 587:A148, Mar 2016.

[91] J. Rho, H. L. Gomez, A. Boogert, and others. A dust twin of Cas A: cool dust and 21 μm silicate dust feature in the supernova remnant G54.1+0.3. *Monthly Notices of the Royal Astronomical Society*, 479(4):5101–5123, Oct 2018.

[92] Brian J. Williams and Tea Temim. *Infrared Emission from Supernova Remnants: Formation and Destruction of Dust*, page 2105. 2017.

[93] O. Löhmer, A. Wolszczan, and R. Wielebinski. A search for cold dust around neutron stars. *Astronomy & Astrophysics*, 425:763–766, Oct 2004.

[94] Pablo Fosalba, Alex Lazarian, Simon Prunet, and Jan A. Tauber. Statistical Properties of Galactic Starlight Polarization. *The Astrophysical Journal*, 564(2):762–772, Jan 2002.

[95] A. Fletcher, R. Beck, A. Shukurov, E. M. Berkhuijsen, and C. Horellou. Magnetic fields and spiral arms in the galaxy M51. *Monthly Notices of the Royal Astronomical Society*, 412(4):2396–2416, Apr 2011.

[96] Rainer Beck. Magnetic fields in the nearby spiral galaxy IC 342: A multi-frequency radio polarization study. *Astronomy & Astrophysics*, 578:A93, Jun 2015.

[97] Rainer Beck. Magnetic fields in spiral galaxies. *The Astronomy and Astrophysics Review*, 24(1):4, Dec 2015.

[98] Rainer Beck, Axel Brandenburg, David Moss, Anvar Shukurov, and Dmitry Sokoloff. Galactic magnetism: Recent developments and perspectives. *Annual Review of Astronomy and Astrophysics*, 34(1):155–206, 1996.

[99] A. Ordog, J. C. Brown, R. Kothes, and T. L. Landecker. Three-dimensional structure of the magnetic field in the disk of the Milky Way. *Astronomy & Astrophysics*, 603:A15, Jul 2017.

[100] A. Saintonge, C. D. Wilson, T. Xiao, and others. JINGLE, a JCMT legacy survey of dust and gas for galaxy evolution studies - I. Survey overview and first results. *Monthly Notices of the Royal Astronomical Society*, 481:3497–3519, December 2018.

[101] Martin Houde, Talayeh Hezareh, Scott Jones, and Fereshte Rajabi. Non-Zeeman Circular Polarization of Molecular Rotational Spectral Lines. *The Astrophysical Journal*, 764(1):24, Feb 2013.

[102] B. Adebahr, M. Krause, U. Klein, and others. <ASTROBJ>M 82</ASTROBJ> - A radio continuum and polarisation study. I. Data reduction and cosmic ray propagation. *Astronomy & Astrophysics*, 555:A23, Jul 2013.

[103] Serena Bertone, Corina Vogt, and Torsten Enßlin. Magnetic field seeding by galactic winds. *Monthly Notices of the Royal Astronomical Society*, 370(1):319–330, Jul 2006.

[104] T. J. Jones, C. D. Dowell, E. Lopez Rodriguez, and others. SOFIA Far-infrared Imaging Polarimetry of M82 and NGC 253: Exploring the Supergalactic Wind. *The Astrophysical Journal Letters*, 870:L9, January 2019.

[105] E. Lopez-Rodriguez, R. Antonucci, R.-R. Chary, and M. Kishimoto. The Highly Polarized Dusty Emission Core of Cygnus A. *The Astrophysical Journal Letters*, 861:L23, July 2018.

[106] F. H. Vincent, W. Yan, O. Straub, A. A. Zdziarski, and M. A. Abramowicz. A magnetized torus for modeling Sagittarius A* millimeter images and spectra. *Astronomy & Astrophysics*, 574:A48, Jan 2015.

[107] F. H. Vincent, M. A. Abramowicz, A. A. Zdziarski, and others. Multi-wavelength torus-jet model for Sagittarius A*. *Astronomy & Astrophysics*, 624:A52, Apr 2019.

[108] Pei-Ying Hsieh, Patrick M. Koch, Woong-Tae Kim, and others. A Magnetic Field Connecting the Galactic Center Circumnuclear Disk with Streamers and Mini-spiral: Implications from 850 μm Polarization Data. *The Astrophysical Journal*, 862(2):150, Aug 2018.

[109] Event Horizon Telescope Collaboration, Kazunori Akiyama, Antxon Alberdi, and others. First M87 Event Horizon Telescope Results. I. The Shadow of the Supermassive Black Hole. *The Astrophysical Journal Letters*, 875(1):L1, Apr 2019.

[110] S. Issaoun, M. D. Johnson, L. Blackburn, and others. The Size, Shape, and Scattering of Sagittarius A* at 86 GHz: First VLBI with ALMA. *The Astrophysical Journal*, 871(1):30, Jan 2019.

[111] A. P. Marscher. Relativistic Jets in Active Galactic Nuclei. In P. A. Hughes and J. N. Bregman, editors, *Relativistic Jets: The Common Physics of AGN, Microquasars, and Gamma-Ray Bursts*, volume 856 of *American Institute of Physics Conference Series*, pages 1–22, September 2006.

[112] E. I. Robson, J. A. Stevens, and T. Jenness. Observations of flat-spectrum radio sources at λ850 μm from the James Clerk Maxwell Telescope - I. 1997 April to 2000 April. *Monthly Notices of the Royal Astronomical Society*, 327:751–770, November 2001.

[113] S. G. Jorstad, A. P. Marscher, J. A. Stevens, and others. Multiwaveband Polarimetric Observations of 15 Active Galactic Nuclei at High Frequencies: Correlated Polarization Behavior. *The Astronomical Journal*, 134:799–824, August 2007.

[114] A. P. Marscher. Turbulent, Extreme Multi-zone Model for Simulating Flux and Polarization Variability in Blazars. *The Astrophysical Journal*, 780:87, January 2014.

[115] J. W. Lee, S.-S. Lee, S. Kang, D.-Y. Byun, and S. S. Kim. Detection of millimeter-wavelength intraday variability in polarized emission from S5 0716+714. *Astronomy & Astrophysics*, 592:L10, August 2016.

[116] E. Lopez-Rodriguez, A. Alonso-Herrero, T. Diaz-Santos, and others. The origin of the mid-infrared nuclear polarization of active galactic nuclei. *Monthly Notices of the Royal Astronomical Society*, 478(2):2350–2358, Aug 2018.

[117] S.-S. Lee, S. Kang, D.-Y. Byun, and others. First Detection of 350 Micron Polarization from a Radio-loud AGN. *The Astrophysical Journal Letters*, 808:L26, July 2015.

[118] R. M. Crutcher, B. Wandelt, C. Heiles, E. Falgarone, and T. H. Troland. Magnetic Fields in Interstellar Clouds from Zeeman Observations: Inference of Total Field Strengths by Bayesian Analysis. *The Astrophysical Journal*, 725:466–479, December 2010.

[119] A. Lazarian and Thiem Hoang. Radiative torques: analytical model and basic properties. *Monthly Notices of the Royal Astronomical Society*, 378(3):910–946, Jul 2007.

[120] B. G. Andersson, A. Lazarian, and John E. Vaillancourt. Interstellar Dust Grain Alignment. *Annual Review of Astronomy and Astrophysics*, 53:501–539, Aug 2015.

[121] Archana Soam, Kate Pattle, Derek Ward-Thompson, and others. Magnetic Fields toward Ophiuchus-B Derived from SCUBA-2 Polarization Measurements. *The Astrophysical Journal*, 861(1):65, Jul 2018.

[122] T. J. Jones, M. Bagley, M. Krejny, B. G. Andersson, and P. Bastien. Grain Alignment in Starless Cores. *The Astronomical Journal*, 149(1):31, Jan 2015.

[123] T. J. Jones, Michael Gordon, Dinesh Shenoy, and others. SOFIA Mid-infrared Imaging1 and CSO Submillimeter Polarimetry Observations of G034.43+00.24 MM1. *The Astronomical Journal*, 151(6):156, Jun 2016.

[124] Kate Pattle, Shih-Ping Lai, Tetsuo Hasegawa, and others. JCMT BISTRO Survey observations of the Ophiuchus Molecular Cloud: Dust grain alignment properties inferred using a Ricean noise model. *arXiv e-prints*, page arXiv:1906.03391, Jun 2019.

[125] R. H. Hildebrand, J. L. Dotson, C. D. Dowell, D. A. Schleuning, and J. E. Vaillancourt. The Far-Infrared Polarization Spectrum: First Results and Analysis. *The Astrophysical Journal*, 516(2):834–842, May 1999.

[126] John E. Vaillancourt, C. Darren Dowell, Roger H. Hildebrand , and others. New Results on the Submillimeter Polarization Spectrum of the Orion Molecular Cloud. *The Astrophysical Journal Letters*, 679(1):L25, May 2008.

[127] T. J. Bethell, A. Chepurnov, A. Lazarian, and J. Kim. Polarization of Dust Emission in Clumpy Molecular Clouds and Cores. *The Astrophysical Journal*, 663(2):1055–1068, Jul 2007.

[128] Natalie N. Gandilo, Peter A. R. Ade, Francesco E. Angilè, and others. Submillimeter Polarization Spectrum in the Vela C Molecular Cloud. *The Astrophysical Journal*, 824(2):84, Jun 2016.

[129] Jamil A. Shariff, Peter A. R. Ade, Francesco E. Angilè, and others. Submillimeter Polarization Spectrum of the Carina Nebula. *The Astrophysical Journal*, 872(2):197, Feb 2019.

[130] B. J. Dober, P. A. R. Ade, P. Ashton, and others. The next-generation BLASTPol experiment. In *Millimeter, Submillimeter, and Far-Infrared Detectors and Instrumentation for Astronomy VII*, volume 9153 of *Proc. SPIE*, page 91530H, July 2014.

[131] D. A. Harper, M. C. Runyan, C. D. Dowell, and others. HAWC+, the Far-Infrared Camera and Polarimeter for SOFIA. *Journal of Astronomical Instrumentation*, 7:1840008–1025, 2018.

[132] Richard M. Crutcher. Magnetic Fields in Molecular Clouds. *Annual Review of Astronomy and Astrophysics*, 50:29–63, Sep 2012.

[133] Martin Houde, John E. Vaillancourt, Roger H. Hildebrand, Shadi Chitsazzadeh, and Larry Kirby. Dispersion of Magnetic Fields in Molecular Clouds. II. *The Astrophysical Journal*, 706(2):1504–1516, Dec 2009.

[134] M. Houde. Magnetic Fields in Three Dimensions. In Pierre Bastien, Nadine Manset, Dan P. Clemens, and Nicole St-Louis, editors, *Astronomical Polarimetry 2008: Science from Small to Large Telescopes*, volume 449 of *Astronomical Society of the Pacific Conference Series*, page 213, Nov 2011.

[135] P. Goldreich and N. D. Kylafis. On mapping the magnetic field direction in molecular clouds by polarization measurements. *The Astrophysical Journal Letters*, 243:L75–L78, Jan 1981.

[136] N. Galitzki, P. A. R. Ade, F. E. Angilè, and others. The Next Generation BLAST Experiment. *Journal of Astronomical Instrumentation*, 3:1440001, November 2014.

[137] Sean Bryan, Jason Austermann, Daniel Ferrusca, and others. Optical design of the TolTEC millimeter-wave camera. In *Proc. SPIE*, volume 10708 of *Society of Photo-Optical Instrumentation Engineers (SPIE) Conference Series*, page 107080J, Jul 2018.

[138] R. Adam, A. Adane, P. A. R. Ade, and others. The NIKA2 large-field-of-view millimetre continuum camera for the 30 m IRAM telescope. *Astronomy & Astrophysics*, 609:A115, Jan 2018.

[139] Luis Esteras Otal. *The Optical System and the Astronomical Potential of A-MKID, a New Camera Using Microwave Kinetic Inductance Detector Technolog*. PhD thesis, University of Bonn, 08 2014.

STUDIES OF EVOLVED STARS IN THE NEXT DECADE

EAO SUBMILLIMETRE FUTURES PAPER SERIES, 2019

Peter Scicluna[*1] • **Hiroko Shinnaga**[2] • **Jonathan Marshall**[1] • **Jan Wouterloot**[3] • **Iain McDonald**[4]
Steven Goldman[5] • **Sofia Wallström**[6] • **Jacco Th. van Loon**[7] • **Thavisha Dharmawardena**[1]
Lapo Fanciullo[1] • **Sundar Srinivasan**[8]

[1]*Academia Sinica Institute of Astronomy and Astrophysics, AS/NTU Astronomy-Mathematics Building, No 1. Sec. 4 Roosevelt Rd, Taipei, Taiwan*
[2]*Department of Physics and Astronomy, Amanogawa Galaxy Astronomy Research Center (AGARC), Kagoshima University, 1-21-35 Korimoto, Kagoshima, Japan*
[3]*East Asian Observatory (JCMT), 660 N. A'ohōkū Place, Hilo, Hawai'i, USA, 96720*
[4]*Jodrell Bank Centre for Astrophysics, School of Physics and Astronomy, University of Manchester, M13 9PL, Manchester, UK*
[5]*Space Telescope Science Institute, 3700 San Martin Drive, Baltimore, MD 21218, USA*
[6]*Institute of Astronomy, KU Leuven, Celestijnenlaan 200D bus 2401, 3001 Leuven, Belgium*
[7]*Lennard-Jones Laboratories, Keele University, ST5 5BG, UK*
[8]*Instituto de Radioastronomía y Astrofísica, UNAM., Apdo. Postal 72-3 (Xangari), Morelia, Michoacán 58089, Michoacán, México*

ABSTRACT

This white paper discusses recent progress in the field of evolved stars, primarily highlighting the contributions of the James Clerk Maxwell Telescope. It discusses the ongoing project, the *Nearby Evolved Stars Survey* (NESS), and the potential to build upon NESS in the next decade. It then outlines a number of science cases which may become feasible with the proposed 850 μm camera which is due to become available at the JCMT in late 2022. These include mapping the extended envelopes of evolved stars, including in polarisation, and time-domain monitoring of their variations. The improved sensitivity of the proposed instrument will facilitate statistical studies that put the morphology, polarisation properties and sub-mm variability in perspective with a relatively modest commitment of time that would be impossible with current instrumentation. We also consider the role that could be played by other continuum wavelengths, heterodyne instruments or other facilities in contributing towards these objectives.

1 Introduction

Evolved stars play key roles in the chemical enrichment of the Universe; most directly, they return material to the interstellar medium (ISM), fuelling future star formation with hydrogen, and enrich the ISM with dust and the products of nucleosynthesis [1]. The rates at which this mass is lost are also critical; in low- and intermediate-mass stars, taking place primarily on the asymptotic giant branch (AGB), it impacts the amount of metals they process (He, C, N, O), and s-process enrichment [2]. Meanwhile for massive stars, mass-loss controls their lifetimes (and hence the injection of ionising photons into the ISM) and which supernova channel will consume them, dictating the production of iron-peak elements and the turbulence of the ISM [e.g. see 3, for a recent review]. To understand the physics and chemistry of the ISM, it is therefore crucial to understand the physics of mass loss and its impact on stellar evolution and the ISM.

Nevertheless, a number of important questions remain open. We do not yet understand how, when and how much mass-loss takes place on the AGB, meaning that yields for low- and intermediate-mass stars are difficult to predict, as they are sensitive to the total length of the AGB phase. While the winds are expected to be driven by radiation pressure on dust, it is not clear when this becomes relevant and how it depends on the properties of the dust, whose formation process remains similarly poorly understood [e.g. 4]. For low-mass stars, mass loss on the red giant branch

[*]peterscicluna@asiaa.sinica.edu.tw

(RGB) has a significant impact on their AGB evolution and on the initial–final mass relation for white dwarves. We know that mass-loss from red supergiants (RSGs) can dramatically alter the evolution of massive stars, controlling their lifetimes and dramatically altering their pre-supernova nucleosynthesis, yet the mechanisms driving the mass loss remain elusive with several competing suggestions [3]. In all of these cases, the time-variability of the mass loss will also play an important role, as will any companions, if present, which may shape the outflow [e.g. 5, 6] or entirely alter the evolutionary pathway [e.g. 7].

Sub-mm astronomy has a key role to play in exploring these questions. The low-J rotational transitions of CO are the most direct means of estimating gas mass-loss rates for evolved stars, while the ^{13}CO isotopologues are an effective way of measuring the outcomes of nucleosynthesis when the photosphere is obscured by circumstellar dust and provide an independent constraint on the optical depth of the envelope [e.g. 8]. If the winds are dust-driven, the properties of the dust are key to driving the wind, and the sub-mm continuum is sensitive to both the size and composition of dust grains.

2 Current Status of Evolved-Star Science in the Sub-mm

Single-dish sub-mm studies of evolved stars have a long and fruitful history. As luminous sources with abundant molecules, CO-line emission from evolved stars has been a particular target. This has allowed us to determine mass-loss rates for samples of objects [e.g. 9, 10, 11]. While many observations of the low-J CO lines exist, homogeneous compilations for large, volume-limited samples are rarer [e.g. 12, 13, 14]. Such samples are essential to robustly estimate the total return of gas to the ISM from evolved stars and their lifetimes, and the large samples are useful for other scientific objectives such as studying the relationships between pulsations, dust formation and mass loss.

However, continuum studies have been more limited, with the relatively weak dust emission more difficult to observe. Recently, [15] and [16] have published the results of observing small samples of evolved stars using APEX/LABOCA [17] and JCMT/SCUBA-2 [18] respectively. Both studies detect bright continuum emission from the sources observed. However, where the low mapping speed of LABOCA was insufficient to resolve the envelopes [15], [16] were able to detect extended emission throughout the sample with SCUBA-2, which is able to reach the same depth in roughly 1 per cent of the time. This extended emission traces the historic mass loss, and hence the variation of mass loss on timescales of centuries, and almost all sources appear to be inconsistent with a constant mass-loss rate [16].

Motivated by the sensitivity of SCUBA-2 and the need to compare volume-limited samples of Galactic sources to the extragalactic samples studied with e.g. *Spitzer*, the Nearby Evolved Stars Survey (NESS) was initiated at the JCMT. NESS is exploiting both heterodyne and continuum observations to constrain the total gas- and dust-return rates to the Solar Neighbourhood, the dust-to-gas ratios of the outflows, the importance of cold, historic mass loss, and the physical processes driving mass loss, for a statistical sample of ~ 400 nearby evolved stars. NESS has since expanded to include the Southern sky, using APEX, and lower frequency lines, using the Nobeyama 45-metre telescope. Preliminary results from the JCMT are favourable, with a high detection rate in both lines and continuum ($\gtrsim 75\%$, Scicluna et al., in prep; Wallström et al., in prep).

While NESS is observing a large sample at relatively low resolution to obtain a statistical picture, it is important to complement this with higher-resolution studies. For example, Atacama Large Millimeter/sub-millimeter Array (ALMA) observations at $\sim$ mas resolution are exploring which molecules are involved in dust formation [e.g. 19] while the new extreme adaptive optics instruments are able to trace the distribution of the newly-formed dust [e.g. 20]. Combining these with the large database of mass-loss rates provided by NESS will enable an exploration of the relationships between mass loss and the physics and chemistry of mass loss, by providing a robust sample for which the density, momentum and chemistry of the outflow is known. This will help to put studies observing smaller samples in greater detail, such as the ALMA projects DEATH STAR and ATOMIUM in perspective.

The keys to observing extended emission from evolved stars are sensitivity and dynamic range; the typical evolved star has a bright, point-like (to the JCMT) central component, surrounded by a faint halo of emission that extends to very large radii [e.g. 16, find radii up to an arcminute, and results from *Herschel* suggest that higher sensitivity would most likely detect emission at larger distances]. Successful recovery of this halo requires that the observation be sensitive enough to identify it, but it must also not be filtered out by observing or data-reduction techniques; chopping and high-pass filtering remove unwanted background or atmospheric emission, but also filter out interesting astronomical signals if they are on the wrong size scale. Therefore, improved techniques for the recovery of faint emission on intermediate angular scales will be key to continuing these studies in future. While recent projects have made advances in ensuring that all the flux is recovered from a source of this kind [e.g. JINGLE, 21], this remains an intensive process with many open problems.

3 The Next Decade

In spite of ongoing progress, many questions remain open. In this section, we explore some of these issues and how current and future instrumentation in the sub-mm can contribute to them.

3.1 Current Facilities

Enrichment While NESS provides the data to estimate the total mass return to the Solar Neighbourhood, and hence the fuel for future star formation, to understand the chemical evolution of galaxies, it is critical to understand the origins of heavy elements. Different mass-ranges of evolved stars will undergo significantly different nucleosynthetic processes, returning different ranges of metals to the ISM [2, provide a good review relevant to this section]. For example, the triple-α process produces carbon-12, and dredge-up from C-rich AGB stars is expected to be a major contributor to the carbon budget, particularly at low metallicity when C-stars are more numerous. On the other hand, Hot Bottom Burning (HBB) converts ^{12}C into ^{13}C and N, reducing C production for massive AGB stars and increasing surface N. Finally, rotational mixing in massive stars enriches the surfaces of RSGs and Wolf-Rayets (WRs) with fusion products from a variety of processes. All of these elements are then returned to the ISM through winds.

Hence, in order to understand the enrichment of the ISM by evolved stars, we must understand not only how much each star contributes, but how the mass-loss rate changes and how the composition of the ejecta evolves with time. The large NESS sample can begin to answer the first of these two unknowns through its large, volume-limited sample by constraining the lifetimes of the different phases, however for the shortest phases, which may be disproportionately important, more sources are required to avoid the problem of small-number statistics. Doubling the NESS sample, corresponding to an increase in distance of $\approx \sqrt{2}$, would provide substantially larger samples of less common objects, including C-stars, S-stars and RSGs without a significant increase in integration time, providing the data required to crack this problem.

To explore the evolution of the outflow composition, ^{13}CO provides a useful proxy [e.g. 8], as the ^{13}C abundance is sensitive to both of the key AGB nucleosythetic processes, the triple-α process and HBB. However, the lower abundance compared to ^{12}CO necessitates longer integration times to achieve the same SNR [e.g. compare the ^{12}CO and ^{13} CO observations of 22]. However, the new receivers of Nāmakanui provide a substantial improvement in sensitivity for compact sources compared to RxA3m and HARP, providing the means to observe large samples to significantly greater depths. This will provide the means to achieve constraints on the isotope ratio across the entire NESS sample, revealing the evolution of the ^{13}C abundance. Furthermore, new large single-dish telescopes such as the Large Millimeter Telescope (LMT), or future projects such as AtLAST, provide the further sensitivity improvements required to probe weaker isotopologues to trace the evolution of other elements that play roles in AGB nucleosynthesis, such as C^{18}O or HC^{15}N.

3.2 Future Developments

While the size of the NESS sample provides a useful statistical overview, it is fundamentally limited in its ability to answer key questions by the nature of the observations. NESS is collecting sub-mm photometry for many sources, but only a subset of observations were designed to detected the extended emission associated with historic mass loss. As intrinsically variable sources, it is also important to consider the changes in the sources at all wavelengths, requiring many observing periods. In particular, the variations are driven by pulsations, which are believed to play an important role in initiating the mass loss. And magnetic fields, whose importance to various classes of evolved stars has been debated over the years, remain poorly understood. However, with current instrumentation, exploring these issues for large samples would be prohibitively expensive.

The proposed future instrument is expected to provide the same rms noise at 850 μm in roughly one tenth the time SCUBA-2 can achieve. Thanks to its intrinsic polarisation sensitivity, this increases to a factor of 20 improvement for polarimetry. These improvements are driven by improved per-pixel sensitivity, higher detector yield, and larger field of view. In the future, a similar improvement is projected for 450 μm as well, either through a second instrument or an upgrade of the first. This order-of-magnitude improvement will be transformative for several areas of evolved-star science, and we will examine the potential impact of these and other potential developments below, along with how it fits in with other facilities.

Mass-loss histories Studying the dust mass-loss histories of AGB stars is a key goal of NESS. However, due to the increased depth required to consistently detect extended emission, only a subset ($\approx 10\%$) of NESS sources have been selected for this. These sources are preferentially nearby ($d \leq 300$ pc) with moderate mass-loss rates; not only is the sample barely large enough to develop a statistical picture, but it is likely to be biased as well. While other sources may

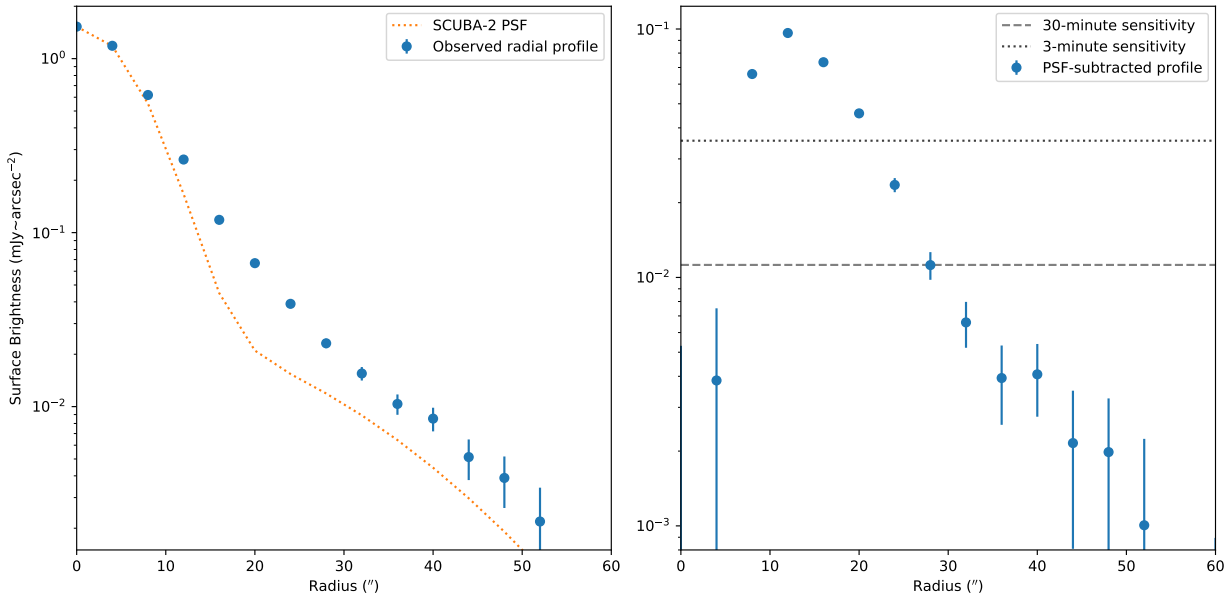

Figure 1: Deep radial profile of o Cet from SCUBA-2 observations (left) and PSF-subtracted radial profile (right). This profile required 40 hours with SCUBA-2, and is expected to require $\sim$ 4 hours with the proposed 850 μm camera. The dashed lines on the right panel indicate the expected sensitivity to extended emission for 30 and 3 minutes of integration with the new camera, and the regions of extended emission to which they would be sensitive.

also show resolved emission, these will tend to be the brightest sources with the highest mass-loss rates where less depth is required to detect the emission, injecting new biases into the sample.

An improvement of a factor of 10 in mapping speed would mean that even our shortest observations would begin to approach the confusion limit, highlighting the superior sensitivity of the future instrument. At present, all NESS sources are observed using a single 30-minute Daisy, sufficient for photometry, while selected sources are observed a factor of two deeper (2 hours). However, a 30-minute scan with the proposed camera would provide sensitivity equivalent to 5 hours with SCUBA-2, and the confusion limit would be reached in under an hour for reasonable conditions, enabling a much deeper search for extended emission than is currently possible.

An idea of what can be obtained can be seen from observations of the archetypal source o Cet (Mira), which has a moderate mass-loss rate [$\sim 2.5 \times 10^{-7}\,\mathrm{M}_\odot\,\mathrm{yr}^{-1}$, 22] and is rather nearby ($\sim 100\,$pc. Because it is used as a pointing source, [16] were able to compile all SCUBA-2 observations to provide $\approx$ 40 hours of integration. The resulting radial profile can be seen in Fig. 1. Such an observation could be repeated in just 4 hours with the proposed instrument – given that this would allow for a better choice of observing conditions, this might even result in deeper data. Also indicated on the plot are the expected depths that would be achieved with the new instrument in 30 minutes or 3 minutes (the latter is equivalent to 30 minutes with SCUBA-2), under the assumption that noise scales with $\sqrt{t_{\mathrm{int}}}$ and including the advantages of azimuthal averaging. It is immediately clear that the new camera will reveal a vastly larger area around any individual star than SCUBA-2 is able to detect, with a $\sim$50% increase in the radius for a single scan. This corresponds to a longer look-back time, giving a longer history of mass loss. Along with probing a longer history for any given source, this will expand the sample of stars amenable to having their mass-loss history studied in dust continuum in two ways: by being sensitive to fainter extended emission, it will enable to study of sources with lower surface brightness (i.e. lower mass-loss rates); by probing longer timescales, sources at larger distances (harder to resolve) will become feasible. A future large program comparable to NESS could provide mass-loss histories for all 400 stars in roughly 200 hours. For the nearest AGB stars in such a sample ($\sim 60\,$pc), the resolution of the JCMT would correspond to a timescale of $\sim$500 yr, while for the furthest stars ($\sim 2\,$kpc) we could expect to recover emission covering timescales up to 100 000 yr ($\sim 90''$).

Beyond improved sensitivity, the new camera will provide several other advantages to the study of mass-loss history. The improved stability of MKIDs vs. TESs is expected to improve the fidelity of images and our ability to combine multiple scans. This would give a corresponding improvement in our confidence of the reality of structures, particularly low-surface-brightness emission, which might be further aided if increases in the field-of-view provide improvements

in the estimation of the background and recovery of total power. This will be key to interpreting mass-loss histories and, potentially, asymmetry in AGB stars, but also depends strongly on the eventual data-reduction method employed. As noted above, SCUBA-2 data reduction becomes difficult when the required dynamic range is high or the source is faint but extended, and it will be important to mitigate these issues for evolved-star science in future.

While improved sensitivity will probe longer timescales than SCUBA-2 is able to, the only way to probe shorter timescales in the continuum is through higher resolution. A comparable improvement in sensitivity at 450 μm would probe variations on timescales a factor $\sim$2 shorter, particularly in the bright inner outflow. A byproduct of the addition of 450 would be to probe the wavelength-dependence of the emission (α), which is primarily determined by the size and composition of dust grains. The ability to map variations in α would probe the mechanisms driving the variable mass loss, by revealing whether dust properties change as a result. While 450 offers an optimal choice of resolution and available time, other, longer wavelengths could provide comparable insights. In particular, there are suggestions that C-stars have a significant flux excess at wavelengths $> 500\mu$m, but the origin of this excess remains elusive. Whether this represents a change in the wavelength dependence of the dust opacity or an additional population of dust requires further observations at longer wavelengths. Observations in the 1 – 3 mm range, particularly in regions that avoid contamination from CO or other bright lines, are essential to determine whether this is a bump or a double power-law. While the longer part of this range is perfectly suited to 50 m-class facilities such as the LMT thanks to their higher resolution, the ability to observe at e.g. 1.1 mm with the JCMT may prove particularly interesting, especially in worse weather.

An alternative way of probing shorter timescales (rather than shorter wavelength) is to combine JCMT observations with data from the SMA or ALMA. While *uv*-filtering prohibits large-scale mapping with interferometers, the combination of sensitive interferometric mosaics with JCMT maps will enable the recovery of both large- and small-scale structures. By tuning the resolution of the interferometric data, this could help to homogenise the shortest timescales probed by the maps, rather than losing the shortest timescales in more distant sources.

While the continuum is easy to trace, dust makes up only a small fraction of the outflowing material, and it will be difficult to distinguish between variations in mass loss and variations in dust-to-gas ratio from the continuum alone. It is therefore vital to have comparable probes of the mass-loss history from lines. As with the continuum, the gas mass-loss history can be probed by mapping low-excitation line emission from the outer envelope (see e.g. Fig. 2, which shows a preliminary reduction of NESS data for this purpose showing extended CO emission out to $\sim 30''$); this has certain advantages for comparison with the continuum, primarily that by tracing the cold gas the results are directly comparable to the cold dust revealed in the continuum, and that these low-J lines are sensitive to the external photodissociation of the envelope. This has the added benefit of allowing the line contribution to the continuum flux to be determined, which has been shown to be small but have a significant impact on the interpretation of extended continuum emission [e.g. 23].

However, since different lines are primarily emitted in different regions of the outflow thanks to the differences in excitation temperature of different lines, gas mass-loss histories can also be explored through the use of multiple lines [e.g. 24, 25]. The bright lines of CO, HCN and their isotopologues are particularly useful for this, and the limitation of angular resolution can be circumvented by going further up the rotational ladder. A number of useful lines lie within atmospheric windows, primarily the (4–3), (6–5) and (7–6) lines of CO, which can be observed in ALMA bands 8, 9 and 10 respectively. Previous studies have used these lines along with the lower-J lines to infer multiple epochs of mass loss on timescales of centuries [25]. While these higher-frequency lines require good weather to observe them, the highly efficient flexible scheduling enjoyed by the JCMT makes this one of the few sites where this would be a reasonable proposition, and at present the only site in the Northern Hemisphere. However, in future the Greenland telescope may provide an alternative site for these THz windows [e.g. 26].

Sub-mm variability Evolved stars are intrinsically variable, with bolometric pulsation amplitudes as high as a factor of 2.5 [27]. This variability initiates the mass loss as the pulsations launch material on ballistic trajectories suitable for dust to form; the dust is then able to provide sufficient radiation pressure to accelerate the outflow to escape [e.g. 28, and references therein]. The shocks and changes in luminosity created by these pulsations sculpt the inner outflow in a number of ways: the high densities associated with the shocks drive dust formation, while the intense radiation field near maximum light destroys some of the closest dust [e.g 28]; energy from shocks ionises a substantial fraction of material in the inner envelope, leading to free-free emission from the radio photosphere, while also fuelling a number of chemical pathways [29, 30]; and the changes in luminosity lead to large changes in the pumping of high-excitation lines and hence the energy balance of the circumstellar gas [31, 32].

Historically, this variability has typically been explored in the optical and near-infrared, however longer wavelengths provide a number of advantages. The sub-mm is free from extinction, and avoids confusion caused by changes in spectral type by primarily detecting the circumstellar emission. Furthermore, it has the potential to directly probe the influence of the variations on the outflow, rather than having to infer them indirectly: radio photospheres, dust

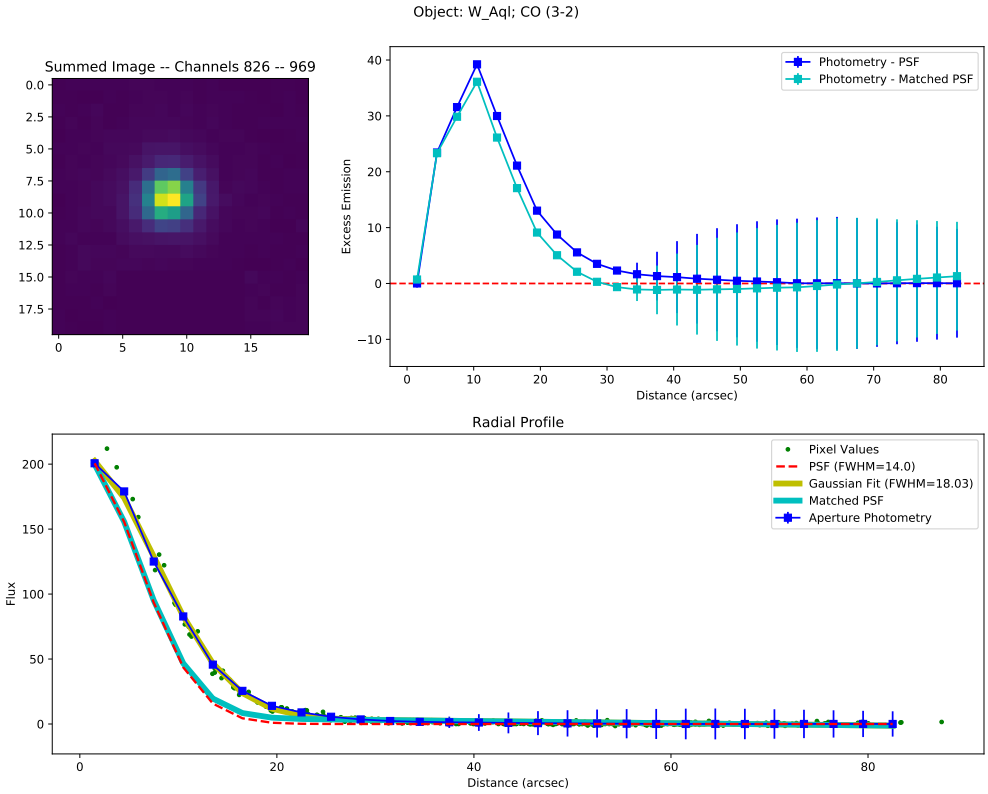

Figure 2: Example of CO map from JCMT observations, revealing significant extended emission that is likely linked to gas from historic mass loss.

and molecules all contribute to the sub-mm emission and its variability and their role can be traced through different observables. By studying variability in the sub-mm and relating that to the behaviour of the stars themselves (as probed in the optical and near-IR) we can unravel the influence of the pulsations on the inner envelope, where the outflow is launched.

A preliminary study [33] exploring the two nearby AGB stars used by SCUBA-2 as pointing sources (IRC+10216 and o Cet) found variability at 850 μm in both sources of factors ≥ 1.6 on periods that agree with those found in the optical; while the sub-mm lightcurve of o Cet is in phase with the optical, IRC+10216 was out of phase, showing better agreement with the cm-wave lightcurve of [29] for reasons that are not yet clear. However, this exploited some 40 hours of short calibration observations spread over several years for each source to construct the lightcurves. These observations were all in the regime where the photometric uncertainty is dominated by the uncertainty in the absolute flux calibration of SCUBA-2; assuming that the calibration uncertainty for the new instrument is similar to that of SCUBA-2 ($\sim$8%) there are at least 50 sources in the NESS sample that would be similarly calibration-dominated in 3 minutes of integration with the new instrument, and likely a substantial population of other sources similarly amenable to observation. For such short integration, a total of 1 hour of integration is required to detect the source in 20 epochs, sufficient to evenly sample the lightcurve if a good estimate of the period is available from short wavelengths. This suggests that samples of several tens of sources each could be feasibly explored in PI time, while a large program could potentially follow a sample of hundreds of evolved stars over a window of several years. This will provide unprecedented insights on the behaviour of the inner envelopes of evolved stars in the sub-mm. It will be particularly interesting to combine sub-mm monitoring with very high angular resolution snapshots of the inner envelope, for example mid-infrared interferometry or optical polarimetric imaging, which are also sensitive to the formation and properties of dust, and radio VLBI, which is dominated by the radio photosphere. This would reveal the relative importance of these two mechanisms, probing the importance of dust formation and shock heating across the pulsation cycle.

However, such studies depend critically on the calibration uncertainty. Given the current calibration of SCUBA-2, there is clearly a significant sample of sources that could be observed. Should the flux ratio seen in IRC+10216 and o Cet prove typical, a large number of sub-mm variables could be analysed, as 8% uncertainty would be sensitive to flux

ratios between two epochs of 1.35 – although this ignores the statistical gains from sampling over the full lightcurve. Further improvements to the calibration uncertainty would reveal smaller levels of variability, but require more time per epoch or a smaller sample. Should calibration uncertainty reach just 5%, flux ratios as low as 1.2 become observable.

Once again, a multi-wavelength capability is important, and particularly useful if it is simultaneous, giving the ability to probe phase differences between the different wavelengths. The spectral behaviour of the variability is able to distinguish between different sources of emission, which may reveal the underlying mechanism driving the variations. The exact choice of band is not particularly important, although more is always better: with mechanisms such as free-free typically being more important at longer wavelengths and dust in the sub-mm, having three or more wavelengths makes it possible to distinguish between e.g. a change in the relative importance of dust and free-free or a change in the sub-mm properties of the dust. The upcoming MKID array for the LMT, TolTEC [e.g. 34], will provide a complementary capability by mapping the 1 – 2 mm range at high efficiency in 3 bands; combined observations between the JCMT and LMT will break these degeracies, but the 850 μm window is expected to be most sensitive to the dust.

Complementary to the continuum, recent studies have found significant variability in sub-mm lines, particularly those with high excitation temperatures [e.g. 31, 32]. The variability of some of these lines correlates strongly with the changes in luminosity (probed by the near-IR), while others are strongly anti-correlated. This may be tracing changes in thermal and radiative excitation in the inner envelope as the star pulsates. However, many of these lines are weak, and although there have been some successful observations with APEX, such monitoring remains challenging. Very wide bandwidth, enabling the observation of many lines simultaneously, is useful as it both maximises the integration time per spectral point and enables robust relative calibration of the lines. Alternatively, the greater collecting area and lower beam dilution of the SMA, Morita Array or large single dishes such as the LMT may fill an important niche here.

Polarisation and Magnetic Fields Despite being fully convective and probably slow rotators, a number of studies have found significant magnetic fields in evolved stars, both at their surfaces [35] and in their envelopes [e.g. 36, 37]. These have typically relied upon Zeeman splitting of either the photospheric or maser lines, which may therefore be biased as they sample only a small fraction of the emission; photospheric lines may be affected by the presence of starspots, whose lifetimes are similar to the rotation period making it difficult to sensibly average them out, while masers naturally sample dense clumps in the inner outflow. To see the big picture and understand the typical behaviour of magnetism in evolved stars, we must observe the large-scale field in the envelope. This requires us to map the field throughout the envelope, most easily achieved in the far-IR and sub-mm.

A commonly used tracer of the magnetic field orientation is continuum polarisation at far-IR and submm wavelengths. This arises from the thermal emission of non-spherical dust grains whose angular momenta are aligned. In the ISM, grains typically align with magnetic field lines, so that the observed polarisation angle traces the magnetic field projected on the plane of the sky [38, 39, 40]. However, the envelopes of AGB stars are faint in dust, requiring deep integrations to map their extended envelopes. To date, few studies have succeeded in detecting continuum polarisation from evolved stars, and it is only with the exquisite sensitivity of ALMA that the bright RSG VY CMa has been detected [41]. Furthermore, as a rare case, Zeeman splitting of SiO transition is detected towards VY CMa [42]. Based on the deep radial profile of IRC+10216 (the brightest AGB star in the sub-mm) from [16], POL-2 is expected to need $\sim$ 30 hours of band-1 weather to detect 5% polarisation in the outer envelope. Therefore, while observations of a few sources might be feasible with SCUBA-2, a 20$\times$ increase in speed would be transformative to these studies. The brightest sources would be feasible to observe in 1 – 2 hours each, including 7 of the 15 sources observed by [16]. For the big picture, it would be feasible for a potential large program to observe scores or hundreds of evolved stars and map the polarisation in their envelopes, particularly if informed by the results of NESS or a future effort to map the outflows in the continuum with the proposed 850 μm instrument.

The currently favoured theory of grain alignment is that of radiative torques, or RATs, according to which the alignment of grains with the magnetic field is driven by the torque of an anisotropic radiation field on an asymmetrical (non-zero helicity) grain [43, 44, 45]. In the case of a weak magnetic field and/or a strong radiation field, and depending on the grains' properties, they may be aligned with the radiation field rather than the magnetic field [44, 46]. The presence of iron inclusions, which make the grains superparamagnetic, improves the efficiency of the alignment with the magnetic field [45, 47]. While RATs are currently favoured by observations [40], observational constraints on this model are for the moment mostly qualitative. Studying them in the well-constrained radiation field of evolved stars provides an opportunity to better understand RATs and dust formation at the same time.

Observations of continuum polarisation would probe a number of fundamental questions regarding evolved stars. How many of them have large-scale magnetic fields? What is the typical geometry? There is some debate as to the origin of the fields, whether they are produced by angular-momentum transfer from a companion or if another mechanism is required to explain their existence. Statistics of the presence and morphology of the large-scale field will be a key observable, as they can be compared to models of the expected population of companions, and with known binary stars.

Furthermore, comparison between the field morphology and the mass-loss history will reveal whether magnetic fields play any role in shaping the outflow. Finally, correlating the magnetic field properties with the evolutionary stage of a sample will explore how fields evolve with the stars, and if they play a role in the changes that occur as stars evolve off the AGB.

Observations of polarisation will also have important implications for studying the mass-loss process itself. For evolved stars losing significant amounts of mass the outflows are expected to be driven by radiation pressure on dust that forms close to the star, fuelled by the pulsating atmosphere of the star. As a result, the properties of the dust that forms should have a strong influence on the properties of the outflow, such as the velocity and outflow rate. Models of dust formation in the outflows of cool evolved stars typically assume the grains to be compact, uniform spheres, however this is unlikely to be the case. Deviations from symmetry have significant impacts on the absorption and scattering cross-sections [e.g. 48], and hence the radiation pressure. Similarly, one might also expect changes in the efficiency of gas-grain coupling. Fortunately, the shape – or more precisely, the axial ratio – of the grains is one of the main factor influencing the sub-mm polarisation fraction, making this a relatively straightforward property to explore.

In addition, there are interesting consequences for studying dust formation and processing. As mentioned above, grain alignment with magnetic fields is boosted by inclusions that makes grains superparamagnetic and, when the grains are rotating fast enough, exert a torque to align the grains with the field lines. In AGB stars, the most likely candidate for this is iron, which in O-rich stars is expected to be a significant component of the dust from both abundance and energy-balance arguments, although the state of the iron (metallic, oxide or in silicates) remains unknown. However, in C-rich stars, it is unclear whether iron condenses into dust as metal, ferruginous compounds or not at all. Hence, the coupling of the dust with the magnetic field will probe whether iron is incorporated into dust grains, probed through the morphology of the polarisation. The naive assumption is that there should be a systematic difference between O-rich and C-rich sources, with O-rich sources showing magnetic alignment, and C-rich radial alignment. If the polarisation pattern around around O-rich and C-rich stars were more complex than that, this could provide an opportunity to better test the RATs model itself. For instance, a shift from radial alignment to magnetic field alignment beyond a certain radius would provide better constraints on the environmental conditions needed for the two alignment regimes. Evolved stars, where the radiation field is central and has a well-understood relation with radial distance, could provide better constraints on this than molecular clouds.

Whether or not – and how – iron is incorporated into dust grains directly probes the conditions in the dust-formation region, as the temperature and pressure in that zone determine the composition and size of the grains that form. Differences in composition also have a major impact on the wavelength dependence of the polarised emission in the sub-mm [49, 50]. However, unlike other observables – which are influenced not just by composition, but by size, shape, alignment efficiency and magnetic-field morphology – the wavelength dependence of the polarisation fraction cancels out all the degeneracies: the orientation of the average magnetic field, the turbulent component of the field and, eventually, imperfect grain alignment affect polarisation in the same way independently of wavelength [51, 52]. This leaves the wavelength dependence of polarisation as a direct probe of the properties of the dust itself [e.g. 53]. Hence, multi-wavelength continuum polarimetry has an important role to play in understanding the properties of dust in evolved stars, although as yet no models exist to explore this possibility. While TolTEC at the LMT would provide a powerful complementary capability in polarisation, our ability to map extended dust emission at the longer wavelengths that it is sensitive too has yet to be thoroughly tested. On the other hand, [16] have already demonstrated efficient mapping of the 450 μm emission on scales only moderately smaller than at 850 μm. Hence, a complementary 450 μm capability at the JCMT would provide an efficient and low-risk way to probe the wavelength dependence of polarisation.

While ALMA or the SMA would be able to image polarisation at multiple wavelengths with higher resolution, it is presently unclear whether mosaicing of polarimetric observations is feasible. However, it is important to observe as far out in the shell as possible to minimise projection effects, which may introduce degeneracies between the 3D structure of the magnetic field and the alignment efficiency or changes in the dust properties with radius. Hence, being able to observe the largest possible fields – where the JCMT excels – is important to minimising the biases in polarisation studies.

In the case of continuum polarisation, there is a key degeneracy between the magnetic field and alignment. For example, in the case of no polarisation, it is unclear whether there is no magnetic field, the grains are spherical or they are simply not aligned. In the case of evolved stars, the last issue can probably be ignored – the radiation field is so strong that RATs will spin them up to high velocities and align them with the radiation field if they are non-spherical – leaving two options which can be selected through observations of gas polarisation. Observations of thermally-excited lines have previously been employed, exploiting both the Goldreich-Kylafis and Zeeman effects [e.g. 54, 55], to explore the magnetic field strength and morphology including velocity information, breaking the aforementioned degeneracy. Hence, the ability to map polarisation with heterodyne instruments will provide an important route to constraining the large-scale magnetic fields of evolved stars, and be highly complementary to studies of the continuum polarisation.

4 Summary

Evolved stars have been studied in the sub-mm, and particularly with the JCMT, for many decades, primarily for their role in providing chemical and material feedback to the ISM. Nevertheless, many important questions remain unsolved, and thanks to new instrumentation the JCMT will play a key role alongside other current and future facilities. This white paper has presented a number of science cases where future instrumentation at the JCMT, particularly a proposed 850 μm continuum camera which would have a factor of 10 improvement in mapping speed, can make significant contributions to the field, focusing on the study of the time-variation of mass-loss, the origins of sub-mm variability and the role of magnetic fields in mass loss. These science goals will make key contributions to our understanding of the enrichment of the ISM with heavy elements and the physics that drives the mass-loss process.

The three key science cases we have proposed can all be achieved with a moderate time investment, thanks to the expected factor of 10 improvement in mapping speed along with necessary upgrades to the data reduction software (e.g. improving dynamic range, reducing large-scale structure filtering). Mapping the extended emission, and hence mass-loss histories, of a sample of 400 evolved stars could be achieved in 200 hours of band 2 weather, reaching depths of roughly 10 μJy arcsec^{-2} in azimuthally-averaged profiles. This would provide a statistical overview of the long (500 – 100 000 yr, depending on distance) timescale variations in mass loss, revealing their importance to mass loss and enrichment. Monitoring the brightest 100 of these sources could, provided that the optical periods are known, probe sub-mm variability at the level of tens of per cent in 100 hours of observations in band 2 weather, split into many short observations spread over months or years, depending on the periods of individual sources. This will reveal the mechanisms driving sub-mm variability in evolved stars and trace processes involved in dust formation and the formation of the radio photosphere. A sample of 100 bright, extended evolved stars could be mapped in polarisation in 200 hours of band 1 weather to a depth required to detect 5% polarisation in their outer envelopes. By providing a statistical overview of the morphology of polarised emission in evolved stars, this would answer key open questions about the role of magnetic fields in shaping their outflows, the composition and shape of dust (with important consequences for driving the outflow with radiation pressure) and the physics of grain alignment.

Mapping in the sub-mm, where dust dominates the continuum in evolved stars, is a unique niche for the JCMT. The combination of large field of view and high sensitivity of the proposed receiver provide a natural means for exploring extended emission, which is key to several future studies of evolved stars. Observations in the sub-mm, particularly at 850 μm are decidedly important as this probes dust temperatures in the same range as the gas temperatures probed by the low-J rotational transitions of CO, the favoured way of measuring the gas in the outflow. Other facilities, such as the LMT, can complement the proposed studies through similar capabilities at longer wavelengths, which can help to decouple the influence of different emission mechanisms and constrain the properties of the dust. Despite its exquisite sensitivity, the small field of view and *uv*-filtering mean that ALMA is unable to compete, although it can supplement the JCMT by probing variations on smaller angular scales, corresponding to shorter times. The combination of these facilities, supporting the proposed continuum instrument, represent a bright future for studies of evolved stars in the sub-mm continuum.

References

[1] Amanda I. Karakas. Stellar yields for chemical evolution modelling. In Sofia Feltzing, Gang Zhao, Nicholas A. Walton, and Patricia Whitelock, editors, *Setting the scene for Gaia and LAMOST*, volume 298 of *IAU Symposium*, pages 142–153, Jan 2014.

[2] Amanda I. Karakas and John C. Lattanzio. The Dawes Review 2: Nucleosynthesis and Stellar Yields of Low- and Intermediate-Mass Single Stars. *Publ. Astron. Soc. Australia*, 31:e030, Jul 2014.

[3] Georges Meynet, André Maeder, Cyril Georgy, and others. Massive stars, successes and challenges. In J. J. Eldridge, J. C. Bray, L. A. S. McClelland, and L. Xiao, editors, *The Lives and Death-Throes of Massive Stars*, volume 329 of *IAU Symposium*, pages 3–14, Nov 2017.

[4] Susanne Höfner and Hans Olofsson. Mass loss of stars on the asymptotic giant branch. Mechanisms, models and measurements. *A&ARv*, 26(1):1, Jan 2018.

[5] Hyosun Kim, Sheng-Yuan Liu, Naomi Hirano, and others. High-resolution CO Observation of the Carbon Star CIT 6 Revealing the Spiral Structure and a Nascent Bipolar Outflow. *ApJ*, 814(1):61, Nov 2015.

[6] Hyosun Kim, Alfonso Trejo, Sheng-Yuan Liu, and others. The large-scale nebular pattern of a superwind binary in an eccentric orbit. *Nature Astronomy*, 1:0060, Mar 2017.

[7] Nathan Smith and Ryan Tombleson. Luminous blue variables are antisocial: their isolation implies that they are kicked mass gainers in binary evolution. *MNRAS*, 447(1):598–617, Feb 2015.

[8] J. S. Greaves and W. S. Holland. High mass-loss carbon stars and the evolution of the local $^{12}C/^{13}C$ ratio. *A&A*, 327:342–348, Nov 1997.

[9] K. Young. A CO(3–2) Survey of Nearby Mira Variables. *ApJ*, 445:872, Jun 1995.

[10] G. R. Knapp and M. Morris. Mass Loss from Evolved Stars. III. Mass Loss Rates for 50 Stars from CO J = 1–0 Observations. *ApJ*, 292:640, May 1985.

[11] C. Kahane and M. Jura. Circumstellar CO around bright oxygen-rich semi-regulars. *A&A*, 290:183–197, Oct 1994.

[12] F. L. Schöier and H. Olofsson. Models of circumstellar molecular radio line emission. Mass loss rates for a sample of bright carbon stars. *A&A*, 368:969–993, Mar 2001.

[13] H. Olofsson, D. González Delgado, F. Kerschbaum, and F. L. Schöier. Mass loss rates of a sample of irregular and semiregular M-type AGB-variables. *A&A*, 391:1053–1067, Sep 2002.

[14] S. Ramstedt, F. L. Schöier, H. Olofsson, and A. A. Lundgren. Mass-loss properties of S-stars on the AGB. *A&A*, 454(2):L103–L106, Aug 2006.

[15] D. Ladjal, K. Justtanont, M. A. T. Groenewegen, and others. 870 μm observations of evolved stars with LABOCA. *A&A*, 513:A53, Apr 2010.

[16] Thavisha E. Dharmawardena, Francisca Kemper, Peter Scicluna, and others. Extended Dust Emission from Nearby Evolved Stars. *MNRAS*, 479(1):536–552, Sep 2018.

[17] G. Siringo, E. Kreysa, A. Kovács, and others. The Large APEX BOlometer CAmera LABOCA. *A&A*, 497(3):945–962, Apr 2009.

[18] W. S. Holland, D. Bintley, E. L. Chapin, and others. SCUBA-2: the 10 000 pixel bolometer camera on the James Clerk Maxwell Telescope. *MNRAS*, 430(4):2513–2533, Apr 2013.

[19] T. Kamiński, K. T. Wong, M. R. Schmidt, and others. An observational study of dust nucleation in Mira (o Ceti). I. Variable features of AlO and other Al-bearing species. *A&A*, 592:A42, Jul 2016.

[20] K. Ohnaka, G. Weigelt, and K. H. Hofmann. Clumpy dust clouds and extended atmosphere of the AGB star W Hydrae revealed with VLT/SPHERE-ZIMPOL and VLTI/AMBER. *A&A*, 589:A91, May 2016.

[21] Matthew W. L. Smith, Christopher J. R. Clark, Ilse De Looze, and others. JINGLE, a JCMT legacy survey of dust and gas for galaxy evolution studies: II. SCUBA-2 850 μm data reduction and dust flux density catalogues. *MNRAS*, 486(3):4166–4185, Jul 2019.

[22] E. De Beck, L. Decin, A. de Koter, and others. Probing the mass-loss history of AGB and red supergiant stars from CO rotational line profiles. II. CO line survey of evolved stars: derivation of mass-loss rate formulae. *A&A*, 523:A18, Nov 2010.

[23] Thavisha E. Dharmawardena, Francisca Kemper, Sundar Srinivasan, and others. The nearby evolved stars survey - I. JCMT/SCUBA-2 submillimetre detection of the detached shell of U Antliae. *MNRAS*, 489(3):3218–3231, Nov 2019.

[24] F. Kemper, R. Stark, K. Justtanont, and others. Mass loss and rotational CO emission from Asymptotic Giant Branch stars. *A&A*, 407:609–629, Aug 2003.

[25] L. Decin, S. Hony, A. de Koter, and others. The variable mass loss of the AGB star WX Piscium as traced by the CO J = 1-0 through 7-6 lines and the dust emission. *A&A*, 475(1):233–242, Nov 2007.

[26] Hiroyuki Hirashita, Patrick M. Koch, Satoki Matsushita, and others. First-generation science cases for ground-based terahertz telescopes. *PASJ*, 68(1):R1, Feb 2016.

[27] P. R. Wood. Evolutionary and pulsation properties of AGB stars . *Mem. Soc. Astron. Italiana*, 81:883, Jan 2010.

[28] S. Liljegren, S. Höfner, W. Nowotny, and K. Eriksson. Dust-driven winds of AGB stars: The critical interplay of atmospheric shocks and luminosity variations. *A&A*, 589:A130, May 2016.

[29] K. M. Menten, M. J. Reid, E. Krügel, M. J. Claussen, and R. Sahai. Radio continuum monitoring of the extreme carbon star IRC+10216. *A&A*, 453(1):301–307, Jul 2006.

[30] I. Cherchneff. A chemical study of the inner winds of asymptotic giant branch stars. *A&A*, 456(3):1001–1012, Sep 2006.

[31] J. H. He, Dinh-V-Trung, and T. I. Hasegawa. Monitor Variability of Millimeter Lines in IRC+10216. *ApJ*, 845(1):38, Aug 2017.

[32] J. H. He, T. Kamiński, R. E. Mennickent, and others. ALMA Monitoring of Millimeter Line Variation in IRC +10216. I. Overview of Millimeter Variability. *ApJ*, 883(2):165, Oct 2019.

[33] Thavisha E. Dharmawardena, Francisca Kemper, Jan G. A. Wouterloot, and others. The sub-mm variability of IRC+10216 and o Ceti. *MNRAS*, 489(3):3492–3505, Nov 2019.

[34] J. E. Austermann, J. A. Beall, S. A. Bryan, and others. Millimeter-Wave Polarimeters Using Kinetic Inductance Detectors for TolTEC and Beyond. *Journal of Low Temperature Physics*, 193(3-4):120–127, Nov 2018.

[35] A. Lèbre, M. Aurière, N. Fabas, and others. Search for surface magnetic fields in Mira stars. First detection in χ Cygni. *A&A*, 561:A85, Jan 2014.

[36] F. Herpin, A. Baudry, C. Thum, D. Morris, and H. Wiesemeyer. Full polarization study of SiO masers at 86 GHz. *A&A*, 450(2):667–680, May 2006.

[37] W. H. T. Vlemmings, E. M. L. Humphreys, and R. Franco-Hernández. Magnetic Fields in Evolved Stars: Imaging the Polarized Emission of High-frequency SiO Masers. *ApJ*, 728(2):149, Feb 2011.

[38] Roger H. Hildebrand. Magnetic fields and stardust. *QJRAS*, 29:327–351, Sep 1988.

[39] Planck Collaboration, P. A. R. Ade, N. Aghanim, and others. Planck intermediate results. XIX. An overview of the polarized thermal emission from Galactic dust. *A&A*, 576:A104, Apr 2015.

[40] B. G. Andersson, A. Lazarian, and John E. Vaillancourt. Interstellar Dust Grain Alignment. *ARA&A*, 53:501–539, Aug 2015.

[41] W. H. T. Vlemmings, T. Khouri, I. Martí-Vidal, and others. Magnetically aligned dust and SiO maser polarisation in the envelope of the red supergiant VY Canis Majoris. *A&A*, 603:A92, Jul 2017.

[42] H. Shinnaga, M. J. Claussen, S. Yamamoto, and M. Shimojo. Strong magnetic field generated by the extreme oxygen-rich red supergiant VY Canis Majoris. *PASJ*, 69:L10, December 2017.

[43] A. Z. Dolginov and I. G. Mitrofanov. Orientation of Cosmic Dust Grains. *Ap&SS*, 43(2):291–317, Sep 1976.

[44] A. Lazarian and Thiem Hoang. Radiative torques: analytical model and basic properties. *MNRAS*, 378(3):910–946, Jul 2007.

[45] Thiem Hoang and A. Lazarian. A Unified Model of Grain Alignment: Radiative Alignment of Interstellar Grains with Magnetic Inclusions. *ApJ*, 831(2):159, Nov 2016.

[46] Ryo Tazaki, Alexandre Lazarian, and Hideko Nomura. Radiative Grain Alignment In Protoplanetary Disks: Implications for Polarimetric Observations. *ApJ*, 839(1):56, Apr 2017.

[47] J. S. Mathis. The Alignment of Interstellar Grains. *ApJ*, 308:281, Sep 1986.

[48] R. Siebenmorgen, N. V. Voshchinnikov, and S. Bagnulo. Dust in the diffuse interstellar medium. Extinction, emission, linear and circular polarisation. *A&A*, 561:A82, Jan 2014.

[49] Bruce T. Draine and Aurélien A. Fraisse. Polarized Far-Infrared and Submillimeter Emission from Interstellar Dust. *ApJ*, 696(1):1–11, May 2009.

[50] V. Guillet, L. Fanciullo, L. Verstraete, and others. Dust models compatible with Planck intensity and polarization data in translucent lines of sight. *A&A*, 610:A16, Feb 2018.

[51] J. Mayo Greenberg. *Interstellar Grains*, page 221. 1968.

[52] H. M. Lee and B. T. Draine. Infrared extinction and polarization due to partially aligned spheroidal grains : models for the dust toward the BN object. *ApJ*, 290:211–228, Mar 1985.

[53] Planck Collaboration, P. A. R. Ade, N. Aghanim, and others. Planck intermediate results. XXI. Comparison of polarized thermal emission from Galactic dust at 353 GHz with interstellar polarization in the visible. *A&A*, 576:A106, Apr 2015.

[54] J. M. Girart, N. Patel, W. H. T. Vlemmings, and Ramprasad Rao. Mapping the Linearly Polarized Spectral Line Emission around the Evolved Star IRC+10216. *ApJ*, 751(1):L20, May 2012.

[55] A. Duthu, F. Herpin, H. Wiesemeyer, and others. Magnetic field in IRC+10216 and other C-rich evolved stars. *A&A*, 604:A12, Jul 2017.

SUBMILLIMETER GALAXY STUDIES IN THE NEXT DECADE

EAO SUBMILLIMETRE FUTURES PAPER SERIES, 2019

Ran Wang[*1] • **Wei-Hao Wang**[2] • **Clements David L.**[3] • **Haojing Yan**[4] • **Yiping Ao**[5]

[1]*Kavli Institute for Astronomy and Astrophysics, No. 5 Yiheyuan Road, Haidian district, Beijing, 100871, China*
[2] *Academia Sinica Institute of Astronomy and Astrophysics (ASIAA), No. 1, Section 4, Roosevelt Rd., Taipei 10617, Taiwan*
[3]*Department of Physics and Astronomy, McMaster University, Hamilton, ON, L8S 4M1 Canada*
[4]*Department of Physics and Astronomy University of Missouri Columbia, MO, 65211 USA*
[5]*Purple Mountain Observatory, Chinese Academy of Sciences, Nanjing, 210034, China*

ABSTRACT

Over the last two decades, the Submillimetre Common-User Bolometer Array (SCUBA) and SCUBA-2 on the James Clerk Maxwell Telescope (JCMT) achieved great success in discovering the population of dusty starburst galaxies in the early universe. The SCUBA-2 surveys at 450 μm and 850 μm set important constraints on the obscured star formation over cosmic time, and in combination with deep optical and near-IR data, allows the study of protoclusters and structure formation. However, the current submillimeter (submm) surveys by JCMT are still limited by area of sky coverage (confusion limit mapping of only a few deg^2), which prevents a systematic study of large samples of the obscured galaxy population. In this white paper, we review the studies of the submm galaxies with current submillimeter/millimeter (submm/mm) observations, and discuss the important science with the new submm instruments in the next decade. In particular, with a 10 times faster mapping speed of the new camera, we will expect deep 850 μm surveys over 10 to 100 times larger sky area to i) largely increase the sample size of submm detections toward the highest redshift, ii) improve our knowledge.

1 Introduction

The thermal dust continuum emission at far-infrared wavelengths is an important tracer of the dust and gas contents and star forming activities in galaxies [1, 2, 3]. At high redshift, the UV and optical emission from the stellar component is dimming dramatically. However, the hump of the thermal dust emission is shifted to the submm bands, and due to the negative k-correction, the observing flux densities at submillieter (submm) and millimeter wavelengths do not drop with redshift. Thus, the submm/mm windows open a unique opportunity to probe active star formation and galaxy evolution toward the earliest epoch. Over the last two decades, the submm facilities, such as the Submillimetre Common-User Bolometer Array (SCUBA) and SCUBA-2 on the JCMT and the SPIRE on the *Herschel* Space telescope etc., achieved great success in discovering the population of dusty starburst galaxies in the early universe [3, 4, 5].

Dusty starbursts have been found into the epoch of reionization (EoR; $z > 6.3$). Some of them are found as quasar hosts and/or companions [6, 7], and yet some are found in "blind" sub-mm/mm surveys [8, 9]. In terms of IR luminosities, they are all ULIRGs ($L_{IR} > 10^{12} L_{\odot}$) and HyLIRGs ($L_{IR} > 10^{13} L_{\odot}$), which translate to dust-embedded star formation rates (SFRs) of $> 100 - 1000 M_{\odot}/yr$. The very existence of such high-z U/HyLIRGs has important implications. The burst of star formation traces the most active stage of galaxy evolution. The submm sources detected in the core of overdensity regions also probe the early evolution of galaxy clusters. In addition, The prevalence of dust at $z \approx$ 6-7 means that there must be very active star formations at even earlier epochs ($z \sim 10$ and beyond).

Bright submm/mm emission was also detected in the host galaxies of optically luminous quasars at z$\sim$2 to 7 [10, 11, 12, 13, 14]. The single dish surveys at sub-mJy sensitivity reveal that about 30% of them are hosted in dusty starburst systems with FIR luminosities comparable to that of the ULIRGs and HyLIRGs, suggesting massive star formation co-eval with rapid supermassive black hole (SMBH) accretion. These quasar-starburst systems became important targets for further interferometer observations to search and resolve the gas and dust content. The follow-up molecular

[*]rwangkiaa@pku.edu.cn

CO and [C II] observations probe the distribution of dust, gas, and star forming activity, as well as the host dynamics [7, 15, 16, 17, 18, 19], and thus, set key constraints on the early growth of the SMBH-galaxy systems [20, 21].

The obscured star formation discovered in submm surveys provides essential complement to probe the cosmic star formation history (SFH). Traditionally, tracing the evolution with cosmic time of the galaxy luminosity density from the far-UV (FUV) to the far-infrared (FIR) offers the prospect of an empirical determination of the global star formation history (SFH) and heavy element production of the Universe [22, 23, 24]. However, lacking precise astrometry at FIR wavelengths at high redshifts often prevents us from connecting FUV to FIR data and providing the required complete understanding of cosmic SFH. To study the formation and evolution of galaxies, it is crucial to determine the redshift distribution of sources. Large samples of high redshift galaxies have been imaged with space facilities like *Hubble*, *Spitzer*, *Herschel* and ground-based telescopes at multiple wavelengths and their redshifts can be determined by photometric observations at multiple bands. Alternatively, a small fraction of sources have been confirmed with spectroscopic measurements and narrow-band imaging. Due to large extinction, observations at optical and/or near-infrared are difficult and only bright sources can be detected at high redshifts. For some sources with large amount of dust, they are very likely to be invisible with current optical facilities in a limited observing time.

The mapping capabilities of the single dish telescopes at submm wavelengths are also becoming important in tracing overdensity and structure formation in the early universe. Clusters of galaxies are the most massive bound structures in the local universe. They are largely dominated by 'red and dead' elliptical galaxies, and the oldest and most massive elliptical galaxies lie at their cores (eg. [25]). Studies of the stellar populations of these massive galaxies reveal them to be old, with inferred formation redshifts $z > 3$ and with the bulk of their stellar populations forming over a short time scale. This would imply that the progenitors of the massive elliptical galaxies in the cores of clusters must have formed in major starbursts.

Finding galaxy clusters in formation at these high redshifts is a difficult task. The standard methods of cluster detection include X-ray and Sunyaev Zel'dovich (SZ) observations of the hot intracluster medium, and the search for red sequence galaxies in the optical and near-IR. All of these methods fail for forming galaxy clusters; the first two since young systems are yet to virialize and thus lack a significant intracluster medium that can be detected by X-rays or SZ, and the last because the galaxies making up the cluster are still star-forming and thus do not lie on the red sequence. The high star formation rates (SFRs) of forming giant elliptical galaxies, however, in principle allow us to search for these objects in the far-IR, since, like starbursts in the local universe, they should be luminous at these wavelengths. Recent results using *Herschel* and *Planck* data in the far-IR and submm have begun to find candidate protoclusters in this way.

2 Current Status

Submm surveys of galaxies were carried out with JCMT in the last two decades (Table 1), e.g., the SCUBA program which discovered the first submm galaxy sample at high redshift, the SCUBA-2 Cosmology Legacy Survey (S2CLS, [3]), The Hawaii SCUBA-2 Lensing Cluster Survey [26], the Submillimeter Perspective on the GOODS Fields (SUPER GOODS, [27]), the SCUBA-2 Large eXtragalactic Survey (S2LXS[2]), S2COSMOS/eS2COSMOS[3], and SCUBA-2 Ultra Deep Imaging EAO Survey (STUDIES, [28]). The SCUBA-2 surveys image the submm sky to a 1σ noise level of $0.9 \sim 2$ mJy, discovering the extreme starburst systems with FIR luminosities on orders of 10^{12} to 10^{13} $L_{\odot}$. These observations, together with the data from *Spitzer* and *Herschel* at shorter wavelengths, measure the submm source number densities and update the star formation rate density [3, 4, 23, 28, 29, 30], revealing that the submm galaxies contribute significantly to the cosmic star formation history over a wide range of redshift [22, 23].

To study the SFH in the early Universe, observations by space telescopes at far-infrared and ground facilities at submm become an important tool to detect highly dust-obscured galaxies. However, due to the poor resolution and confusion level of the space telescopes, the observations will only select bright sources and therefore largely underestimate the SFR at high redshifts. Ground-based facilities like JCMT/SCUBA2 can provide better sensitivity and resolution in comparison with space facilities like *Herschel*. However, due to a relatively low mapping speed the statistical results still suffer from large uncertainties by the cosmic variance from small surveyed fields. Large area, deep surveys are highly required in future.

In addition, to fully understand the early cosmological star formation history, we will need large samples of high-z dusty starbursts selected in a systematic manner. The most promising method to construct such samples is through the use of FIR/sub-mm colors in blind, un-biased surveys. The typical cold-dust emission (as being heated by star formation) in galaxies has its peak at around rest-frame 100 μm, and the color selection is to utilize this characteristics. The so-called "500 μm riser" technique is an implementation tailored for the BLAST and the *Herschel*/SPIRE bands [31, 32]: a dusty

[2] https://www.eaobservatory.org/jcmt/science/large-programs/s2lxs/

[3] https://www.eaobservatory.org/jcmt/science/large-programs/s2-cosmos/

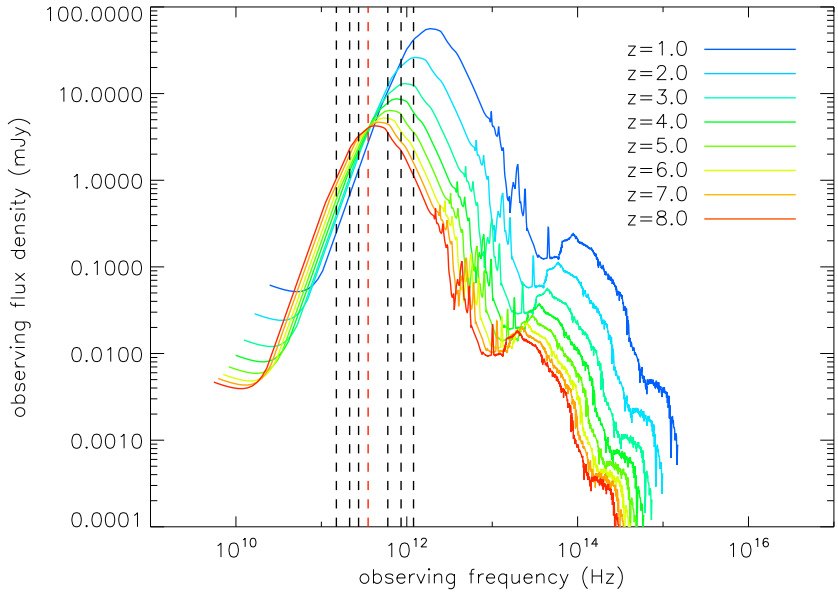

Figure 1: The spectral energy distribution (SED) of a dusty star forming galaxy at redshift from z=1 to 8. We use the SED of M82 from the SWIRE library as a template [34]. The SEDs are normalized at an 850 μm observing flux density of 4mJy, which are the typical 4σ detection limit for JCMT/SCUBA-2 surveys. The vertical lines shows the observing windows at 250 μm, 350 μm, 500 μm, 850 μm, 1.1 mm, 1.4 mm, 2 mm. The 850 μm window is marked as a red line, which samples the peak of the dust continuum bump at the highest redshift.

galaxy at $z > 4$ should have red colors in 250, 350 and 500 μm bands because its SED is "rising" through these three bands as the peak is redshifted to $\sim$ 500 μm and redder wavelengths. An extension of this technique to higher redshifts is the "850/870 μm riser" method, where a redder band at 850 or 870 μm is added to the selection [33].

A growing number of protoclusters and protocluster candidates are being found using far-IR and submm techniques. Casey [35] summarises results on five specific protoclusters at $2 < z < 3.1$ with spectroscopic confirmation, as well as a further three candidates at higher redshifts. Meanwhile, there is an increasing number of candidate protoclusters with estimated redshifts around 2 to 3 emerging from work on the *Herschel* and *Planck* surveys, including at least 27 candidates emerging from investigating *Planck* sources lying within the large area *Herschel* surveys [36], [37], and 228 resulting from colour selection from the *Planck* [38] all sky survey. The nature of these sources is currently unclear since nearly all the sources lack the spectroscopic followup necessary to confirm, or otherwise, their protocluster nature. One of the *Planck* candidates has been found to be a superposition of two galaxy overdensities at different redshifts (1.7 and 2.0, [39]) while photometric redshifts suggest that several others are genuine protoclusters ([37], [35]). Over the next ten years the spectroscopic study of these candidates should allow considerable progress in confirming their nature and studying the detailed physics of the processes driving the star formation in their member galaxies.

Theoretically, protoclusters at $z \sim$2 are expected to be very large structures. Theoretical models show that the eventual members of a Coma-sized cluster at zero redshift will be spread over scales of 10s of Mpc [41]. Observations of several confirmed protoclusters ([42]; [43]; [44]) seem to confirm this result, with structures seen on scales of 3 to 15 Mpc. However, there is a mismatch between the detailed predictions of SFRs and other properties for protocluster galaxies from theoretical models and what we appear to be seeing in the population revealed by *Herschel* and *Planck* (see eg. [36]). At higher redshifts, theoretical predictions suggest a different picture, with the cores of eventual protoclusters showing high rates of star formation on scales of a few 100kpc at $z \sim 6$ [27]. The observational situation at higher redshift is somewhat confused, however. Starbursting cluster cores may have been seen at $z \sim 4$, rather lower than the predicted redshift, in followup observations of very red sources from *Herschel* [40] and the South Pole Telescope [45], but protocluster candidates at $z \sim 6$ selection through Lyα emission by HyperSuprime Cam [46] show structures, including far-IR luminous sources, extended on scales of 10 Mpc instead. It is thus clear that much remains to be learnt about the early stages of galaxy cluster formation.

In summary, the submm/mm bands are unique in tracing obscured star formation and galaxy evolution over the cosmic time. The great success of the existing JCMT/SCUBA and SCUBA-2 survey proved that the 850 μm band on Maunakea

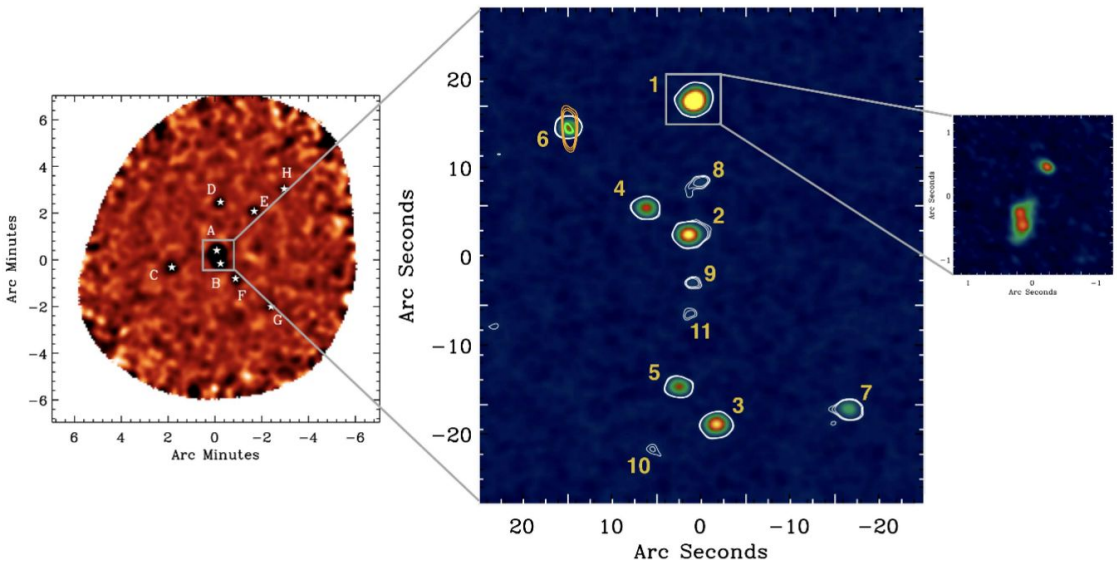

Figure 2: From [40]: A candidate protocluster core at a redshift of 4.001 discovered through colour selection from *Herschel* and follow-up submm imaging. On the left is a LABOCA image of a very red *Herschel* source selection from its 250 to 350 to 500 μm colour. The *Herschel* source breaks up into several 870μm sources. In the centre is an ALMA image of the central region of this clump of sources, showing that they too break up into numerous submm sources. These sources have spectroscopic redshifts measured by ALMA. On the right is the brightest of these sources which, in higher reslution ALMA data, is found to be a pair of submm sources. This is consistent with the picture of [27] for protocluster core formation, but it is found at $z = 4$ rather than the predicted $z \sim 6$ for this stage of cluster formation. For details see [40] and references therein.

is the most efficient window for deep imaging to detect the submm population at high redshift. However, the current submm surveys by JCMT are limited by the small area of sky coverage (Table 1). e.g., The deep SCUBA-2 surveys (S2CLS, S2COSMOS) cover only ≤ 5 deg^2 of sky area. For comparison, much large sky area are aleardy covered with deep optical, near-infrared, and radio observations (e.g., Stripe 82 of 300 deg^2). The lack of deep submm data in these region prevent a systematic study of large samples of the obscured galaxy population. Thus, the new JCMT 850 μm camera with a 10 times faster mapping speed becomes an urgent request for developing large submm surveys.

3 The Next Decade

We would like to propose wide field surveys at 850 μm using the new camera on the JCMT when the instrument is available in 2022. The 10 times faster mapping speed of the new 850 μm camera will allow submm mapping over hundred deg^2 of sky area at mJy sensitivity level in the next decade. The fields covered by the deep X-ray, optical, near-infrared, and radio observations will have the highest priority for such submm surveys. As we discussed above, the previous submm/mm surveys with sky coverages of 100 to 1000 deg^2, such as the HerS and HerMes Surveys at 250μm, 350μm, and 500μm, the SPT survey at 1.4mm, 2mm, and 3mm, are insufficient in both sensitivity and angular resolution, to fully recover the obscured star formation population toward the highest redshift and identify the counterpart of galaxy samples and protocluster members discovered in deep optical and near-IR observations. The new 850 μm continuum survey will largely increase the sample size of submm sources, and combined with data at other wavelengths, will significantly improve our knowledge of galaxy and structure evolution in the early universe.

3.1 Selection of Dusty Starbursts at Very High Redshifts

High-z dusty starbursts are rare. Depending on the exact color criteria adopted, the surface density of 500 μm risers in the HerMES and the H-ATLAS areas is ~ 10 deg^{-2} or less. While there is not yet sufficient statistics of 850/870 μm risers, there is evidence that they are even rarer (e.g. Duivenvoorden et al. 2018). By providing an increase of $10 \sim 20\times$ in the mapping speed than SCUBA-2, the planned JCMT new wide-field camera will be the most powerful tool in our search for dusty starbursts at $z > 7$ and beyond. Furthermore, the increase in mapping speed will bring JCMT to the same league as the new millimeter camera, TolTEC, on the LMT [61]. Combining wide-area submm/mm data from

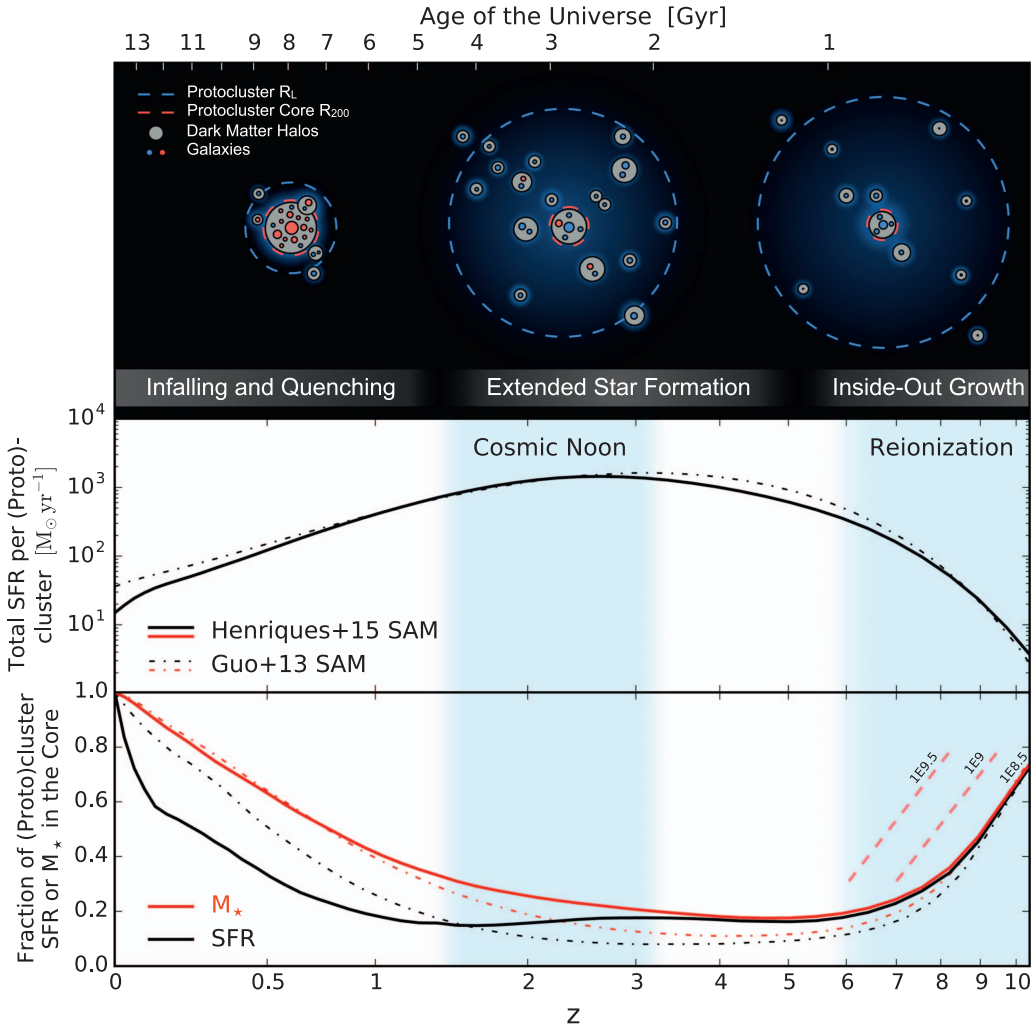

Figure 3: From [27]: predictions for the evolution of protoclusters showing the core formation phase at high redshift and the growth phase at $z = 2 - 3$. For details see [27] and references therein.

JCMT and LMT will greatly boost our capability to study the high-redshift dusty population in terms of both sample size and robust sample selection.

3.2 Understanding the connection between star formation and SMBH accretion

Large populations of quasars and active galactic nuclei (AGN) are discovered from the optical and near-IR surveys. Previous submm/mm observations discovered a small fraction of the quasar host galaxies that are still efficiently forming stars. However, the connection between star formation activity and AGN properties are still unclear. In particular, the limit sky coverage of previous submm/mm observations cannot provide enough sample in different bins of AGN activities for such studies at high redshift. The new 850 μm survey will increase the sample size of submm observed quasars by factors of $>$a few tens and significantly improve the statistics.

The detection of dust continuum at 850 μm will intermediately constrain the dust mass and star formation rate in the quasar host galaxies. The sky coverage of large quasar samples will allow detections of the stacking signals with objects in bins of redshifts, SMBH masses, and quasar luminosities. This will address the evolutionary connection between star formation and SMBH accretion over a wide range of redshift. Based on the assumption of dust-to-molecular gas ratio, the gas mass could also be constrained. The gas fraction in quasar hosts is an important parameter to address the effect of AGN feedback (e.g., [62, 63]). i.e., a low gas fraction compared to the normal star forming galaxies may indicate that the molecular gas are removed and the star formation are suppressed due to the AGN power. In addition, More

Table 1: Submillimeter and millimeter surveys

Survey	Sky Area deg^2	Wavelength μm	1σ rms mJy beam^{-1}	Reference
SCUBA/JCMT SHADES	0.2	850	2	[1]
SCUBA/JCMT HDF	0.0025	850	0.45	[4]
SUPER GOODS	0.125	850/450	0.28/2.6	[47]
Hawaii SCUBA-2 Lensing Cluster Survey	0.137	450	4.4[c]	[26]
S2CLS	5	850	1.2	[3]
S2COSMOS/eS2COSMOS	2	850	0.9	[48]
STUDIES	0.08	450	0.55	[28]
S2LXS	10	850	2	a
HerMes	380	250/350/500	5.2$\sim$12.8	[49]
H_ATLAS	570	250/350/500	9	[50]
HerS	79	250/350/500	13.0/12.9/14.8	[5]
BGS-Wide	10	250/350/500	36/31/20	[51]
BGS-Deep	0.9	250/350/500	11/9/6	[51]
LESS	0.25	870	1.2	[52]
AzTEC GOODS-S	0.075	1100	0.48$\sim$0.73	[53]
AzTEC GOODS-N	0.068	1100	0.96$\sim$1.16	[54]
AzTEC SHADES	0.7	1100	0.9	[55]
AzTEC COSMOS	0.72	1100	1.26	[56]
SPT	2500	1400/2000/3000	4/1.2/2	[57, 58]
IRAM/GISMO survey	0.07	2000	0.23	[59]
NIKA2 GOODS-N[d]	0.04	1200/2000	0.2$\sim$0.6/0.1$\sim$0.3	[60]
NIKA2 COSMOS[d]	0.4	1200/2000	0.1/0.07	[60]
Planned surveys				
TolTEC Ultra-Deep Galaxy Survey	1	1100/1400/2000	0.026/0.024/0.018	b
TolTEC Large Scale Structure Survey	100	1100/1400/2000	0.26/0.24/0.18	b

[a]Geach et al. M17BL001; [b]http://toltec.astro.umass.edu/science_legacy_surveys.php [c]Before lensing amplification correction. [d]See also Beelen et al. https://lpsc-indico.in2p3.fr/Indico/event/1765/session/9/contribution/52

quasar-starburst systems will be discovered at high redshift. These objects will be the targets for further ALMA and JWST observations to image the dust, gas, and stellar components. These systems will be the key examples to probe the early growths of the SMBH and their host galaxies.

3.3 Cosmic Star Formation History Based on the Large, Deep Surveys

Large samples of SMGs have been detected with the JCMT/SCUBA-2 (e.g., [3]), and follow-up observations with ALMA have mapped some SCUBA-2 sources. Machine-learning algorithm can efficiently identify the likely counterparts at optical/NIR for the SCUBA-2 sources by using ALMA observations as a training sample [64]. A new bolometer camera at JCMT with a mapping speed of 10 times faster than the current SCUBA-2 can be used to finish a much wider field with multiple optical/NIR archival data in an efficient way. Together with the machine-learning method, this can well constrain the cosmic SFH and significantly reduce the cosmic variance for the measurements.

However, it is difficult to efficiently search for high redshift sources even with ALMA. Currently, lacking of identified high redshift sources will largely underestimate their corresponding SFRs at z >5. ALMA observations show some SCUBA-2 sources without any optical/NIR counterparts. The latter could be good high-redshift candidates. The deep continuum observations with single dishes can reveal a large sample of SMGs and the follow-up high resolution observations with the interferometers like ALMA can locate their accurate positions. Together with archival multi-wavelength data and possible follow-up deep observations at optical/NIR with large optical/NIR telescopes or on-going facility like TMT, one can constrain the cosmic SFH at high redshift. The machine-learning method is also helpful to identify the likely high-redshift candidates without any optical/NIR counterparts. It may provide informative clues or constraints on the cosmic SFHs at high redshift when ultra-deep optical/NIR observations are currently not available yet.

To compare with the cosmology simulation, we always require a large survey area to reduce the cosmic variance and to find some extreme sources or extreme environments, which are important astrophysical laboratories. The number density of massive galaxies at high redshifts can be use to test different galaxy evolution models, which predict massive galaxies decline very rapidly at z>4.

Other large area surveys with IRAM30m/NIKA2 and LMT/TolTEC will provide deep images at mm wavelength, reaching a superior sensitivity. Together with the data from the next-generation of the 850 μm camera at JCMT, one can efficiently select high redshift candidates based on the color criterion. Ultra-deep radio surveys at LOFAR and SKA precursors can be important for getting cross identifications and accurate positions due to their superior sensitivities and large field of views in comparison to the submm surveys.

3.4 Protoclusters and the Galaxy Cluster Formation

The far-IR/submm based protocluster surveys discussed above were not designed for protocluster work. They have found protocluster candidates with total SFRs $> 10,000 M_{\odot}$/yr, with individual member galaxies forming stars at rates of 100s to 1,000s of $M_{\odot}$/yr, but it is likely that they are seeing only the peak of the luminosity function both of protoclusters and of galaxies within protoclusters because of the relatively limited sensitivity of these surveys to sources at such high redshifts. Meanwhile, dependence on selection at short submm wavelengths, typically 350, 500 or 550 μm for the *Herschel* and *Planck* surveys, hampers studies of the highest redshift protoclusters at $z \geq 6$. At the same time, the existing samples have been selected using a range of rather heterogeneous methods, making statistical assessments of luminosity functions and evolution rather difficult.

The next decade will see a range of developments that will move these studies forward. Firstly, spectroscopic followup of the existing samples will significantly increase the number of confirmed protoclusters known at $z \geq 2$. This will be achieved using both mm/submm spectroscopy using ALMA and NOEMA, and optical/near-IR observations with instruments like KMOS and MUSE. Secondly, theoretical models for these objects, which require detailed n-body-hydro codes with high spatial resolution, will improve our insight into this population. Thirdly, large area surveys at mm wavelengths using instruments such as NIKA2 and TOLTEC will provide new candidate protoclusters for detailed examination. It is here where JCMT will be able to contribute, since the addition of large area surveys at higher frequency submm wavelengths will greatly enhance our ability to select candidate protoclusters from $z \sim 2$ to the highest redshifts. The protocluster candidates we currently know have an area density of about 1 per 40 sq. degrees, so the necessary surveys will have to be large area and ideally reaching a sensitivity of $\sim$ 1mJy. Such surveys will be sensitive to not only the population we already know but also fainter protoclusters and protocluster galaxies, allowing us to examine the luminosity function of these objects. The proposed 10x enhanced mapping speed over SCUBA-2 will make a few hundred sq. deg. 850 μm survey to these sensitivities possible as part of a large area Legacy Survey, which will also be useful for many other studies. At the same time a larger field submm instrument will be needed to survey the $\sim$15 Mpc region around known protoclusters to search for starbursting galaxies in their infall region that, if the predictions of Muldrew et al. [41] are current, will subsequently fall into the clusters. Other instrumentation developments, such as KIDS-based submm imaging spectrometers, able to measure redshifts for all submm sources in a field simultaneously, would be ideal to followup the protocluster candidates detected in these surveys, and to characterise the molecular and atomic gas properties of their member galaxies, allowing this population to be confirmed and analysed much more rapidly than is possible with current instruments. The JCMT thus has a huge potential for studying rare submm emitters, such as protoclusters, using the proposed new instrumentation.

3.5 Further Request of the 450μm Capability

Surveys at 850 μm will play a leading role in discovering the dusty star forming sources. However, detections at a single submm band is insufficient to constrain the nature of the detections. Measurements of dust temperature and IR luminosity, as well as the photometric-redshift require observations at more submm/mm bands. For objects at z$\geq$3, the 450μm window samples the peak of the thermal dust emission (Figure 1), thus is critical in determine the dust SED. The *Herschel* data at 350μm and 500μm are confusion limited and are only available for a small fraction of the sky (HerMes, H_ATLAS, and HerS fields). The 450μm window at Maunakea and the 450μm capability of JCMT will remain unique. JCMT has an angular resolution at 450μm that is similar to that of the LMT in the millimeter. Therefore, JCMT can detect 450 μm sources that are much fainter than the *Herschel*/SPIRE limits and the 850 μm limit of JCMT. The imaging capability of JCMT at 450μm will become a very important complement for future multi-bands surveys. It will also provide a unique band for the color selections of the dusty objects toward the highest redshift, and for probing the normal galaxy population at the peak epoch ($z \sim 2$) of the cosmic star formation and AGN.

3.6 Time and Sensitivity Requests

With the new 850 μm wide field camera, we will be able to carry out surveys that cover very wide areas and still achieve very deep sensitivities. For example, we could conduct a survey over 300 deg^2 to $rms = 2.0$ mJy in 2500 hours under the Band 2/3 weather condition with matched-filter applied (assuming that $\tau_{225GHz} = 0.08$, and that the new camera is 10 times faster than that of the current SCUBA-2 in PONG3600 mode with 660 pointings). We could choose the fields that have already been covered by the previous Herschel surveys and/or will be covered by the coming LMT/TolTEC surveys. The much larger survey area compared to those of the existing SCUBA-2 surveys will allow us to select a very large sample (on the order of $\times 10^4$) of 850 μm risers that are candidates of very high redshift dusty starburst galaxies. The combination of 850 μm data with the Herschel, NIKA2, and TOLTEC data will also allow the selection of protocluster candidates. Moreover, the large sky area will cover a significant number of optically-selected quasars. According to the Sloan Digital Sky Survey fourteen data release of quasar catalog, about 5000 quasars at 2<z< 3 (i.e., the peak of SMBH and galaxy evolution) are expected within 300 deg^2 [65]. While only a small fraction of them would be directly detected, the shear number of the undetected ones will provide enough stacking signal to obtain the average dust continuum emission and dust mass of the hosts in different SMBH mass and quasar luminosity bins. Meanwhile, deeper surveys could be carried out over tens of deg^2 down to the 0.7$\sim$1 mJy level. As an example, a point source sensitivity of $rms = 0.7$ mJy over 10 deg^2 will need 720 hours in Band 2/3 weather ($\tau_{225GHz} = 0.08$). This is much deeper than the existing Herschel surveys, allowing us to detect dusty star forming galaxies or quasar hosts with FIR luminosities around 1×10^{12} L$_\odot$ at high redshifts. In addition, an area on the order of 10 deg^2 will greatly reduce the cosmic variance, better prob the source counts of submm sources down to 2$\sim$3 mJy level (i.e., $S/N \approx 4$), recover more obscured star forming population at high redshift, and improve our knowledge of the SFH over cosmic time.

3.7 Synergies with Other Instruments

The new 850 μm wide field camera will allow submm surveys of high-z dusty star forming systems in tens to hundreds deg^2 of sky area with a much improved sensitivity compared to the current SCUBA2 surveys. The observations will serve as the sub-mm counterparts of the large-scale optical, infrared, and radio surveys with future telescopes (such as the LSST, EUCLID, and SKA et c.). This will reveal the obscured star forming over cosmic time that is not detectable in optical/IR. For galaxies at z$\geq$5, the measurement at 850 μm samples the dust SED close to the peak (see Figure 1). Thus, the combination of 850μm data with surveys using IRAM/NIKA2 or LMT/TolTEC at longer wavelengths and constraints/upper limits from Herschel/SPIRE at shorter wavelengths will allow the selection of large sample of candidates at very high-z. With the 10 times faster mapping speed, this new 850 μm camera will enlarge the current sample of z>5 dusty starburst galaxies by nearly two orders of magnitude. And finally with ALMA or NOEMA, we will be able to accurately locate/resolve the SCUBA-2 detections (e.g., [66]), and spectroscopically determine the redshift (e.g., [67]). These will provide a large sample of young galaxies that are in the obscured starburst phase in both field and protocluster environments. Further high resolution imaging with ALMA, NOEMA, and the VLA will probe the gas distribution and kinematics into details [68, 69] and allow a full study of the galaxy evolution and structure formation at the earliest epoch.

References

[1] K. Coppin, E. L. Chapin, A. M. J. Mortier, and others. The SCUBA Half-Degree Extragalactic Survey - II. Submillimetre maps, catalogue and number counts. *Monthly Notices of the Royal Astronomical Society*, 372(4):1621–1652, Nov 2006.

[2] N. Scoville, H. Aussel, K. Sheth, and others. The Evolution of Interstellar Medium Mass Probed by Dust Emission: ALMA Observations at z = 0.3-2. *The Astrophysical Journal*, 783(2):84, Mar 2014.

[3] J. E. Geach, J. S. Dunlop, M. Halpern, and others. The SCUBA-2 Cosmology Legacy Survey: 850 μm maps, catalogues and number counts. *Monthly Notices of the Royal Astronomical Society*, 465(2):1789–1806, Feb 2017.

[4] David H. Hughes, Stephen Serjeant, James Dunlop, and others. High-redshift star formation in the Hubble Deep Field revealed by a submillimetre-wavelength survey. *Nature*, 394(6690):241–247, Jul 1998.

[5] M. P. Viero, V. Asboth, I. G. Roseboom, and others. The Herschel Stripe 82 Survey (HerS): Maps and Early Catalog. *The Astrophysical Journal Supplement Series*, 210(2):22, Feb 2014.

[6] F. Bertoldi, C. L. Carilli, P. Cox, and others. Dust emission from the most distant quasars. *Astronomy & Astrophysics*, 406:L55–L58, Jul 2003.

[7] R. Decarli, F. Walter, B. P. Venemans, and others. Rapidly star-forming galaxies adjacent to quasars at redshifts exceeding 6. *Nature*, 545(7655):457–461, May 2017.

[8] Dominik A. Riechers, C. M. Bradford, D. L. Clements, and others. A dust-obscured massive maximum-starburst galaxy at a redshift of 6.34. *Nature*, 496(7445):329–333, Apr 2013.

[9] M. L. Strandet, A. Weiss, C. De Breuck, and others. ISM Properties of a Massive Dusty Star-forming Galaxy Discovered at z 7. *The Astrophysical Journal Letters*, 842(2):L15, Jun 2017.

[10] A. Omont, P. Cox, F. Bertoldi, and others. A 1.2 mm MAMBO/IRAM-30 m survey of dust emission from the highest redshift PSS quasars. *Astronomy & Astrophysics*, 374:371–381, Aug 2001.

[11] A. Omont, A. Beelen, F. Bertoldi, and others. A 1.2 mm MAMBO/IRAM-30 m study of dust emission from optically luminous z ∼2 quasars. *Astronomy & Astrophysics*, 398:857–865, Feb 2003.

[12] Robert S. Priddey, Kate G. Isaak, Richard G. McMahon, and Alain Omont. The SCUBA Bright Quasar Survey (SBQS) - II. Unveiling the quasar epoch at submillimetre wavelengths. *Monthly Notice of the Royal Astronomical Society*, 339(4):1183–1188, Mar 2003.

[13] Ran Wang, Chris L. Carilli, Alexandre Beelen, and others. Millimeter and Radio Observations of z ∼6 Quasars. *The Astronomical Journal*, 134(2):617–627, Aug 2007.

[14] C. Leipski, K. Meisenheimer, F. Walter, and others. Complete Infrared Spectral Energy Distributions of Millimeter Detected Quasars at z > 5. *The Astrophysical Journal*, 772(2):103, Aug 2013.

[15] R. Maiolino, P. Cox, P. Caselli, and others. First detection of [CII]158 μm at high redshift: vigorous star formation in the early universe. *Astronomy & Astrophysics*, 440(2):L51–L54, Sep 2005.

[16] C. L. Carilli, R. Neri, R. Wang, and others. Detection of 1.6 10^{10} M_{solar} of Molecular Gas in the Host Galaxy of the z = 5.77 SDSS Quasar J0927+2001. *The Astrophysical Journal Letters*, 666(1):L9–L12, Sep 2007.

[17] Ran Wang, Jeff Wagg, Chris L. Carilli, and others. Star Formation and Gas Kinematics of Quasar Host Galaxies at z ∼6: New Insights from ALMA. *The Astrophysical Journal*, 773(1):44, Aug 2013.

[18] Roberto Decarli, Fabian Walter, Bram P. Venemans, and others. An ALMA [C II] Survey of 27 Quasars at z > 5.94. *The Astrophysical Journal*, 854(2):97, Feb 2018.

[19] Bram P. Venemans, Fabian Walter, Laura Zschaechner, and others. Bright [C II] and Dust Emission in Three z > 6.6 Quasar Host Galaxies Observed by ALMA. *The Astrophysical Journal*, 816(1):37, Jan 2016.

[20] Marta Volonteri. Formation of supermassive black holes. *The Astronomy and Astrophysics Review*, 18(3):279–315, Jul 2010.

[21] Livia Vallini, Simona Gallerani, Andrea Ferrara, and Sunghye Baek. Far-infrared line emission from high-redshift galaxies. *Monthly Notices of the Royal Astronomical Society*, 433(2):1567–1572, Aug 2013.

[22] Piero Madau and Mark Dickinson. Cosmic Star-Formation History. *Annual Review of Astronomy and Astrophysics*, 52:415–486, Aug 2014.

[23] Michael Rowan-Robinson, Seb Oliver, Lingyu Wang, and others. The star formation rate density from z = 1 to 6. *Monthly Notices of the Royal Astronomical Society*, 461(1):1100–1111, Sep 2016.

[24] R. C. Livermore, S. L. Finkelstein, and J. M. Lotz. Directly Observing the Galaxies Likely Responsible for Reionization. *The Astrophysical Journal*, 835(2):113, Feb 2017.

[25] Russell J. Smith, John R. Lucey, and David Carter. The stellar initial mass function in red-sequence galaxies: 1-μm spectroscopy of Coma cluster galaxies with Subaru/FMOS. *Monthly Notices of the Royal Astronomical Society*, 426(4):2994–3007, Nov 2012.

[26] Li-Yen Hsu, Lennox L. Cowie, Chian-Chou Chen, Amy J. Barger, and Wei-Hao Wang. The Hawaii SCUBA-2 Lensing Cluster Survey: Number Counts and Submillimeter Flux Ratios. *The Astrophysical Journal*, 829(1):25, Sep 2016.

[27] Yi-Kuan Chiang, Roderik A. Overzier, Karl Gebhardt, and Bruno Henriques. Galaxy Protoclusters as Drivers of Cosmic Star Formation History in the First 2 Gyr. *The Astrophysical Journal Letters*, 844(2):L23, Aug 2017.

[28] Wei-Hao Wang, Wei-Ching Lin, Chen-Fatt Lim, and others. SCUBA-2 Ultra Deep Imaging EAO Survey (STUDIES): Faint-end Counts at 450 μm. *The Astrophysical Journal*, 850(1):37, Nov 2017.

[29] E. Daddi, M. Dickinson, R. Chary, and others. The Population of BzK-selected ULIRGs at z ∼2. *The Astrophysical Journal Letters*, 631(1):L13–L16, Sep 2005.

[30] C. Gruppioni, F. Pozzi, G. Rodighiero, and others. The Herschel PEP/HerMES luminosity function - I. Probing the evolution of PACS selected Galaxies to z 4. *Monthly Notices of the Royal Astronomical Society*, 432(1):23–52, Jun 2013.

[31] Alexandra Pope and Ranga-Ram Chary. Searching for the Highest Redshift Sources in 250-500 μm Submillimeter Surveys. *The Astrophysical Journal Letters*, 715(2):L171–L175, Jun 2010.

[32] I. G. Roseboom, R. J. Ivison, T. R. Greve, and others. The Herschel Multi-tiered Extragalactic Survey: SPIRE-mm photometric redshifts. *Monthly Notices of the Royal Astronomical Society*, 419(4):2758–2773, Feb 2012.

[33] Dominik A. Riechers, T. K. Daisy Leung, Rob J. Ivison, and others. Rise of the Titans: A Dusty, Hyper-luminous "870 μm Riser" Galaxy at z 6. *The Astrophysical Journal*, 850(1):1, Nov 2017.

[34] M. Polletta, M. Tajer, L. Maraschi, and others. Spectral Energy Distributions of Hard X-Ray Selected Active Galactic Nuclei in the XMM-Newton Medium Deep Survey. *The Astrophysical Journal*, 663(1):81–102, Jul 2007.

[35] Caitlin M. Casey. The Ubiquity of Coeval Starbursts in Massive Galaxy Cluster Progenitors. *The Astrophysical Journal Letters*, 824(1):36, Jun 2016.

[36] J. Greenslade, D. L. Clements, T. Cheng, and others. Candidate high-z protoclusters among the Planck compact sources, as revealed by Herschel-SPIRE. *Monthly Notices of the Royal Astronomical Society*, 476(3):3336–3359, May 2018.

[37] D. L. Clements, F. G. Braglia, A. K. Hyde, and others. Herschel Multitiered Extragalactic Survey: clusters of dusty galaxies uncovered by Herschel and Planck. *Monthly Notices of the Royal Astronomical Society*, 439(2):1193–1211, Apr 2014.

[38] Planck Collaboration, N. Aghanim, B. Altieri, and others. Planck intermediate results. XXVII. High-redshift infrared galaxy overdensity candidates and lensed sources discovered by Planck and confirmed by Herschel-SPIRE. *Astronomy & Astrophysics*, 582:A30, Oct 2015.

[39] I. Flores-Cacho, D. Pierini, G. Soucail, and others. Multi-wavelength characterisation of z $\sim$2 clustered, dusty star-forming galaxies discovered by Planck. *Astronomy & Astrophysics*, 585:A54, Jan 2016.

[40] I. Oteo, R. J. Ivison, L. Dunne, and others. An Extreme Protocluster of Luminous Dusty Starbursts in the Early Universe. *The Astrophysical Journal*, 856(1):72, Mar 2018.

[41] Stuart I. Muldrew, Nina A. Hatch, and Elizabeth A. Cooke. What are protoclusters? - Defining high-redshift galaxy clusters and protoclusters. *Monthly Notices of the Royal Astronomical Society*, 452(3):2528–2539, Sep 2015.

[42] C. M. Casey, A. Cooray, P. Capak, and others. A Massive, Distant Proto-cluster at z = 2.47 Caught in a Phase of Rapid Formation? *The Astrophysical Journal Letters*, 808(2):L33, Aug 2015.

[43] Tiantian Yuan, Themiya Nanayakkara, Glenn G. Kacprzak, and others. Keck/MOSFIRE Spectroscopic Confirmation of a Virgo-like Cluster Ancestor at z = 2.095. *The Astrophysical Journal Letters*, 795(1):L20, Nov 2014.

[44] H. Dannerbauer, J. D. Kurk, C. De Breuck, and others. An excess of dusty starbursts related to the Spiderweb galaxy. *Astronomy & Astrophysics*, 570:A55, Oct 2014.

[45] T. B. Miller, S. C. Chapman, M. Aravena, and others. A massive core for a cluster of galaxies at a redshift of 4.3. *Nature*, 556(7702):469–472, Apr 2018.

[46] Yuichi Harikane, Masami Ouchi, Yoshiaki Ono, and others. SILVERRUSH. VIII. Spectroscopic Identifications of Early Large-scale Structures with Protoclusters over 200 Mpc at z $\sim$ 67: Strong Associations of Dusty Star-forming Galaxies. *The Astrophysical Journal*, 883(2):142, Oct 2019.

[47] L. L. Cowie, A. J. Barger, L. Y. Hsu, and others. A Submillimeter Perspective on the GOODS Fields (SUPER GOODS). I. An Ultradeep SCUBA-2 Survey of the GOODS-N. *The Astrophysical Journal*, 837(2):139, Mar 2017.

[48] J. M. Simpson, Ian Smail, A. M. Swinbank, and others. The East Asian Observatory SCUBA-2 Survey of the COSMOS Field: Unveiling 1147 Bright Sub-millimeter Sources across 2.6 Square Degrees. *The Astrophysical Journal*, 880(1):43, Jul 2019.

[49] S. J. Oliver, J. Bock, B. Altieri, and others. The Herschel Multi-tiered Extragalactic Survey: HerMES. *Monthly Notices of the Royal Astronomical Society*, 424(3):1614–1635, Aug 2012.

[50] S. Eales, L. Dunne, D. Clements, and others. The Herschel ATLAS. *Publications of the Astronomical Society of the Pacific*, 122(891):499, May 2010.

[51] Edward L. Chapin, Scott C. Chapman, Kristen E. Coppin, and others. A joint analysis of BLAST 250-500 μm and LABOCA 870 μm observations in the Extended Chandra Deep Field-South. *Monthly Notices of the Royal Astronomical Society*, 411(1):505–549, Feb 2011.

[52] A. Weiß, A. Kovács, K. Coppin, and others. The Large Apex Bolometer Camera Survey of the Extended Chandra Deep Field South. *The Astrophysical Journal*, 707(2):1201–1216, Dec 2009.

[53] Kimberly S. Scott, Hans F. Stabenau, Filiberto G. Braglia, and others. Spitzer MIPS 24 and 70 μm Imaging Near the South Ecliptic Pole: Maps and Source Catalogs. *The Astrophysical Journal Supplement Series*, 191(2):212–221, Dec 2010.

[54] T. A. Perera, E. L. Chapin, J. E. Austermann, and others. An AzTEC 1.1mm survey of the GOODS-N field - I. Maps, catalogue and source statistics. *Monthly Notices of the Royal Astronomical Society*, 391(3):1227–1238, Dec 2008.

[55] J. E. Austermann, J. S. Dunlop, T. A. Perera, and others. AzTEC half square degree survey of the SHADES fields - I. Maps, catalogues and source counts. *Monthly Notices of the Royal Astronomical Society*, 401(1):160–176, Jan 2010.

[56] I. Aretxaga, G. W. Wilson, E. Aguilar, and others. AzTEC millimetre survey of the COSMOS field - III. Source catalogue over 0.72 deg^2 and plausible boosting by large-scale structure. *Monthly Notices of the Royal Astronomical Society*, 415(4):3831–3850, Aug 2011.

[57] L. M. Mocanu, T. M. Crawford, J. D. Vieira, and others. Extragalactic Millimeter-wave Point-source Catalog, Number Counts and Statistics from 771 deg^2 of the SPT-SZ Survey. *The Astrophysical Journal*, 779(1):61, Dec 2013.

[58] J. D. Vieira, D. P. Marrone, S. C. Chapman, and others. Dusty starburst galaxies in the early Universe as revealed by gravitational lensing. *Nature*, 495(7441):344–347, Mar 2013.

[59] B. Magnelli, A. Karim, J. Staguhn, and others. The IRAM/GISMO 2 mm Survey in the COSMOS Field. *The Astrophysical Journal*, 877(1):45, May 2019.

[60] F. X. Désert, R. Adam, P. Ade, and others. NIKA2, a dual-band millimetre camera on the IRAM 30 m telescope to map the cold universe. In *SF2A-2016: Proceedings of the Annual meeting of the French Society of Astronomy and Astrophysics*, pages 439–442, Dec 2016.

[61] Sean Bryan. The TolTEC Camera for the LMT Telescope. In *Atacama Large-Aperture Submm/mm Telescope (AtLAST)*, page 36, Jan 2018.

[62] Luis C. Ho, Jeremy Darling, and Jenny E. Greene. Properties of Active Galaxies Deduced from H I Observations. *The Astrophysical Journal*, 681(1):128–140, Jul 2008.

[63] Jinyi Shangguan, Luis C. Ho, and Yanxia Xie. On the Gas Content and Efficiency of AGN Feedback in Low-redshift Quasars. *The Astrophysical Journal*, 854(2):158, Feb 2018.

[64] Fang Xia An, S. M. Stach, Ian Smail, and others. A Machine-learning Method for Identifying Multiwavelength Counterparts of Submillimeter Galaxies: Training and Testing Using AS2UDS and ALESS. *The Astrophysical Journal*, 862(2):101, Aug 2018.

[65] Isabelle Pâris, Patrick Petitjean, Éric Aubourg, and others. The Sloan Digital Sky Survey Quasar Catalog: Fourteenth data release. *Astronomy & Astrophysics*, 613:A51, May 2018.

[66] U. Dudzevičiūtė, Ian Smail, A. M. Swinbank, and others. An ALMA survey of the SCUBA-2 CLS UDS field: Physical properties of 707 Sub-millimetre Galaxies. *arXiv e-prints*, page arXiv:1910.07524, Oct 2019.

[67] Fabian Walter, Roberto Decarli, Chris Carilli, and others. The intense starburst HDF 850.1 in a galaxy overdensity at z $\approx$ 5.2 in the Hubble Deep Field. *Nature*, 486(7402):233–236, Jun 2012.

[68] J. A. Hodge, A. M. Swinbank, J. M. Simpson, and others. Kiloparsec-scale Dust Disks in High-redshift Luminous Submillimeter Galaxies. *The Astrophysical Journal*, 833(1):103, Dec 2016.

[69] B. Gullberg, A. M. Swinbank, I. Smail, and others. The Dust and [C II] Morphologies of Redshift 4.5 Sub-millimeter Galaxies at 200 pc Resolution: The Absence of Large Clumps in the Interstellar Medium at High-redshift. *The Astrophysical Journal*, 859(1):12, May 2018.